AD NUMBER
AD864116
LIMITATION CHANGES

TO:

Approved for public release; distribution is unlimited.

FROM:

Distribution authorized to U.S. Gov't. agencies and their contractors; Administrative/Operational Use; 18 JUN 1971. Other requests shall be referred to ARMY AVIATION MATERIEL LABS FORT EUSTIS VA. This document contains export-controlled technical data.

| AUTHORITY |
|---|
| usaamrdl ltr, 18 Jun 1971 |

AD

USAAVLABS TECHNICAL REPORT 69-18

MEASUREMENT OF ROTOR NOISE LEVELS AND EVALUATION OF POROUS BLADE TIPS ON A CH-47A HELICOPTER

By

R. H. Spencer

H. Sternfeld, Jr.

D D C
RECEIVED
JAN 26 1970
D

September 1969

U. S. ARMY AVIATION MATERIEL LABORATORIES
FORT EUSTIS, VIRGINIA

113

Disclaimers

The findings in this report are not to be construed as an official Department of the Army position unless so designated by other authorized documents.

When Government drawings, specifications, or other data are used for any purpose other than in connection with a definitely related Government procurement operation, the United States Government thereby incurs no responsibility nor any obligation whatsoever; and the fact that the Government may have formulated, furnished, or in any way supplied the said drawings, specifications, cr other data is not to be regarded by implication or otherwise as in any manner licensing the holder or any other person or corporation, or conveying any rights or permission, to manufacture, use, or sell any patented invention that may in any way be related thereto.

Disposition Instructions

Destroy this report when no longer needed. Do not return it to the originator.

This contract was initiated to correlate CH-47A noise levels with selected CH-47A parameters and to evaluate over a broad flight spectrum the effect of "porous" blade tips on noise, performance, and fuselage vibration in comparison with the standard rotor blade tips.

It was observed that in the region of rotor overlap, the amount of vertical separation between the forward and aft rotors had a profound influence on rotor noise levels and the occurrence of blade "slap." By comparison, other parameters appeared as second-order influences.

Porous tips only modestly reduced the noise level at hover, had no significant influence on noise levels in forward flight, and failed to demonstrate an appreciable effect on blade slap. It had been estimated that the increased drag of the porous tip represented a power penalty of 120 horsepower in hover, but measured results show this penalty to be 600 horsepower in hover and to diminish with forward speed, reaching zero at 130 knots. Graphic comparison of the power required for porous and standard tips suggests that at forward speeds in excess of 130 knots, the porous tip configuration might be operated at reduced power. Scrutiny of the noise data, however, indicates that noise reductions are not achieved by this reduction in required power.

Task 1F162203A14801
Contract DA 44-177-AMC-330(T)
USAAVLABS Technical Report 69-18
September 1969

MEASUREMENT OF ROTOR NOISE LEVELS
AND EVALUATION OF POROUS BLADE TIPS
ON A CH-47A HELICOPTER

Final Report

D8-0439B

By

R. H. Spencer
and
H. Sternfeld, Jr.

Prepared by

THE BOEING COMPANY
VERTOL DIVISION
Philadelphia, Pennsylvania

for

U.S. ARMY AVIATION MATERIEL LABORATORIES
FORT EUSTIS, VIRGINIA

SUMMARY

This report presents the results of a program to investigate
rotor noise levels of the tandem-rotor CH-47A helicopter. The
program was conducted in two phases:

Phase I

This phase correlated acoustical data with data obtained under
the Dynamic Airloads Program [Contract DA 44-177-AMC-124(T)].
The most significant correlation indicated that relative blade
tip path plane positions played a larger role in setting rotor
noise levels than did other operating parameters such as rotor
speed or gross weight.

Phase II

A set of porous rotor blade tips was evaluated as a means of
achieving noise reduction. These tips effected a 15-db
reduction in hover noise but had no consistent effect on
sound pressure level in forward flight. It was noted, however,
that a qualitative change in the acoustical signature resulted
in decreasing the sharpness of the generated sound at all
airspeeds.

FOREWORD

The two-phase rotor noise investigation was performed by the Acoustics Unit of the Vertol Division of The Boeing Company under U.S. Army Aviation Materiel Laboratories (USAAVLABS) Contract DA 44-177-AMC-330(T), Task 1F162203A14801.

TABLE OF CONTENTS

LIST OF ILLUSTRATIONS

LIST OF TABLES

x

LIST OF SYMBOLS

A	attenuation, decibels
A_ϵ	excess attenuation due to atmospheric absorption, decibels
A/S	airspeed, knots
a_1	longitudinal blade flapping coefficient
a_o	blade coning angle, degrees
BITF	forward rotor longitudinal cyclic trim angle, degrees
BITR	aft (rear) rotor longitudinal cyclic trim angle, degrees
b	number of rotor blades
b_1	lateral blade flapping coefficient
C	speed of sound, feet per second
C_{D_o}	profile drag coefficient
CF	centrifugal force, pounds
C-network	acoustical weighting filter
C_x	coordinate of vortex filament, feet
C_y	coordinate of vortex filament, feet
C_z	coordinate of vortex filament, feet
c	blade chord, feet
c_r	equivalent circumference of blade at radius r, feet
db	decibels, re 0.0002 dyne/cm^2
f	frequency, cycles per second
GW	gross weight, pounds
H	tip path plane separation, feet
Hz	Hertz, cycles per second

xi

h	height of blade tip above fuselage reference line, feet
hp	horsepower
IAS	indicated airspeed, knots
i_s	rotor shaft angle, degrees
kHz	kiloHertz, cycles per second x 10^{-3}
kn	knots
L	port length - porous tip, feet
l	pylon height above fuselage reference plane, feet
lb	force, pounds
M	Mach number
N	North
p	pressure, pounds per square foot
R	rotor blade radius, feet
r	distance from the center of rotation to a particular blade station, feet
r	vortex radius, feet
r, r_o	distance from noise source to microphone, feet
rpm	rotor revolutions per minute
S	South
SPL	sound pressure level, decibels
T	rotor thrust, pounds
TAS	true airspeed, knots
t	time, seconds
t/c	blade thickness ratio
V_{fs}	freestream velocity, feet per second

v_i	induced velocity of the vortex core, feet per second
v_{tot}	blade section total velocity, feet per second
α	angle of attack, degrees
α_f	fuselage angle with respect to the free stream, degrees
β	blade flapping angle, degrees
Δ	incremental notation
λ	wavelength, feet
μ	advance ratio
ρ	density of air, $lb\text{-}sec^2/ft^4$
τ	blade passage period, seconds
ψ	blade azimuth position, degrees
Ω	rotor speed, radians per second

INTRODUCTION

The evolution of rotary-winged aircraft toward higher speeds and higher payloads has produced helicopter rotor systems with greatly increased aerodynamic loading. This loading often results in the predominance of rotor blade noise in the overall noise signature of the aircraft; the level of noise from this source can be relatively strong.

The higher airloading imposed upon the blades gives rise to stronger circulation over the blade, and, therefore, to stronger tip vortex filaments. It is generally accepted that the impulsive acoustic radiation is caused either by large angle-of-attack changes over local sections of the blade or by the effects of local shock fronts on the blade, both of which appear to result from the intersection of the blade with the rolled-up vortex filament. On a single-rotor helicopter, these intersections arise from one blade intercepting the vortex trailed from a previous blade. On a tandem-rotor helicopter, the impulse generally results from a blade on one rotor intersecting a vortex trailed by a blade on the other. For both cases, however, the phenomenon results in similar acoustic effects, regardless of the mechanism of generation; i.e., increased detection signature and annoyance.

Some work has recently been done in the area of lifting-rotor/propeller noise theory by Loewy and Sutton[1] and Schlegel et al[2]; however, a comprehensive experimental program to evaluate the effect of systematic variations in vehicle-operating variables on the external noise of the vehicle has been required in order to examine the relationship of these oscillating pressures with other effects which may be directly or indirectly associated with the mechanism of generation. This report describes such a program, conducted by Vertol Division of Boeing under contract from USAAVLABS.

Since Boeing had already contracted with USAAVLABS to perform an extensive flight test program [Investigation of Dynamic Airloads - Contract DA 44-177-AMC-124(T)], it was arranged to conduct the study described in this report simultaneously with the former program. The Dynamic Airloads Program, which measured the steady and dynamic airloads, blade dynamics, control loads, and airframe response on a CH-47A helicopter, is fully reported in Reference 3. Flight test conditions included three nominal gross weights (25,500, 32,500, and 36,000 pounds), rotor speeds from 202 to 241 rpm, and airspeeds from 0 to 148 knots, to give systematic variations in advance ratio, advancing tip Mach number, and thrust coefficient. Manual adjustment of longitudinal cyclic trim allowed independent control of rotor separation, which exerts a high degree of influence on rotor noise, particularly at high airspeeds. Approximately 250 channels of data were recorded on each flight.

1

By adding four channels of on-board noise-measuring equipment, it was possible to measure rotor noise simultaneously with a large number of other operating variables and to correlate those variables which exerted the highest influence on rotor noise. This effort constituted Phase I of the rotor noise measurement program covered in this report.

It had been theorized earlier that an expanded tip vortex core would result in reduced aerodynamic response of the blade when an intersection occurred. During a wind tunnel program[4] conducted on a section of model blade which simulated flow over the tip region of the rotor, ten blade tip configurations were evaluated to determine the maximum component of tangential velocity induced in the core of the vortex trailed by each configuration. It was shown in this work that a 20-percent porous blade tip was successful in expanding the diameter of the core region, while reducing the maximum velocity to approximately one-fifth that of the standard configuration.

Phase II of the noise measurement program consisted of a separate investigation of the noise-reduction potential of the porous blade tip developed in the course of the Reference 4 program. This investigation was accomplished by installing rotor blades equipped with porous tips on the aircraft previously used for the Dynamic Airloads Program and by conducting an additional flight program.

In general, this program did not meet many of its initial objectives with regard to correlating noise and operating parameters such as gross weight, tip speed, etc. This was primarily due to the fact that the effect of rotor separation proved to be much more powerful than was initially suspected, and the Dynamic Airloads Program from which the data for this program were obtained did not provide the type of flight schedule which would have made it possible to isolate this effect.

Identified and calibrated 1/4-inch magnetic tapes of all noise data recorded under this contract will be on loan from the U.S. Army Aviation Materiel Laboratories to investigators studying helicopter noise.

ANALYSIS OF THE PROBLEM

It is generally accepted that the intersection of a rotor blade
with the rolled-up (or partially rolled-up) portion of the shed
vorticity results in impulsive aerodynamic loading of the rotor
blade. This rapid fluctuation in aerodynamic loading gives
rise to high intensity noise and suggests at least two mecha-
nisms for the generation of this noise:

1. Rapid changes in blade angle of attack with the
   accompanying pressure fluctuations.

2. Local flow over a section of the blade approaching
   the velocity of sound, resulting in a more rapid
   disturbance.

Either mechanism may occur depending upon the velocity of the
blade section. For example, when the blade intercepts a vor-
tex with the total effective velocity over the blade section
well below the critical Mach number for that airfoil, the
mechanism of noise generation is a rapid change in the angle
of attack. However, if the section is operating at high sub-
sonic velocities, the flow over the section of the blade which
passes through the vortex can approach the velocity of sound
and a new mechanism is introduced. In either case, a reduction
in the velocity induced within the core of the vortex reduces
the intensity of the accustical disturbance produced. When
the Mach number of the advancing tip of a rotor blade exceeds
the critical Mach number (neglecting for the moment other dis-
turbing flow fields), transonic or supersonic flow can exist
and the conditions for local shock fronts will then prevail.
The magnitude and extent of the disturbance which exists are
not well understood, but the pressure disturbance on the ground
has been extensively measured.

Two approaches to a solution are: to avoid intersections of
rotor blades with rolled-up tip vortices, or, if this cannot
be accomplished, to reduce excitation of a rotor blade with
the vortex by lowering the velocity induced within the core.

It was the purpose of Phase I of this study to determine the
extent to which changes in operating variables effect changes
in rotor noise levels, and then to correlate the more important
variables with this noise. Phase II was an investigation to
determine, on a full-scale vehicle, the extent of rotor noise
reduction achievable by practical reductions in the velocity
induced in the tip vortex.

3

MEASUREMENT OF NOISE LEVELS

TEST AIRCRAFT

The flight vehicle used for the subject program (Figure 1) is a
tandem rotor U.S. Army CH-47A Chinook helicopter (S/N 94986).
The Chinook has a crew of three and is a medium transport heli-
copter capable of transporting 44 passengers at a maximum
speed of 150 miles per hour over a range of 234 miles. It is
powered by two T55-L-7 turboshaft engines and has a normal
gross weight of 33,000 pounds and a rotor diameter of 59.1
feet. The general arrangement of the CH-47A is shown in
Figure 2.

The control system incorporates longitudinal cyclic trim on
both rotors. This permits the pilot to control the rotor tilt
independently, thus controlling the tip-plane separation be-
tween the rotors.

Development of the Porous Tip

A wind tunnel program[4] to evaluate ten rotor blade tip configu-
rations for the effect on tip vortex core thickening led to the
development of the 20-percent nominal porous tip for the sub-
ject program (Figure 3). In general, the three porous tips,
developed during the Reference 4 program, showed the most
promise for reducing the velocity induced within the core of a
tip vortex filament. Although the 40-percent nominal porosity
blade tip provided a greater reduction in velocity, the incre-
ment in profile drag coefficient involved with this was substan-
tial, and the 20-percent tip was judged to be the optimum.

Although original planning called for the porous blade tips to
be evaluated on the instrumented blades of the Dynamic Airloads
Program, chordwise balance of these instrumented blades was
such that the additional mass required to balance the tips to
the blades could not be retained by the existing tip-attachment
hardware.

Since new fittings for the tip-attachment hardware could not be
installed in the space available, the porous tips were eval-
uated on standard CH-47A noninstrumented rotor blades which
required modification to accept the porous tips; this added an
additional 4.5 pounds to the blade. The modifications consis-
ted of three internal stiffening ribs at the tip and an
external triangular doubler between the blade and tip at the
midchord location.
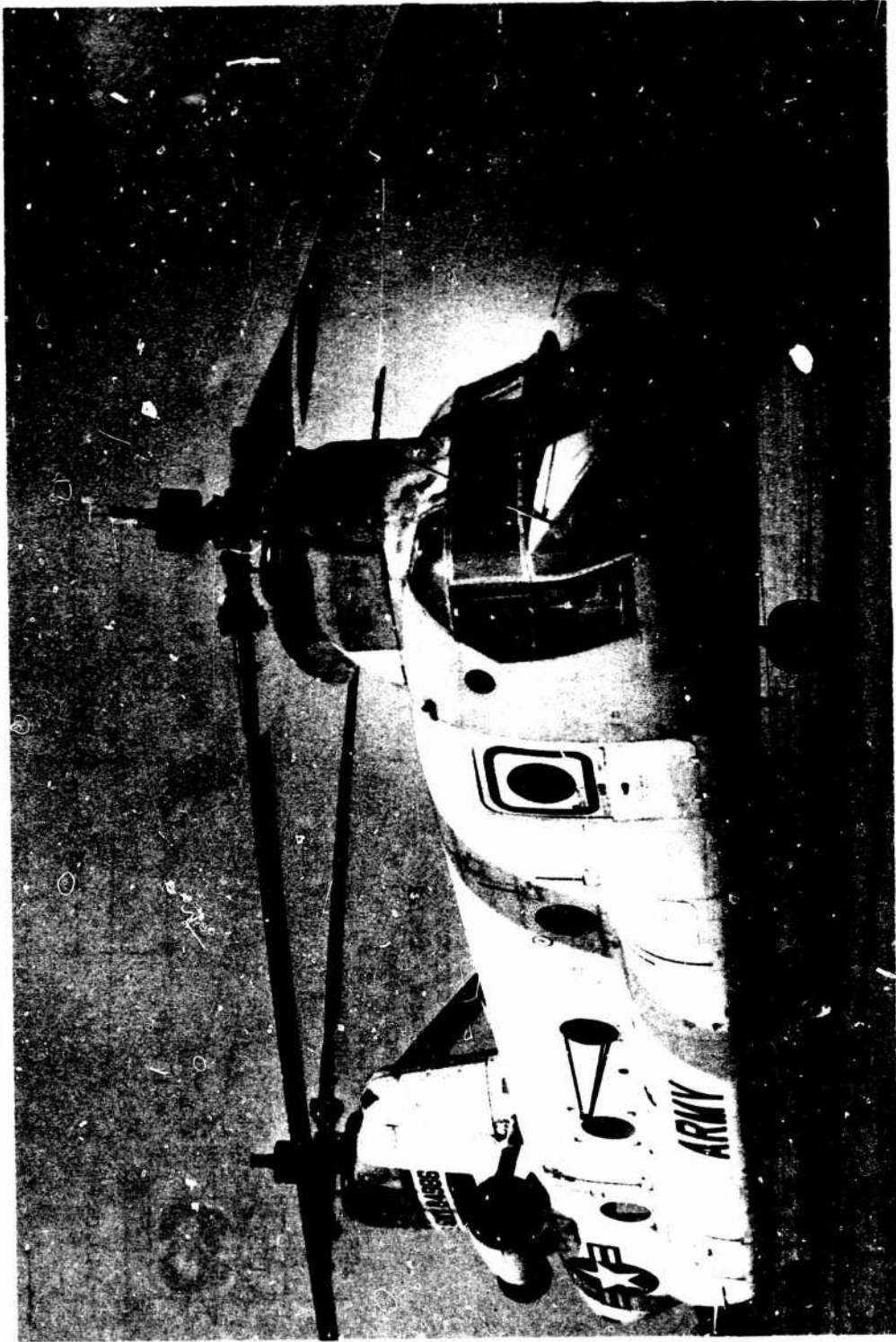
Figure 1. CH-47A Test Aircraft.

5

NOTE: ALL LINEAR DIMENSIONS IN INCHES
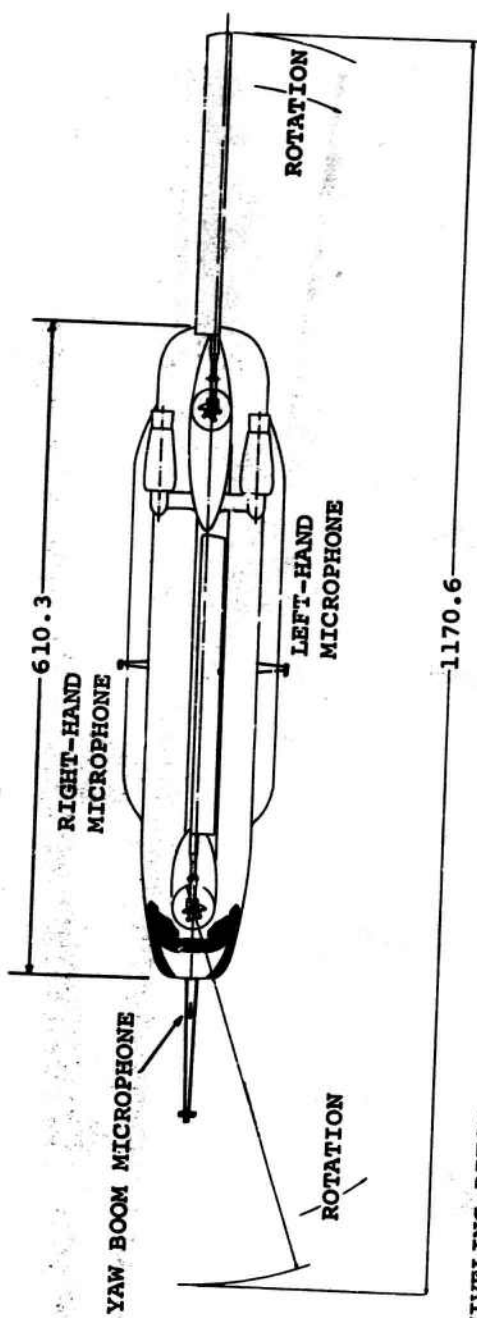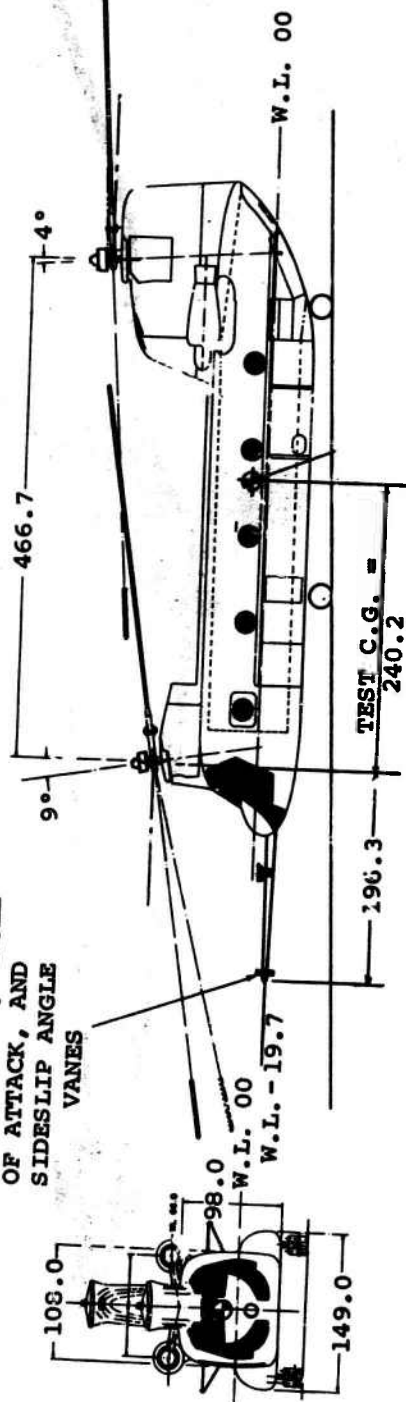
Figure 2. General Arrangement of CH-47A.

6
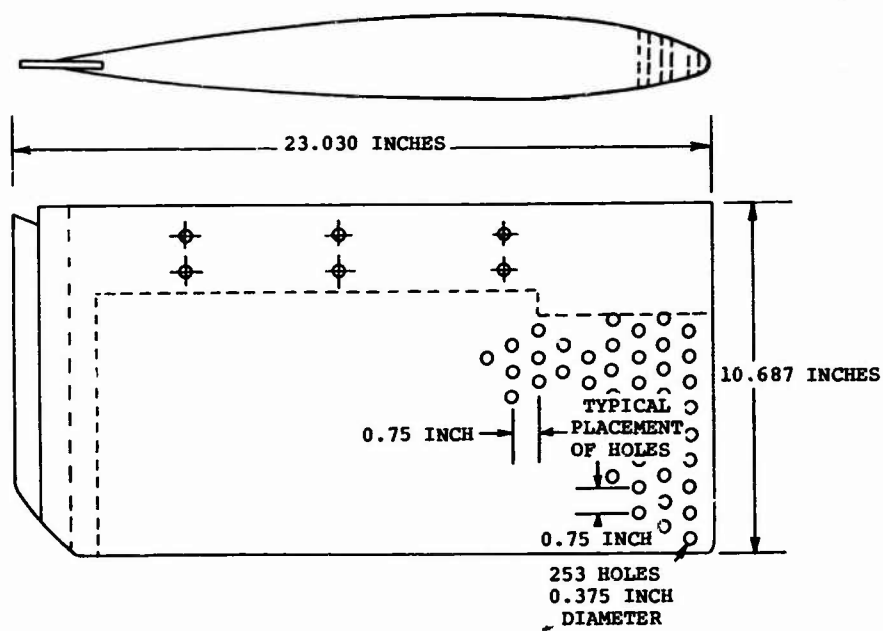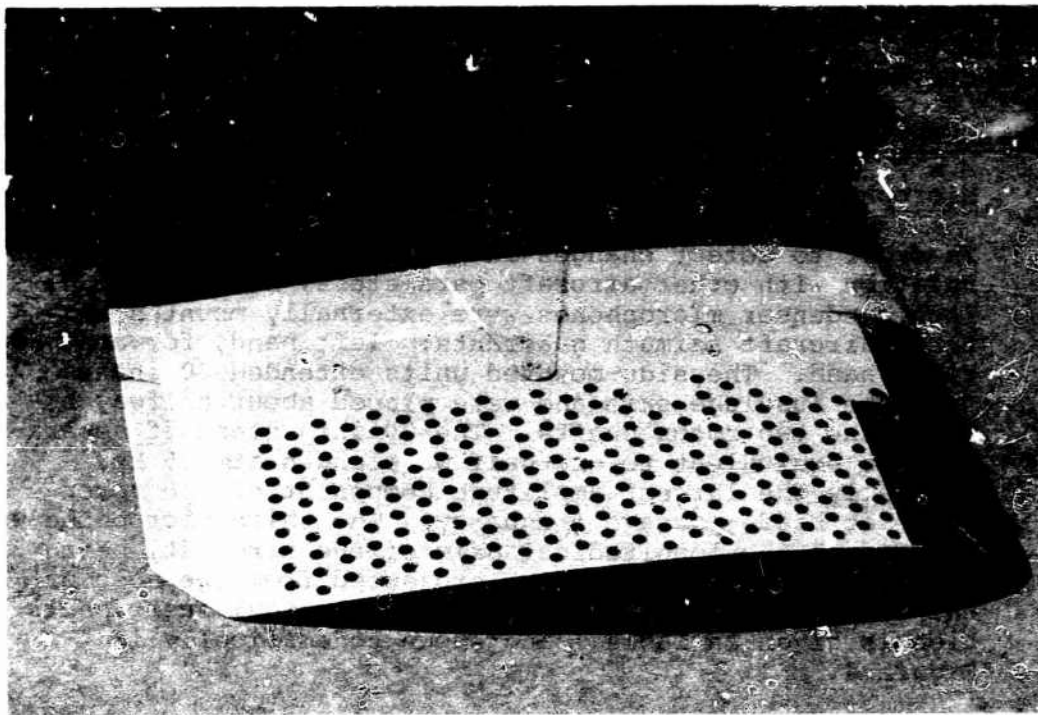
Figure 3.   Details of Rotor Blade Porous Tip.

The modified blades including tips were teeter-balanced, tracked, and endurance-whirled on the whirl-tower facility. In addition, the blades were tracked on the aircraft prior to the flight test program. The final track was accomplished within production tolerances.

INSTRUMENTATION - PHASE I

1. Microphones

In order to detect changes in rotor noise for a valid correlation with other aircraft parameters, sensitive 1/4-inch condenser microphones were externally mounted in three aircraft azimuth quadrants: left hand, forward, and right hand. The side-mounted units extended 30 inches from the fuselage skin and were placed about halfway between the two rotor shafts. The 30-inch standoff separation is equivalent to one-half wavelength at 225 Hz, generally the largest amplitude component of the rotor pulse at blade-passage frequency. The third microphone was located on the longitudinal axis of the aircraft, being placed on the yaw boom which projected from the nose of the aircraft. A complete list of acoustical instrumentation is given in Table I and shown schematically in Figure 4.

The microphone cartridge and cathode follower were mounted in polyurethane foam in U-clamps, in order to eliminate undesirable structurally induced noise. Positioning the longitudinal axis of the cathode follower parallel to the fuselage reference line lowered self-induced aerodynamic noise to a level well below that of the rotor noise at all airspeeds. Cockpit noise levels, which were also recorded, were somewhat higher than in production versions of the CH-47A, since much of the acoustical treatment was removed to permit routing of instrumentation wire packs. Condenser microphones were used for the airborne-measuring system because of their sensitivity and compactness; since they are fed by alternating current power supplies, they remain stable over long periods.

2. Recorder

The three external microphone channels were simultaneously recorded on three direct record channels of a four-channel 1/4-inch magnetic tape recorder. The fourth channel contained a record coder signal and recorded in the FM mode. The same record encoder used for the Reference 3 program was also used for all channels of acoustical data so that precise identification and time correlation could be obtained between the data of both programs.

8

Location	Instrument	Manufacturer	Model	Serial	Location
Airborne External	DC-AC Inverter	Carter	-	-	-
	Recorder Power Pack	Lockheed	1031	-	-
	Tape Recorder	Lockheed	411CDF	0149	-
	Microphone Power Supply	Bruel & Kjaer	2801	107728	Left-Hand Side
	Microphone Power Supply	Bruel & Kjaer	2801	107732	Yaw Boom
	Microphone Power Supply	Bruel & Kjaer	2801	107730	Right-Hand Side
	Cathode Follower	Bruel & Kjaer	2615	141513	Left-Hand Side
	Cathode Follower	Bruel & Kjaer	2615	141563	Yaw Boom
	Cathode Follower	Bruel & Kjaer	2615	141552	Right-Hand Side
	Microphone	Bruel & Kjaer	4136	101292	Left-Hand Side
	Microphone	Bruel & Kjaer	4136	141829	Yaw Boom
	Microphone	Bruel & Kjaer	4136	141765	Right-Hand Side
	Nose Cone	Bruel & Kjaer	0053	-	All External
	Pistonphone	Bruel & Kjaer	4220	85404	-
Airborne Internal	Recorder Power Pack	Lockheed	1031	-	-
	Tape Recorder	Lockheed	411C4D	016R	-
	Microphone Power Supply	Bruel & Kjaer	2801	107731	Cockpit
	Cathode Follower	Bruel & Kjaer	2613	141231	Cockpit
	Microphone	Bruel & Kjaer	4131	123080	Cockpit
	Pistonphone	Bruel & Kjaer	4220	85404	Cockpit
North Side of Runway	DC-AC Inverter	Terado	-	-	200 ft
	Tape Recorder	Ampex	PR-10	-	
	Cathode Follower	Bruel & Kjaer	2630	144605	
	Microphone	Bruel & Kjaer	4131	136272	
	Pistonphone	Bruel & Kjaer	4220	107863	
	Cathode Follower	Bruel & Kjaer	2630	37607	600 ft
	Microphone	Bruel & Kjaer	4131	78601	
	Pistonphone	Bruel & Kjaer	4220	107863	
South Side of Runway	DC-AC Inverter	ATR	-	X-01337	200 ft
	Tape Recorder	Ampex	672	1368	
	Cathode Follower	Bruel & Kjaer	2630	144620	
	Microphone	Bruel & Kjaer	4131	136277	
	Pistonphone	Bruel & Kjaer	4220	85372	
	Cathode Follower	Bruel & Kjaer	2630	102814	600 ft
	Microphone	Bruel & Kjaer	4131	104788	
	Pistonphone	Bruel & Kjaer	4220	85372	

TABLE I. LIST OF ACOUSTICAL INSTRUMENTATION
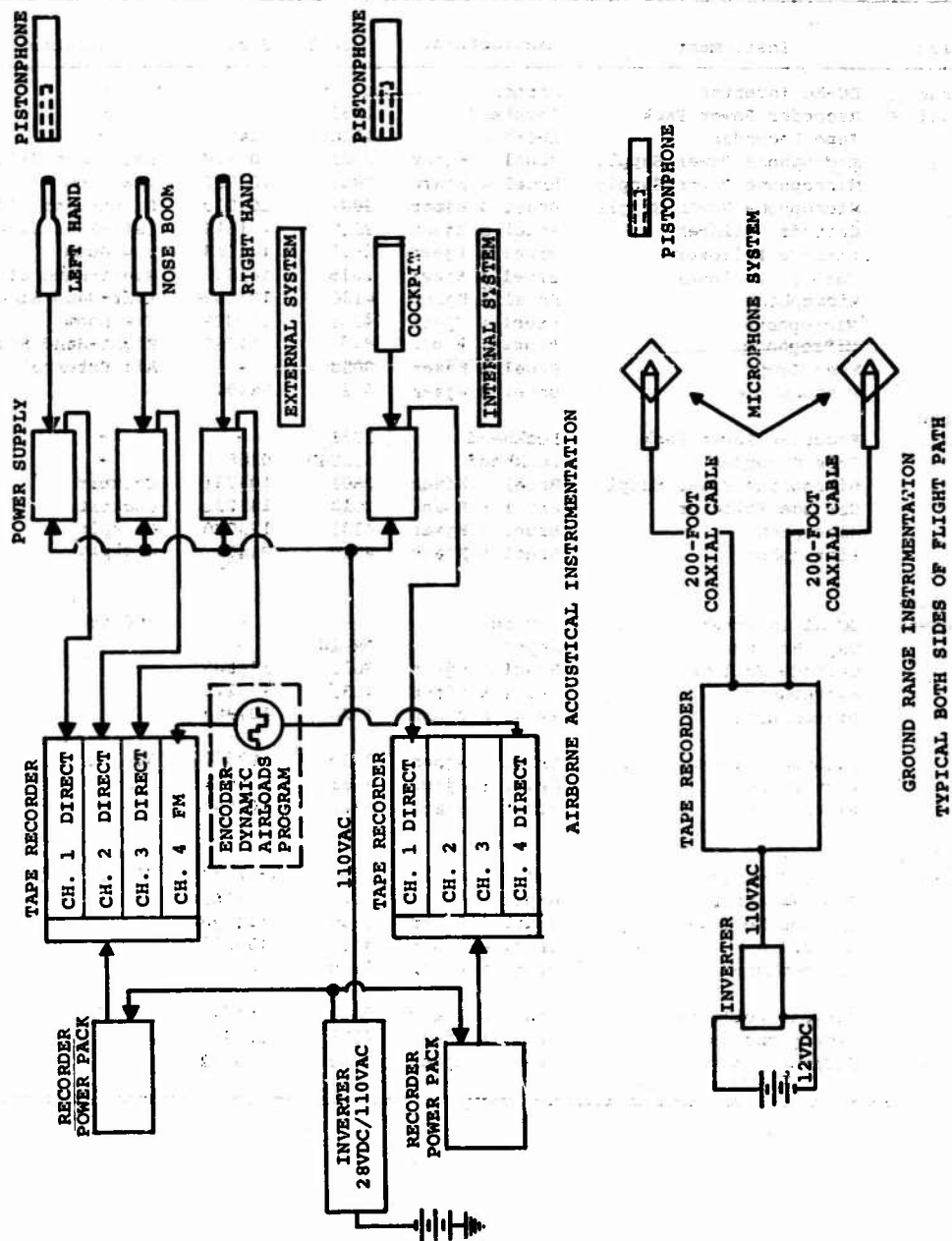
Figure 4. Schematic of Acoustical Instrumentation.

The cockpit microphone data were recorded on a tape recorder which was similar to that used for the aircraft external data and also contained a record identification code from the Reference 4 program instrumentation.

3. Calibration

Frequency response characteristics of the recording system are shown in Figure 5. These data have been determined from rms sine wave inputs and include microphone cartridge calibrations (obtained separately) and cable and recorder system response. Prior to and immediately following each flight, a single frequency tone (250 Hz) was applied to each system using a pistonphone calibrator which produces a 124-db rms level. Because the waveform characteristic of the rotor pulse is not sinusoidal, a response check was performed on the recording system using a comparison of input and output levels for a series of actual recorded pulses. This response is also shown in Figure 5. This type of peak-to-peak waveform input has a flatter response curve in the low frequency (31.5 and 63 Hz) and high frequency (8,000 Hz) regions; therefore, it is more directly applicable to the subject analysis. However, the conventional rms calibration corrections were applied to the data, since this is a recognized calibration procedure and is traceable to standards.

INSTRUMENTATION - PHASE II

1. Microphones

To evaluate the effect of porous tips on external rotor noise of the aircraft, a ground range of microphones was erected and the helicopter was flown over them at low altitudes. Four 1-inch condenser microphones were arranged as shown in Figure 6 for the ground range array. The microphones at 600 feet provided a somewhat less critical transient during fly-over than did the microphones at 200 feet, which were located a short distance inside the acoustic far field.

With ground instrumentation, the absolute change in noise levels could be evaluated even with shifts in azimuth of the noise with respect to the aircraft involved. This would not necessarily be the case with the aircraft instrumentation used for the subject program, since any shift in azimuth of the noise produced by the porous tip might not be fully detected by the microphones mounted on the fixed booms of the near field. The limitations of the ground range instrumentation are that the samples of data obtained are rather limited in time, and analysis of the data must necessarily be of a transient phenomenon. This is discussed more fully under Data Reduction and Analysis.

11
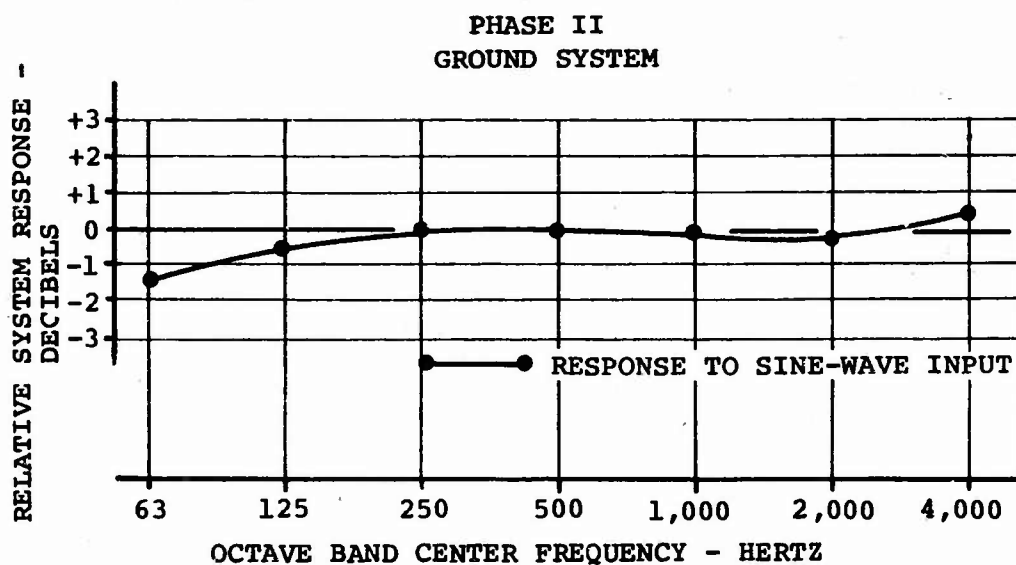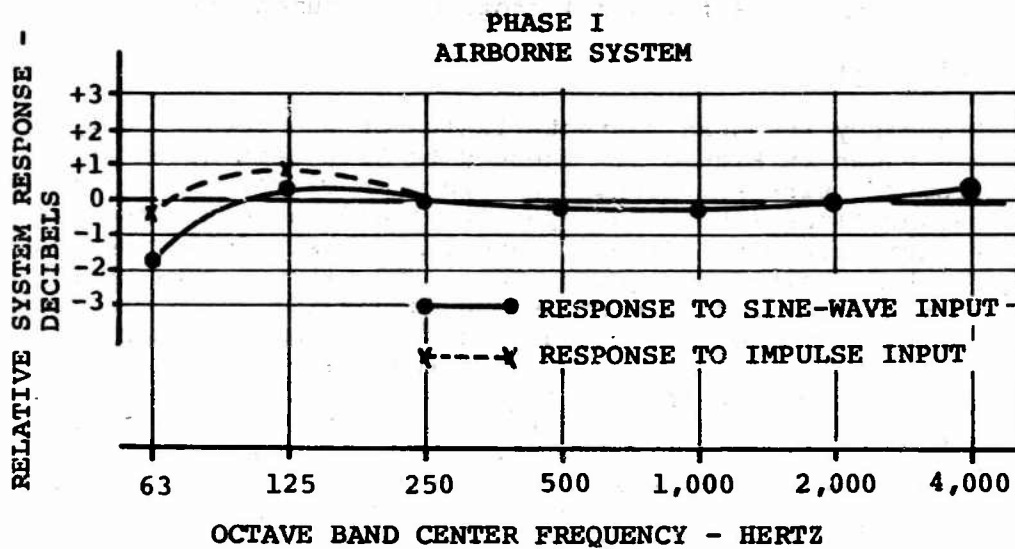
Figure 5. Record System Calibration Curves.

12
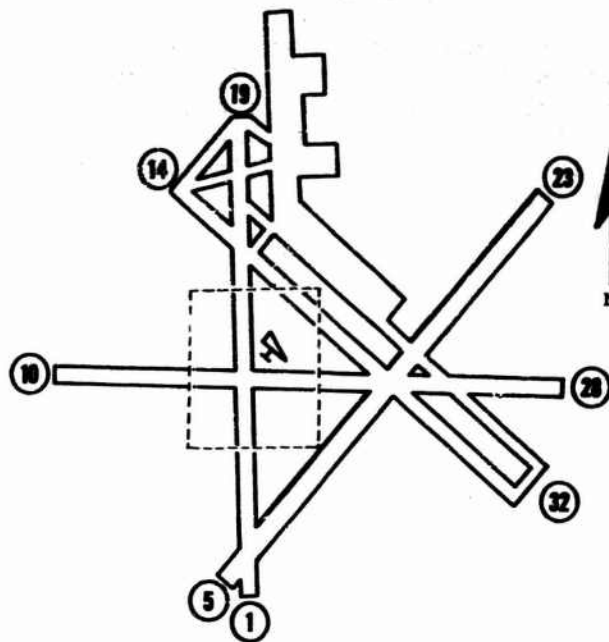
MILLVILLE, N.J., MUNICIPAL AIRPORT
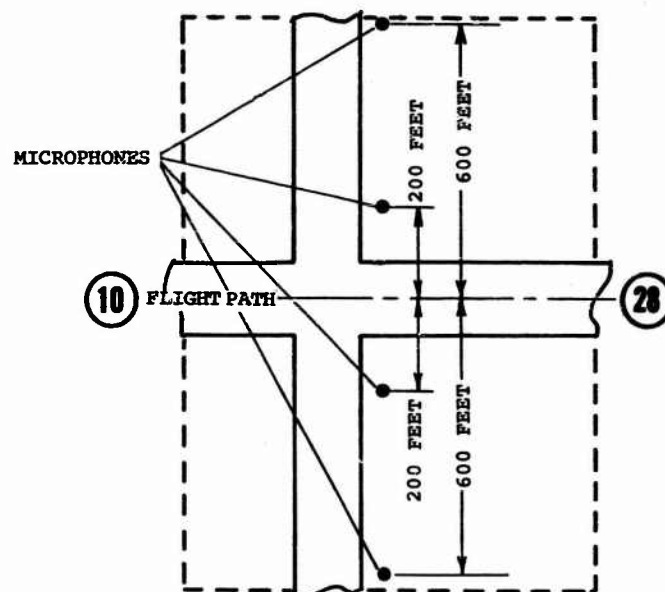
Figure 6.   Phase II Test Site and Ground Range
             Microphone Array.

13

2. Recorder and Calibration

Frequency response characteristics of the recording systems are shown in Figure 5 (Phase II). These data were determined from sine-wave inputs and include microphone cartridge calibration (obtained separately) and recorder response. In the field, a single frequency (250 Hz) was applied to each system prior to and immediately following each flight program. An additional calibration correction was applied in order to correct for galvanometer frequency response. The airborne instrumentation was the same as that used for Phase I.

TEST PROGRAM - PHASE I

The Phase I test program consisted of measuring internal and external noise levels concurrent with the Reference 3 program which investigated variations in rotor speed, airspeed, gross weight, and longitudinal cyclic trim control.

The range of test conditions at which data were obtained was:

Gross weight	23,600 to 36,900 pounds
Airspeed	0 to 148 knots
Rotor speed	202 to 241 rpm
Fwd rotor cyclic trim	0 to 3 degrees forward
Aft rotor cyclic trim	0 to 5 degrees forward
Maneuvers and level flight	

Specific points are defined in Appendix II.

TEST PROGRAM - PHASE II

The purpose of the Phase II test program was to evaluate the effect of porous blade tips on rotor-generated noise over a range of airspeeds and cyclic trim positions. Specific flight conditions are listed in Appendix II. Data on the reference flight were obtained with standard blade tip covers having the form of one-half of a body of revolution generated with an airfoil shape. The fully instrumented rotor blades of the Reference 3 program were utilized for this flight so that blade pressures were obtained.

For the hover conditions, the aircraft was in ground effect with a wheel height of approximately 5 feet. Surface winds were less than 5 knots.

For the fly-by program, the aircraft was flown at an altitude of 200 feet over the test range and maintained in a stabilized level flight condition for a minimum of 1,000 feet prior to and beyond the ground microphone array. To determine what effect minor irregularities in aircraft altitude, course, and gross

14

weight would have on the data acquired throughout the program, four 120-knot fly-bys were performed over the time span of the flight test: two were made at the beginning of the program, one was made at the midpoint, and one was made at the completion of the test. In addition, the effect of ambient winds on rotor-generated noise was investigated by reversing the direction of the aircraft over the course. These effects were minor.

For the approach and flare condition, the landing spot was on the axis of the ground range midway between the left-hand and right-hand microphones. For the maximum rate-of-climb point, the aircraft approached the range at an altitude of 200 feet and began its climb such that when passing over the microphone an altitude of 500 feet had been obtained.

Flight testing with the porous tips was carried out in the same order as with the standard tips in order that the effect of the porous tip could be evaluated at the same gross weight.

DATA REDUCTION AND ANALYSIS

Dynamic Airloads Data

Because of the large amount of instrumentation installed on the aircraft for the Reference 3 program, it was necessary to share the available channels of recording equipment on a time basis; thus, the forward and aft rotor blade instrumentation were sequenced on alternate rotor cycles so that a specific pressure gage on the forward rotor, for instance, time-shared the same recording channel with the respective gage on the rear rotor. The analysis under consideration included five rotor cycles distributed through twenty cycles of data. Results were presented as maximum, minimum, and mean values of the variable. The mean value was used for all correlations in this report. A detailed description of the instrumentation system and analysis methods can be found in Reference 3.

Acoustical Data

Each channel of external microphone data was analyzed by frequency spectrum using full octave bandpass filters of the "preferred" frequency limits[5]. Since circuit ringing can occur when pulse-loading characteristics of rotor noise are filtered through bandpass filters, an investigation to ensure against these false indications was performed.

A representative sample of banging rotor noise was stripped out on an oscillograph using both full octave and one-third octave bandpass filters for that sample. The levels in each group of three one-third octave filters corresponding to the full octave

15

filter over that frequency range were summed and compared with
the level in that equivalent full octave. In each instance
the sum of the levels in the one-third octaves was identical
with the full octave level; presumably, had any one of the
filters been ringing, the sound pressure amplitudes would not
have been identical.

An oscillographic readout system was used for this program in
order to examine the high rates of pressure changes associated
with rotor noise. All external aircraft microphone channels
were stripped out through bandpass filters which have geometric
centers at the following frequencies: 63, 125, 250, 500, 1,000,
2,000, and 4,000 Hz. Sound pressure levels above 5,600 Hz have
not been reported since the galvanometer selected for data
stripouts, which give maximum amplitude over the broadest fre-
quency range, did not respond to these high frequencies.
Restripping with a high frequency galvanometer was not con-
sidered necessary since the problems were completely defined
by frequencies below 5,600 Hz. Other analyses and display
systems were considered but were rejected since they did not
authentically display the rotor bang waveform. Simultaneous
stripout of the three airborne external microphones was per-
formed for the overall frequency records as shown in Figure 7.

Acoustical Data - Phase II

The airborne data, both internal and external, were treated
similarly to data from the Phase I program.

The transient nature of the data resulting from aircraft flown
over a fixed ground array of microphones requires a completely
different approach to analysis. While the maximum value of
the fly-by is useful, it does not relate changes in charac-
teristics which take place prior to and after the fly-by;
namely, the rate of buildup and decay of sound pressure. Thus,
while two aircraft may have the same maximum level, if the
pressure reading on the microphone builds up and decays slowly,
this implies a high sound level over a relatively long period,
whereas rapid buildup and decay characteristics imply short
periods of exposure. This affects both detection and annoy-
ance of the aircraft.

Another aspect of the exposure time which is unrelated to
physical changes in the aircraft is the airspeed at which it
passes over the ground range. To account for this, a fixed
distance was selected as the basis for evaluation of the data,
and after consideration of some representative samples of
data, this distance was selected as 400 feet (250 feet before
maximum and 150 feet following the maximum level), since the
amplitude of the data appeared to be reasonably flat over this
range. The magnitude of each pulse at blade-passage frequency
was tabulated over the time period corresponding to the noted

16
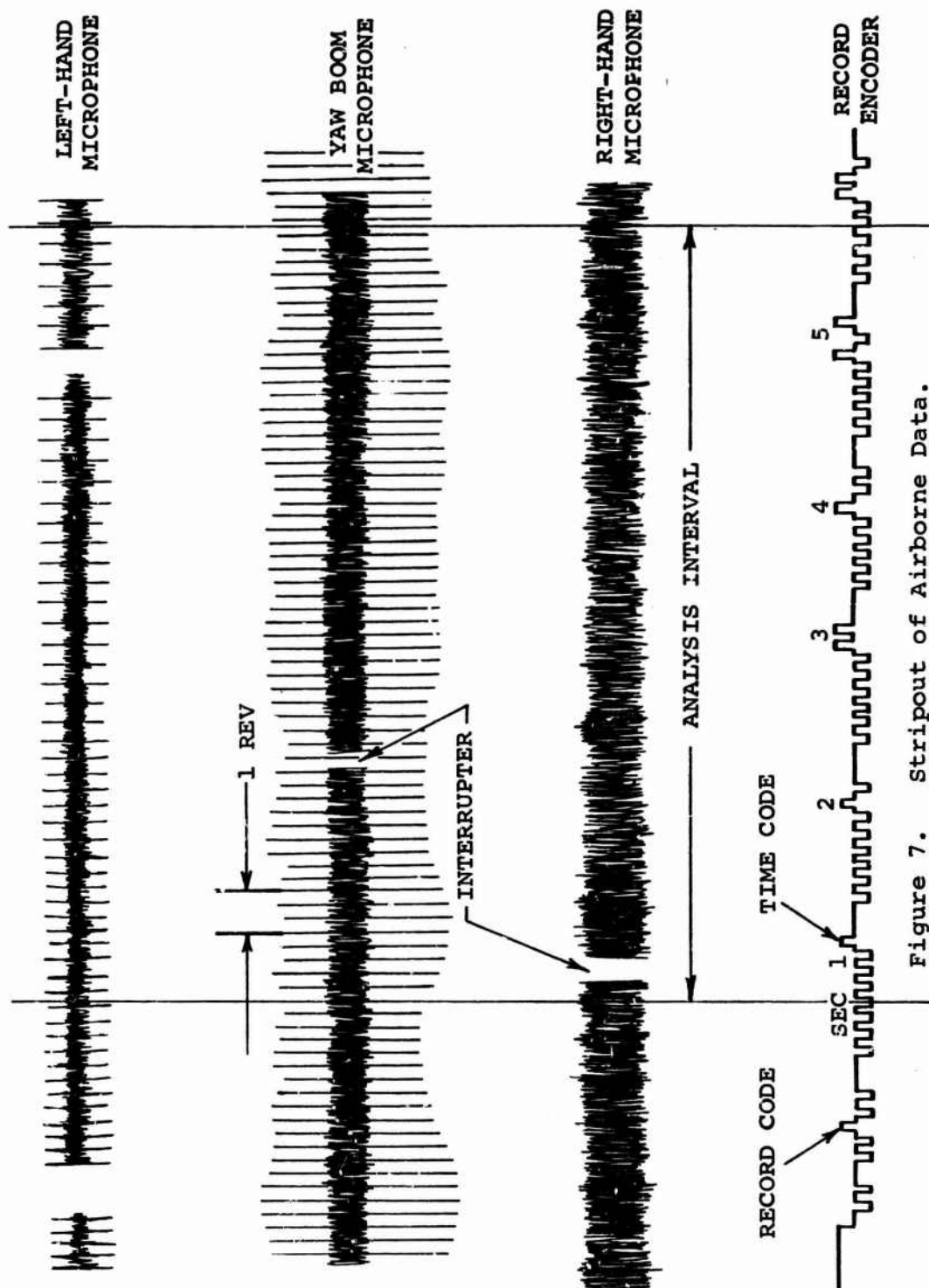
Figure 7.   Stripout of Airborne Data.

17

sample, and the mean value of these amplitudes was computed; this result, then, is the value which has been reported and used for correlation studies.

Statistical Analysis

A large portion of the noise data gathered during the subject program was to be correlated with other variables and parameters obtained from dynamic airloads instrumentation; the only time interval (when the sound pressure levels were read) was the identical interval over which the Reference 3 program data were analyzed, namely, the initial 5 seconds of record (see Figure 8). The peak amplitude of the three-per-revolution rotor bang period was used for correlation purposes. In order to achieve an efficient procedure for determining the representative value for each run, a statistical investigation was then made of several representative flight conditions. The results are presented in Table II.

Data from each of the three external airborne channels were examined. For the same time interval of analysis as the dynamic airloads data, the peak magnitude of every pulse at blade-passage frequency was tabulated and the values of the mean, median, and mode were calculated.* These values were then compared with an average value determined from one-half the sum of the maximum and minimum levels for each run. The absolute value of the difference of the arithmetic mean and average value was found to differ, in general, by less than 0.5 db.

For the two instances noted where this difference exceeded 0.5 db, the data appeared to be bimodal; that is, there was an interval in the record in which banging occurred and another interval in which banging did not occur because of unsteady conditions for that record. In both cases, the indicated airspeed was approximately 51 knots. Further confidence in the grouping of data was noted in the closeness of the mean, median, and mode; these, along with the standard deviation, are shown in Table II. It was concluded that a measure of the mean value of the data, generally within 0.5 db, could be obtained from the average value determined from one-half the sum of the maximum and minimum for each run. All data for each airborne microphone and run were then tabulated, corrected for frequency-response characteristics of the recording and playback system and oscillograph galvanometer response, and then used as input to a computer program which calculated the mean value of all data points.

---

* Mean - arithmetic mean.
  Median - equal number of pulses above as below this value.
  Mode - amplitude which occurs most frequently.

18

ROTOR SEQUENCE FWD
AFT

ROTOR CYCLE

RECORDED
PARAMETERS

INTERVALS DIGITIZED

SEC 1   2   3
TIME CODE
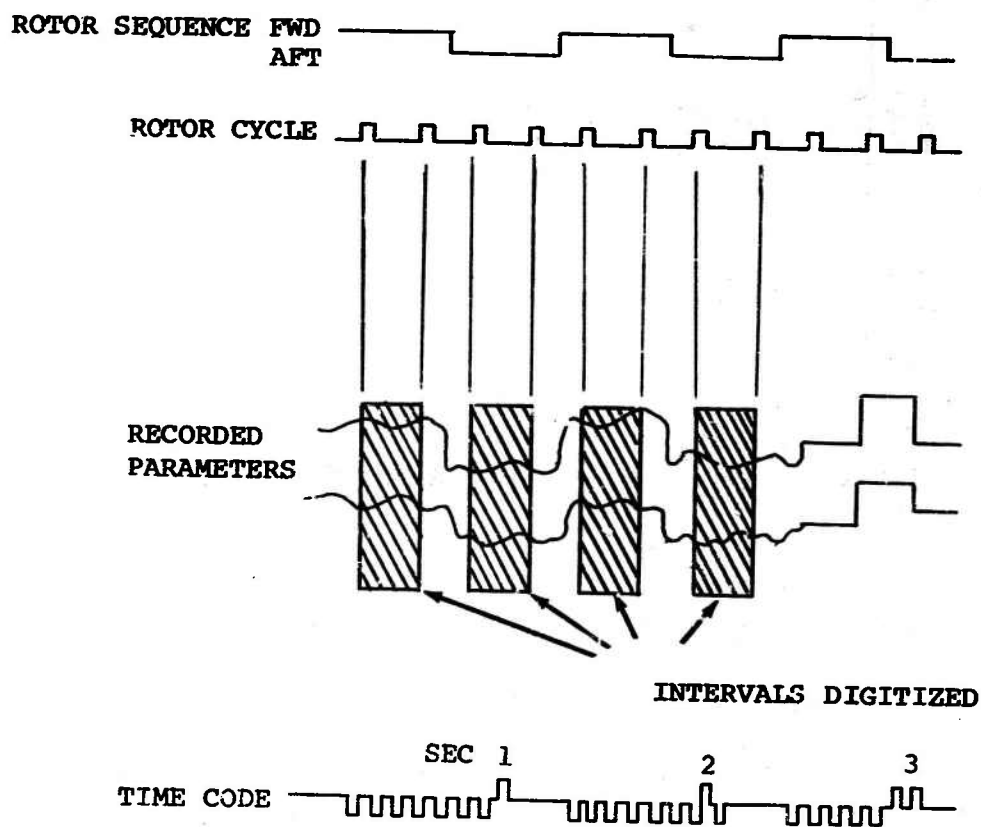
NOTE: SEE REFERENCE 3,
        VOL. III, FIG. 3

Figure 8.   Selection of Flight Data for Digitizing.

19

TABLE II. STATISTICAL ANALYSIS OF AIRBORNE DATA

Micro-phone	Record No.	Approx Gross Weight (lb)	True Air-speed (kn)	Mean (db)	Average (db)	Median (db)	Mode (db)	Standard Deviation (σ)
				FLIGHT 393				
Left	6	36,000	28	125.6	125.5	127	127	0.76
	12	36,000	63	124.8	125	126	126	1.52
Nose	6	36,000	28	122.5	123	123	122	2.23
	12	36,000	63	124.5	124.5	125	125	1.19
Right	6	36,000	28	126.5	127	127	127	1.17
	12	36,000	63	125	125	126	126	1.73
				FLIGHT 394				
Left	1	32,500	58	126.8	127.6	128	130	2.48
	2	32,500	101	125	125.5	126	125	0.83
	3	32,500	85	126	126.5	127	127	1.75
	11	32,500	28	124.5	124	125	125	1.18
Nose	1	32,500	58	128.8	130	130	130	1.23
	2	32,500	101	129.6	130	130	131	1.72
	3	32,500	85	129	129	130	129	1.79
	11	32,500	28	124.5	124.5	124	125	1.58
				FLIGHT 395				
Left	3	23,500	54	126.9	125.5	128	128	1.90
	9	23,500	96	127.5	127	127	126	1.57
Nose	3	23,500	54	127.5	127	127	127	1.80
	9	23,500	96	128.6	128.5	129	130	1.49
Right	3	23,500	54	125.9	126	126	125	1.59
	9	23,500	96	125.6	126	125	125	0.98

The program for calculating mean values also generated a data
listing, which was scanned for check purposes prior to plotting;
it also produced a magnetic tape which was input to an auto-
matic data plotter. With the large quantity of data obtained
in this program, it was judged expedient to review all data for
consistency; thus, all airborne data acquired during the
program were reviewed by an acoustical engineer not previously
associated with the subject program. This procedure is recom-
mended for all large data acquisition programs.

Cockpit internal noise levels were treated from a somewhat
different approach, since internal noise was dominated by
dynamic components, particularly in the test aircraft used
for this program. Because of the large number of wire packs
and cables which were required for the extensive instrumenta-
tion of the Reference 3 program, the normal acoustical treatment
was removed from the aircraft. The internal noise was deter-
mined by full-octave spectrum analysis using a graphic level
recorder for display.

DISCUSSION OF RESULTS

CORRELATION OF ACOUSTIC AND DYNAMIC AIRLOAD DATA - PHASE I

Selection of Data for Correlation

The data parameters of the Dynamic Airloads Program selected for correlation with sound levels measured during the subject program either made a direct contribution to the generation of rotor noise or apparently resulted from the same source.

The three microphones, which were mounted externally to the aircraft, recorded the total acoustical output of the rotor system. Although all of the data from each of the microphones were analyzed for all test conditions (as reported in Appendix III), the following octave bands and microphone locations were selected for purposes of technical discussion:

1. ### Rotational Noise - 63 Hz

   This octave band is set by the primary pressure fluctuations caused by thrust torque and blade thickness, commonly called rotational noise, and also by low-frequency components of blade slap.

   Since the two side microphones sense both of these sources, while the nose-boom microphone did not sense blade slap at 63 Hz, the latter is used for all analyses of rotational noise.

2. ### Blade Slap - 250 Hz

   In much of the correlation of blade slap with other parameters of flight, the sound-pressure amplitude of the band-pass filter centered at 250 Hz was used; the following paragraph established the basis for this selection.

   Determination of differences in spectral content of waveforms with highly transient characteristics such as blade slap is a problem which does not readily yield to solution by ordinary means of analysis. As indicated previously, existing graphic level recorders do not have the ability to respond to rise factors* greater than 5; rotor noise rise factors are generally of the order of 15. Wave analyzers, on the other hand, lend themselves to static

---

* Ratio of peak pulse amplitude to width.

22

or quasi-static functions, but the effective tape-slowing techniques which are required for this type of analysis result in loss of quality in the data. Selection of the 250-Hz band as a primary indicator of blade slap was verified by performing a numerical harmonic analysis of a slapping and nonslapping waveform (Figure 9). Figure 10 shows that the greatest difference between the two sets of data is characterized by the range between the 15th and 30th harmonic of blade passage. The 250-Hz octave band is well centered in this range and was therefore selected as a simplified measurement of blade slap. Figure 11 is an octave band analysis of a banging and nonbanging rotor and supports the use of this octave for comparative purposes. Since the left-hand microphone responded to blade-slap noise at 250 Hz more strongly than the other two, because of directivity effects, data in this octave band will be presented for the left-hand position only.

3. Hlgh Frequency - 4,000 Hz

The high-frequency end of the spectrum is set by blade slap, when it occurs, and has a minimum readable level which is a function of wind noise and dynamic component noise. Although these high-frequency blade-noise levels are not as large in amplitude as the fundamental blade-slap frequencies, it is the existence of these higher harmonics which gives the blade bang a characteristic sharp sound which is an indicator of listener response. Here again, data from the left-hand microphones are presented as being the best indicator of blade slap.

Blade Pressure Time History

The primary purpose of the Dynamic Airloads Program was the measurement of rotor airloads. Since rotor noise levels at the microphone positions are simply rotor-generated oscillatory pressures which have propagated from the blade, a correlation of the strength of the source and position of the blades at the generation of the disturbance can be directly obtained from a study of blade-pressure time histories.

One forward and one aft rotor blade were instrumented for the airloads program with 54 surface-mounted pressure gages on each blade. The blades were positioned on the rotors so that the instrumented rear rotor blade immediately followed the instrumented forward blade and thus permitted a comparison of the effects of the wake of the front rotor on the rear. The processing of data has been described in detail in Volume III of Reference 3, but it should be noted that the data shown in the illustrations have a rather low upper frequency limit. This limitation results from the harmonic analysis procedure which

23
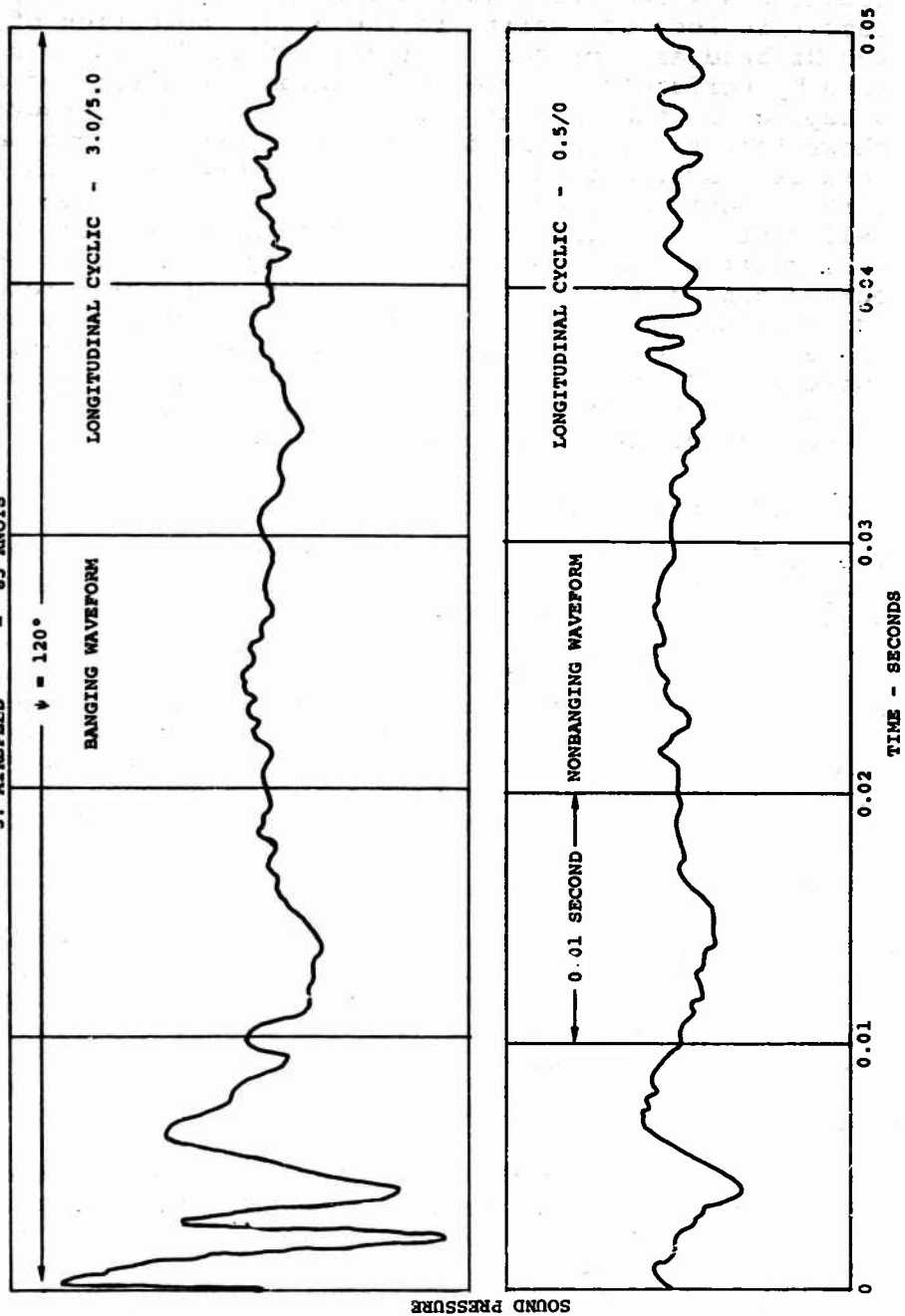
Figure 9. Waveform of Banging and Nonbanging Rotor.

24
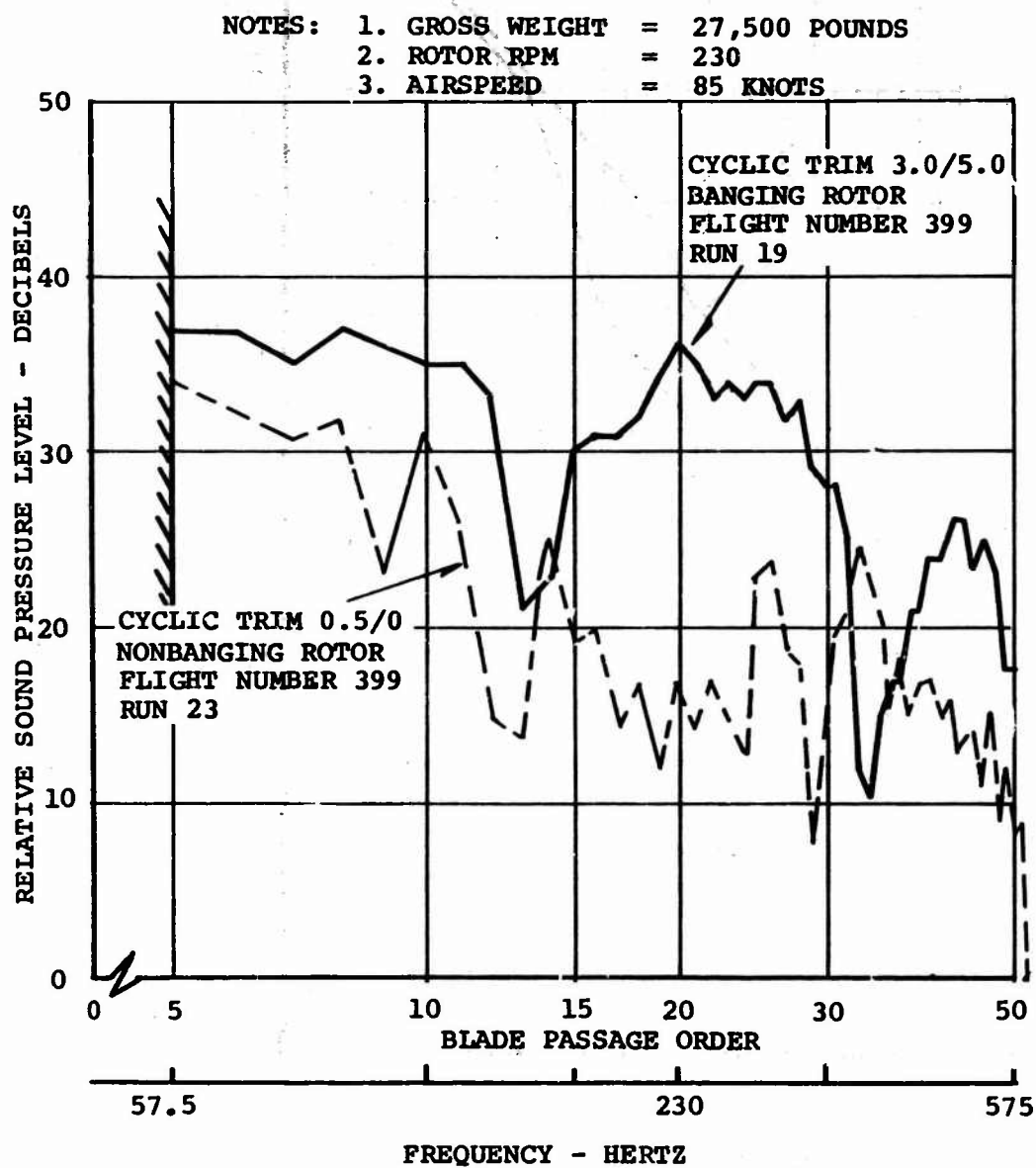
Figure 10. Digital Fourier Analysis of Rotor Blade Noise.

25
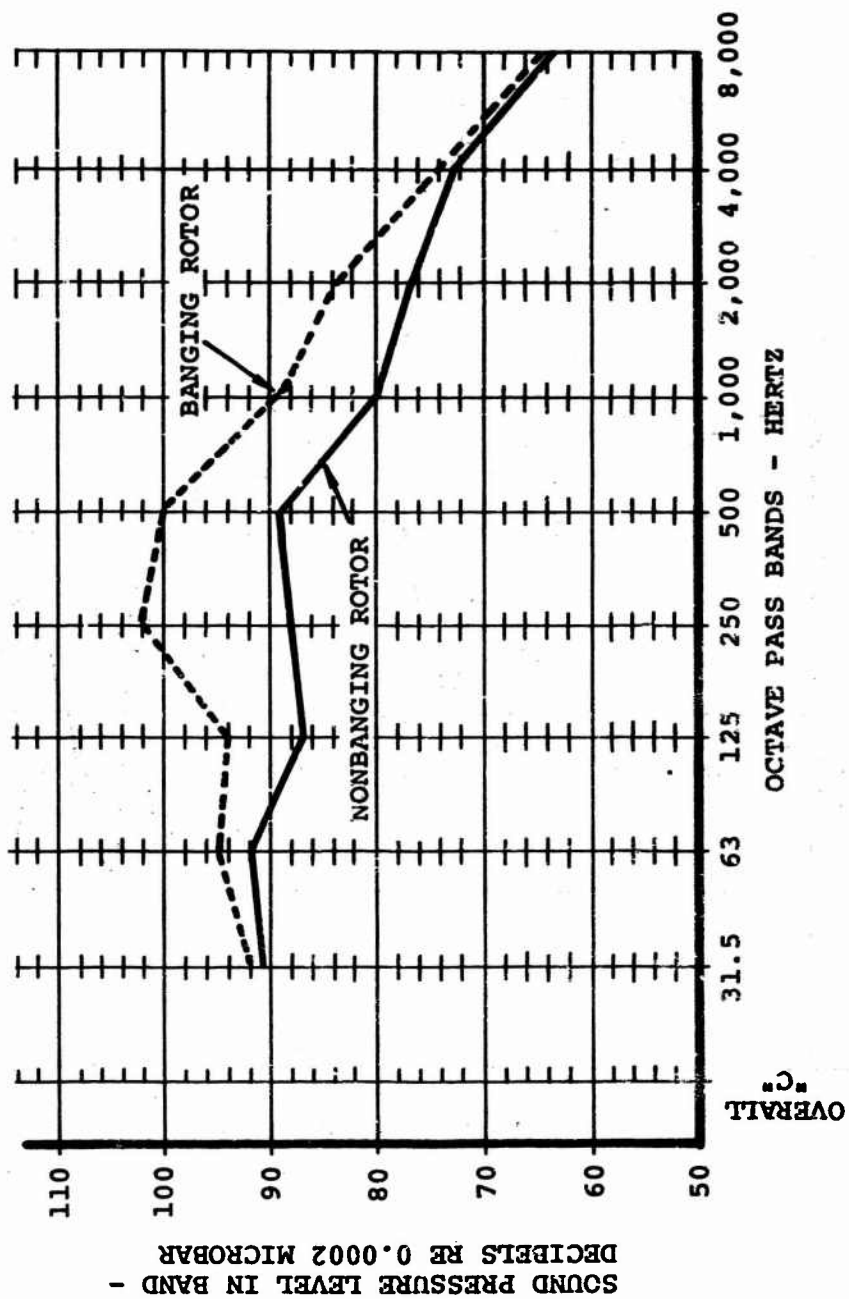
Figure 11. Octave Band Spectra of Helicopter in Forward Flight.

26

digitizes the rotor cycle at a rate of 250 ordinates per second. Since a minimum of four ordinates was utilized to describe any specific waveform, the highest frequency which may be reliably observed was limited to 60 Hz. The digitizing of the pressure waveform was performed for 5 nonconsecutive rotor cycles over a total elapsed period of 20 rotor cycles, as indicated in Figure 8. Nonconsecutive rotor cycles were required since the records were alternately sequenced between forward and aft rotors; transition of rotor sequences occurred between the digitized cycles. The values were then averaged for the five cycles, corrected for phase shift and plotted on an automatic data plotter. The time histories which are illustrated in Figures 12 and 13 report pressures outboard of 0.75R for a forward and aft blade, respectively. Since the largest variations in pressures occur on the aft rotor, a chordwise distribution of time histories is illustrated for that rotor in Figure 14. As would be expected, the leading edge of the blade experiences the largest magnitude low-frequency pressure fluctuation, and all of the pressure data reported herein are either at $X/C = 0.02$ or $X/C = 0.9$, depending upon the availability of complete data for a series of flight records. Figure 15 (Sheets 1 and 2) illustrates forward and aft rotor blade pressures for several airspeeds and two longitudinal trims at 28,500 pounds gross weight. When the aft rotor tip path in the overlap area is trimmed (tilted) forward, as with extended trim (BITF/BITR = 3.0°/5.0°), the planes of the front and rear rotors cross, and the aft rotor intercepts the trailed tip vortex from the front rotor. This effect is particularly noticeable at 43 and 85 knots, where both extended and retracted trims (BITF/BITR = 0.5°/0°) are shown.

Blade Separation

It was noted that the most effective means of changing blade noise was through operation of the longitudinal cyclic trim system. As shown in Figure 16, this system's capability to differentially tilt the rotor disks affords a wide range of tip path separations, with retracted trims opening the gap between tip paths in the overlap region.

The separation of the rotor tip path planes at any rotor azimuth can be predicted from the aircraft geometry if the Fourier coefficients for harmonic blade flapping are known. Figure 17 shows the essential geometry for calculation of rotor blade tip path separation and the rotor azimuth locations used in calculations for the subject program. The height of the blade tip above the fuselage reference plan is established for each rotor. The total blade flapping angle β (with respect to a plane parallel to the horizontal fuselage reference axis and passing through the rotor hub) is defined by

27

$$\beta = a_0 - a_1 \cos \psi - b_1 \sin \psi + i_s \cos \psi \qquad (1)$$

where

a_0, a, and b_1 = harmonic blade-flapping coefficients

i_s = rotor shaft angle with respect to a normal to the fuselage reference plane

ψ = rotor azimuth angle

From this, the tip path separation normal to the free stream may be calculated:

$$H = h \cos \alpha_f = [(R \sin \beta_r + L_r) - (R \sin \beta_f + L_f)] \cos \alpha_f \qquad (2)$$

where

R = blade radius
L = pylon height above the fuselage reference plane
α_f = fuselage angle with respect to the free stream

Measured inputs were utilized for values of longitudinal cyclic trim, the Fourier coefficients were calculated from an existing computer program[6], and the blade separation was determined from equations (1) and (2).

Figure 18 shows the effect of blade separation on a qualitative evaluation of blade noise and reveals that the tendency to bang is a function of the relative blade positions.

In general, there was a lack of nonbanging data recorded since the range of trims specified in the Dynamic Airloads Program did not include many cyclic trim combinations which avoid blade bang. During the Phase II portion of the program, however, a more systematic exploration of the effect of cyclic trim was performed, and these data are shown in Figure 19 for the 200-foot north-side ground microphone. As discussed previously, the 250-Hz band is the strongest indication of blade slap due to the interaction of a rotor blade and a trailed vortex. Examination of the 250-Hz chart of Figure 19 clearly shows the strong effect of blade separation.

28

NOTES: 1. GROSS WEIGHT = 27,500 POUNDS
2. ROTOR RPM = 230
3. TRUE AIRSPEED = 109 KNOTS
4. STANDARD TIP
5. FLIGHT NUMBER 399, RUN 1
6. x/c = 0.09

r/R = 0.98

0.95

0.90

BLADE PRESSURE - PSID

29
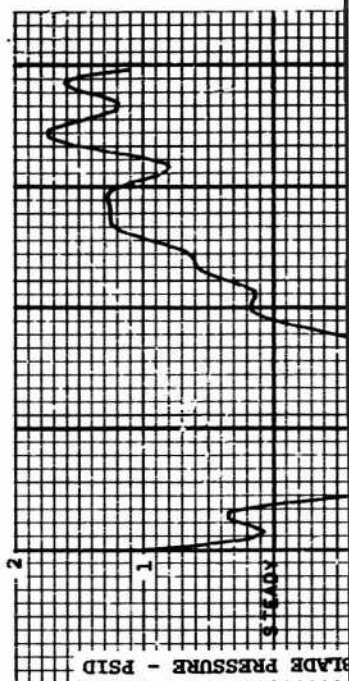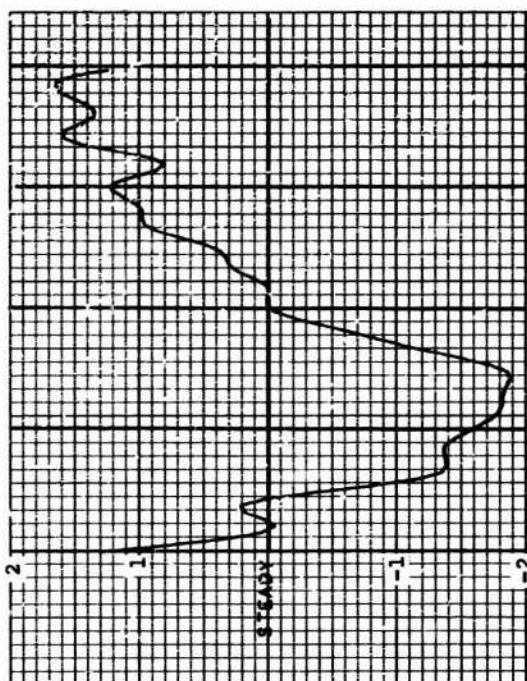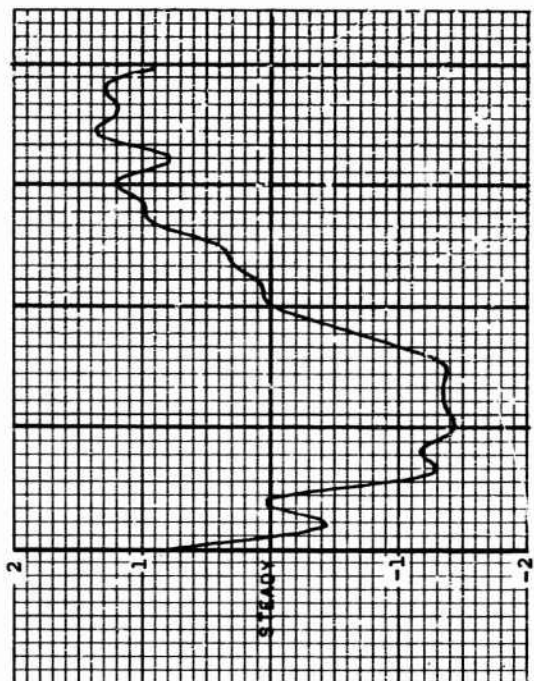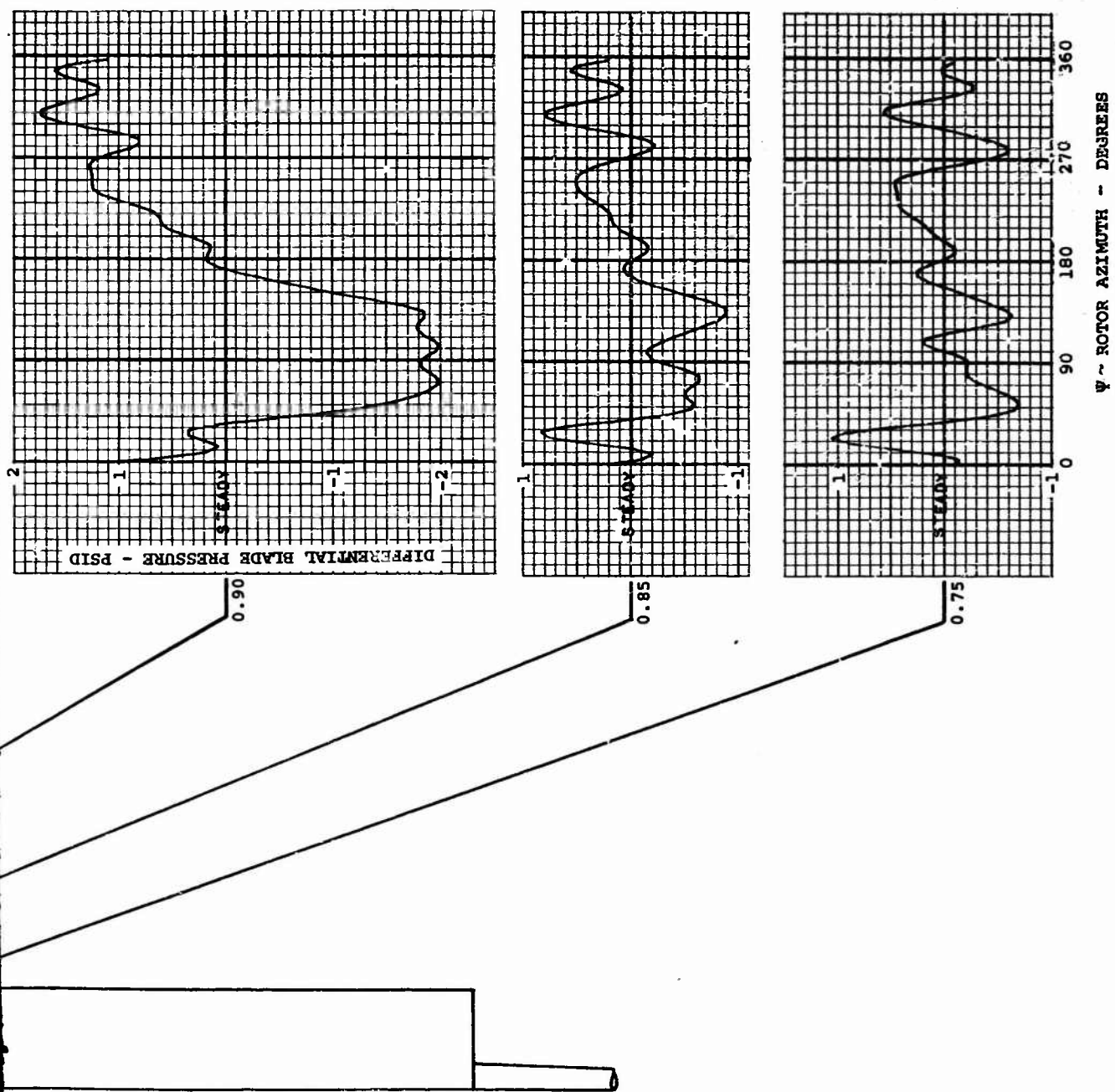
Figure 12. Spanwise Differential Pressure Time History – Forward Rotor.
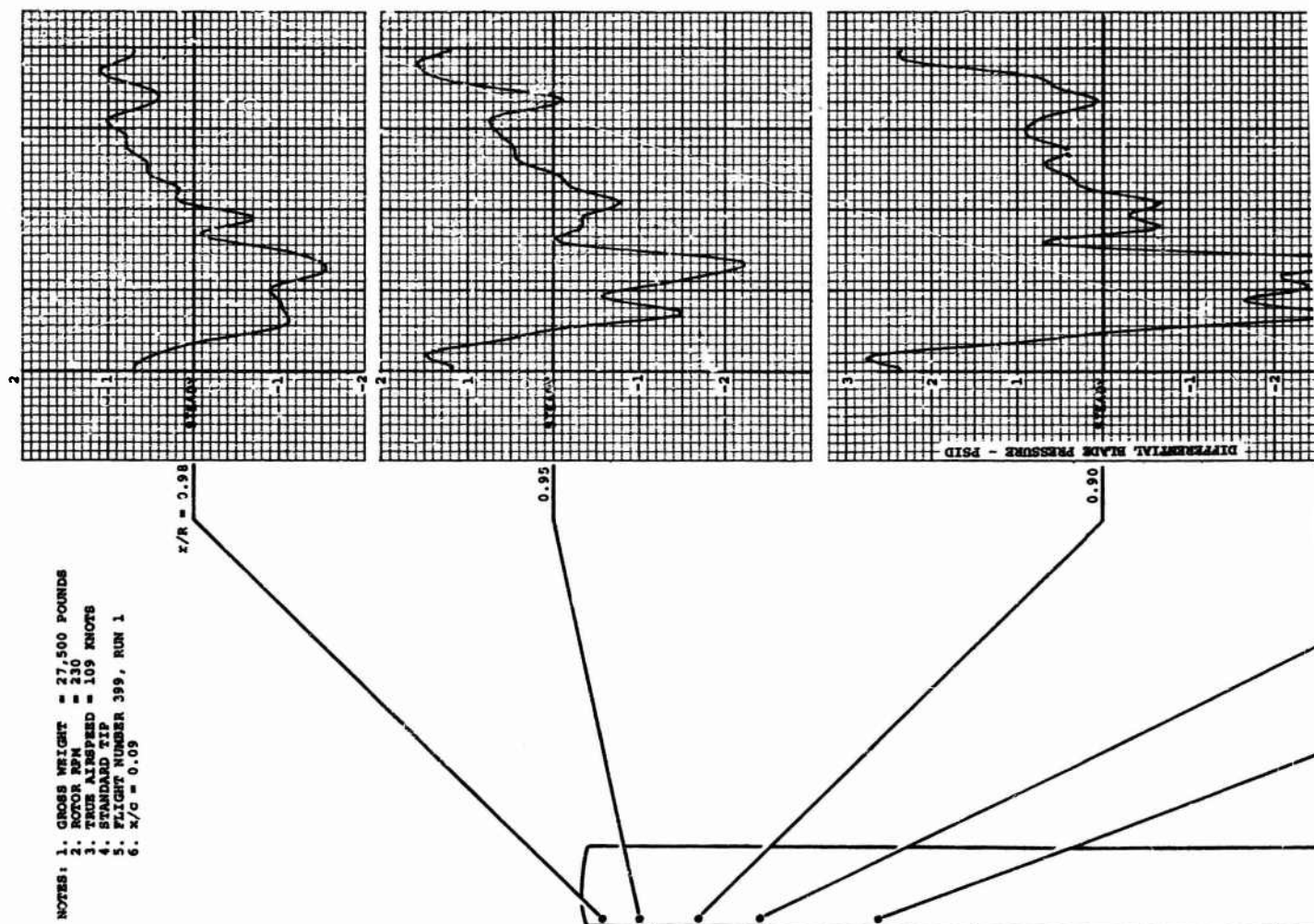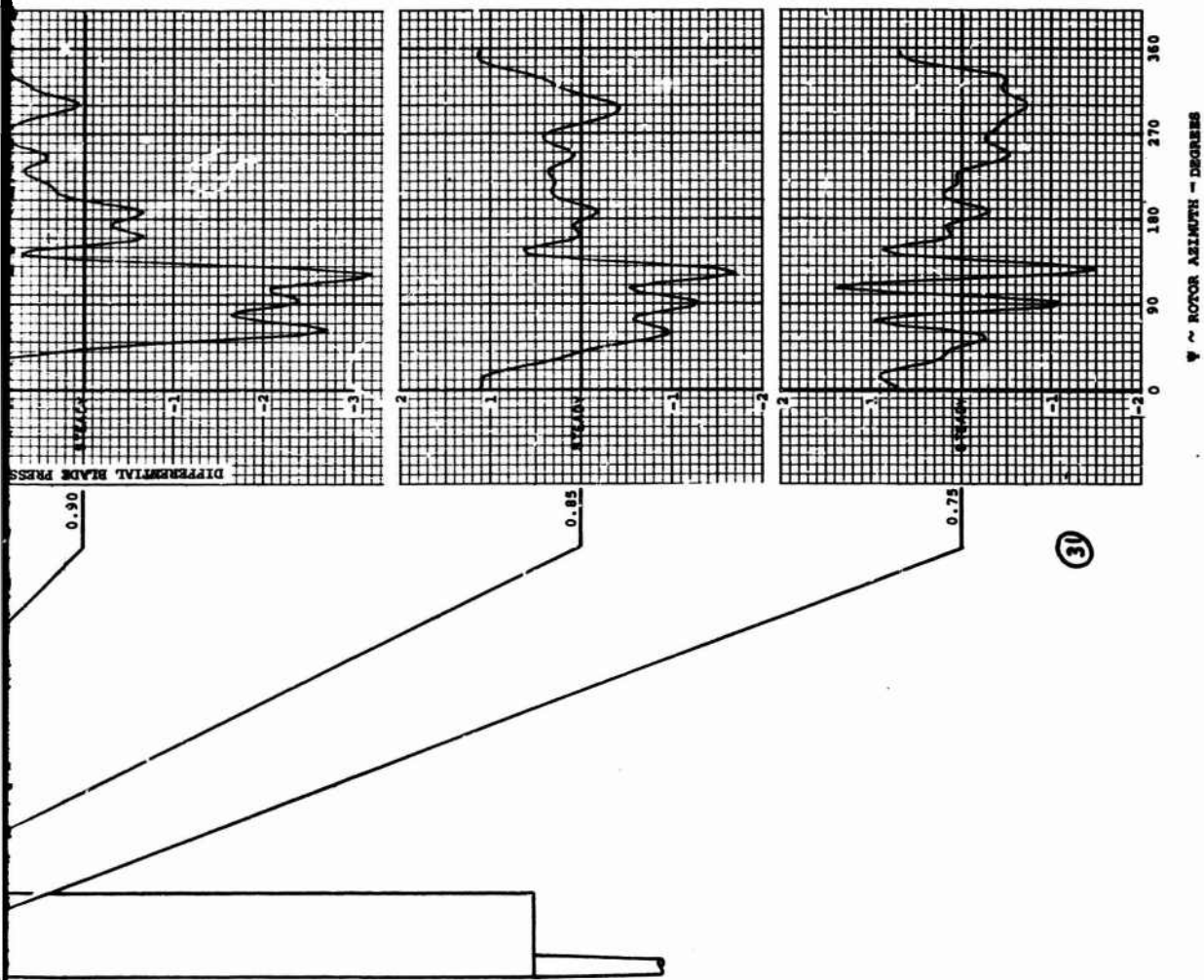
Figure 13. Spanwise Differential Pressure Time History -
Aft Rotor.

NOTES: 1. GROSS WEIGHT = 27,500 POUNDS
2. ROTOR RPM = 230
3. TRUE AIRSPEED = 109 KNOTS
4. STANDARD TIP
5. FLIGHT NUMBER 399, RUN 1
6. r/R = 0.75

x/c = 0.02

0.09

DIFFERENTIAL BLADE PRESSURE - PSID

A

33
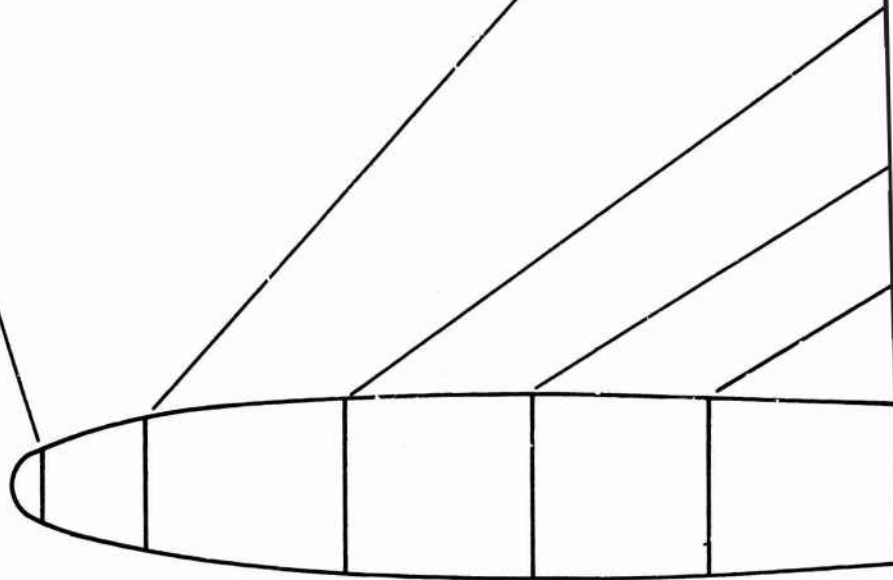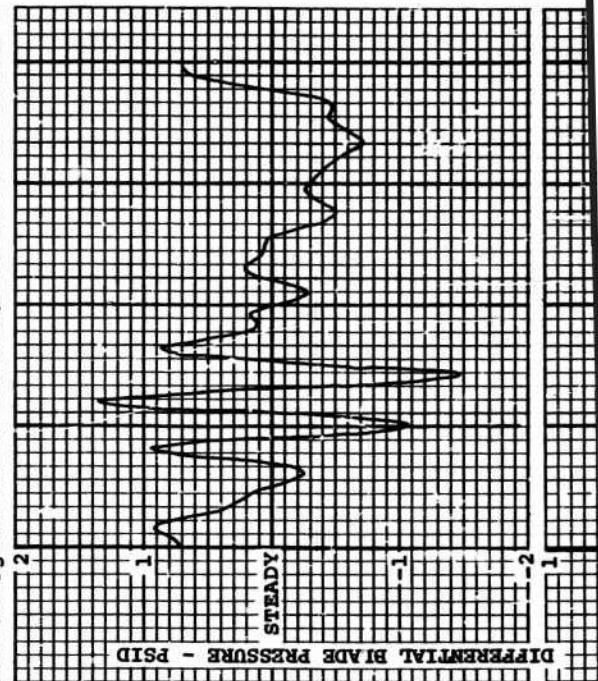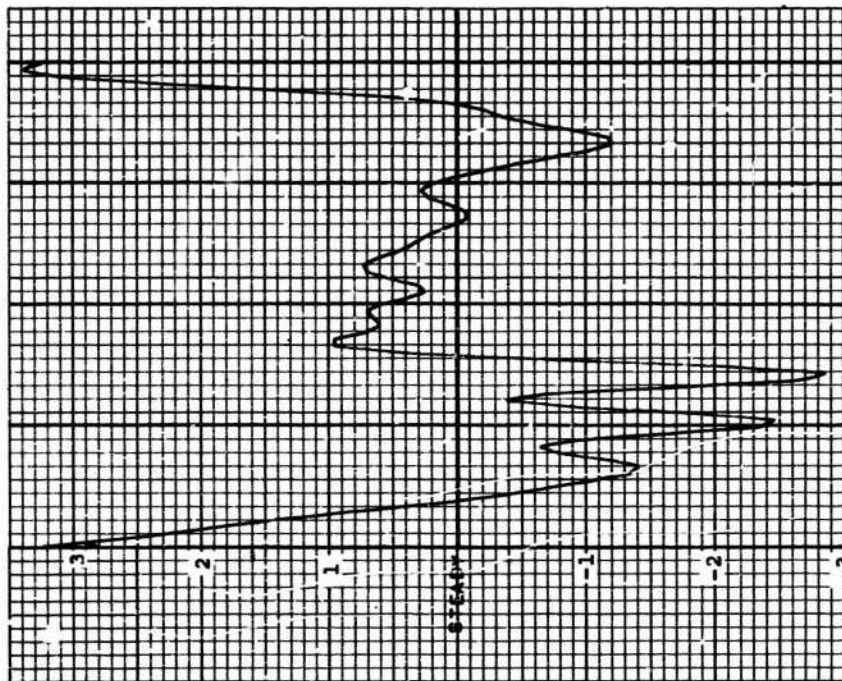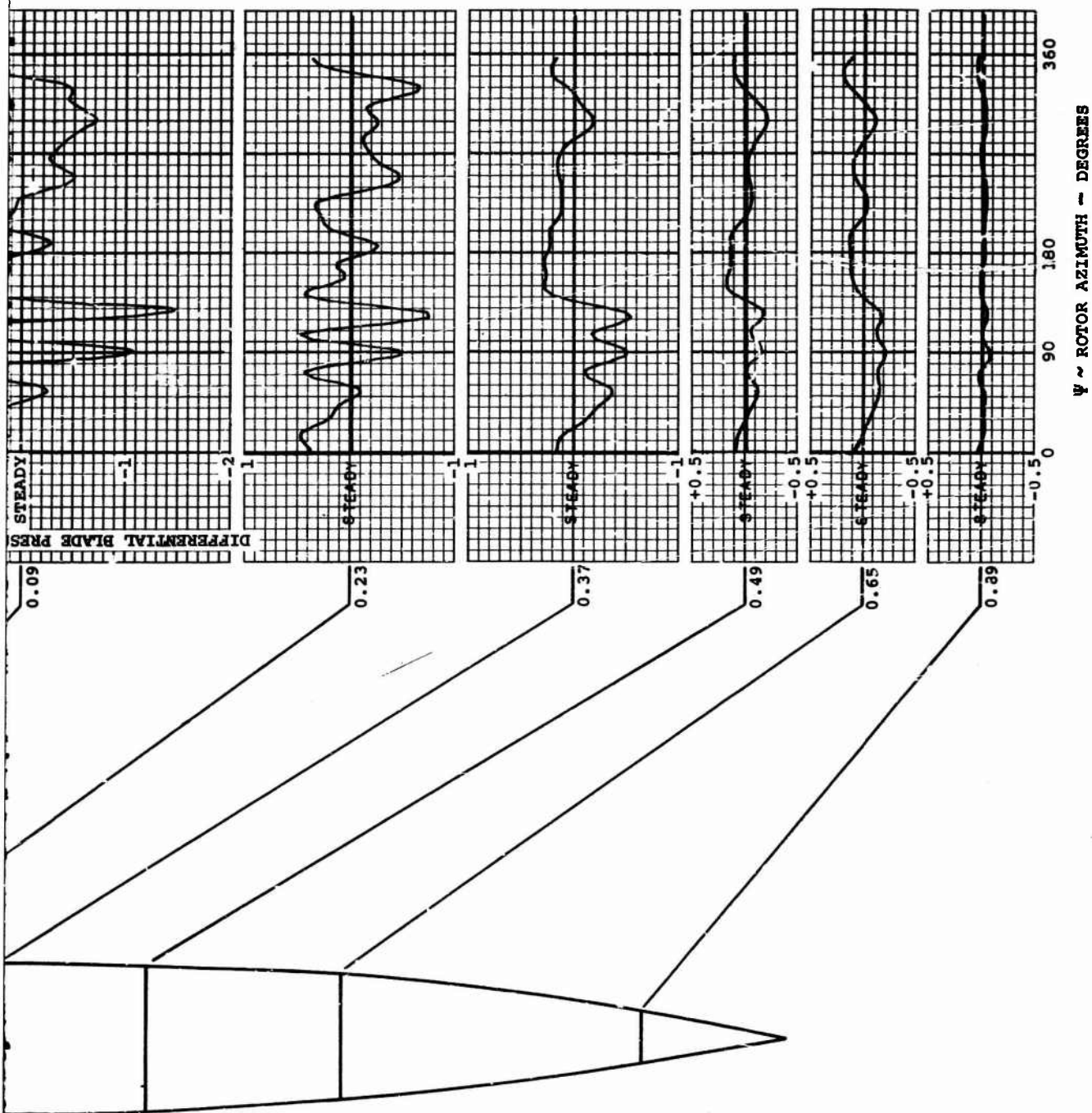
Figure 14. Chordwise Differential Pressure Distribution - Aft Rotor.

TRUE AIRSPEED = 0
$BIT_F/BIT_R = 3.0/5.0$

TRUE AIRSPEED = 43 KNOTS
$BIT_F/BIT_R = 3.0/5.0$

TRUE AIRSPEED = 85 KNOTS
$BIT_F/BIT_R = 3.0/5.0$

TRUE AIRSPEED = 0
$BIT_F/BIT_R = 0.5/0.0$
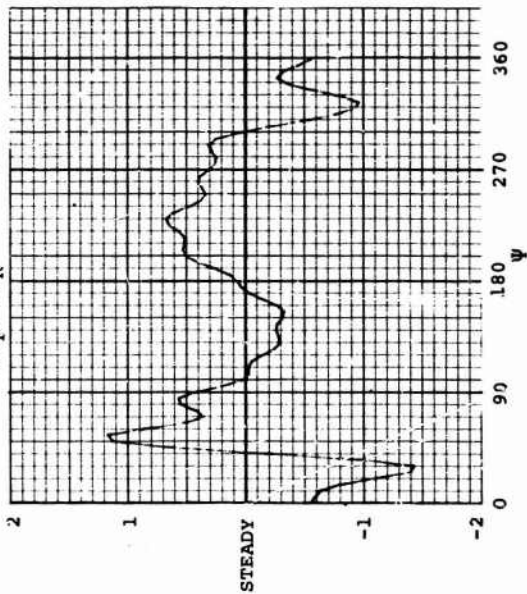
TRUE AIRSPEED = 43 KNOTS
$BIT_F/BIT_R = 0.5/0.0$
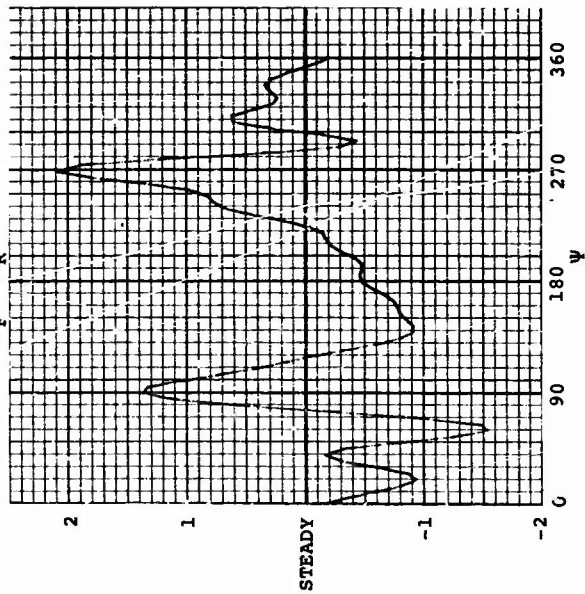
TRUE AIRSPEED = 85 KNOTS
$BIT_F/BIT_R = 0.5/0.0$
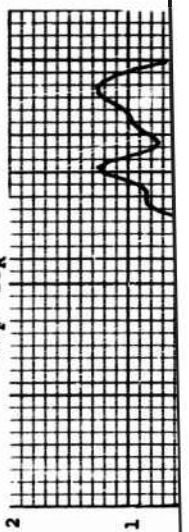
DIFFERENTIAL BLADE PRESSURE - PSID

DIFFERENTIAL BLADE PRESSURE - PSID

35

Figure 15. Differential Blade Pressure Time History – Forward Rotor (Sheet 1 of 2).
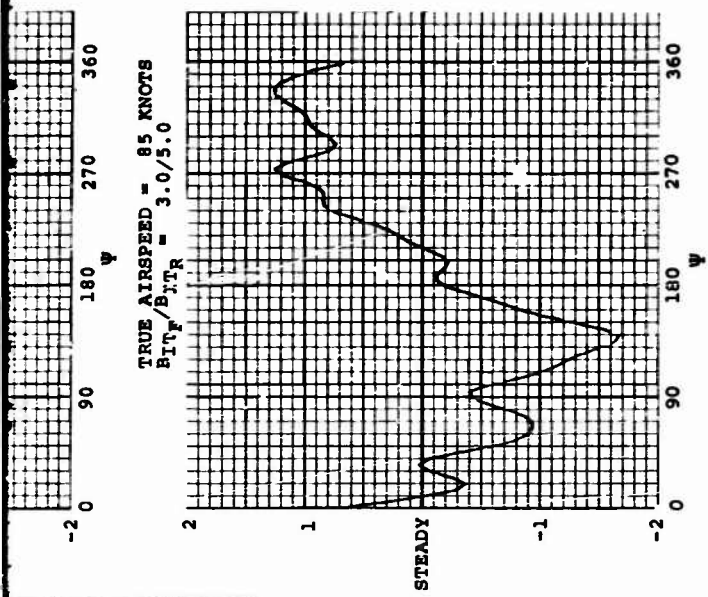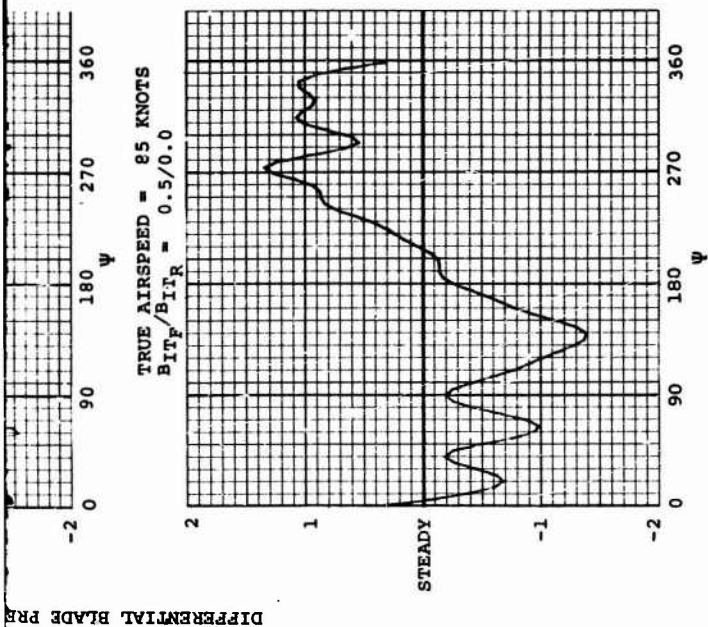
NOTES: 1. ψ = ROTOR AZIMUTH IN DEGREES
2. GROSS WEIGHT = 27,500 POUNDS
3. ROTOR RPM = 230
4. r/R = 0.98
5. x/c = 0.09
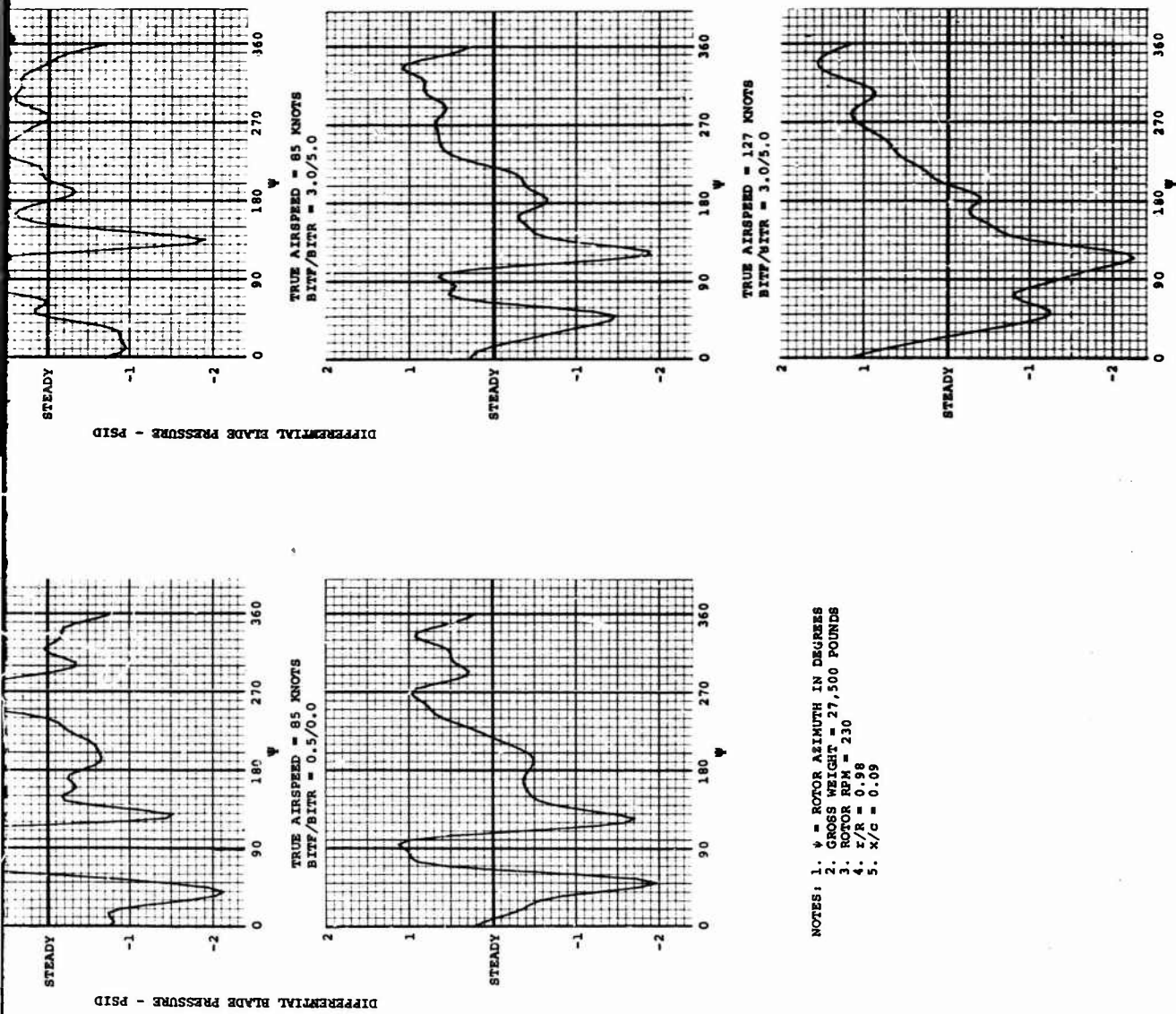
Figure 15. Differential Blade Pressure Time History –
Aft Rotor (Sheet 2 of 2).

RETRACTED TRIM SEPARATION

EXTENDED TRIM SEPARATION
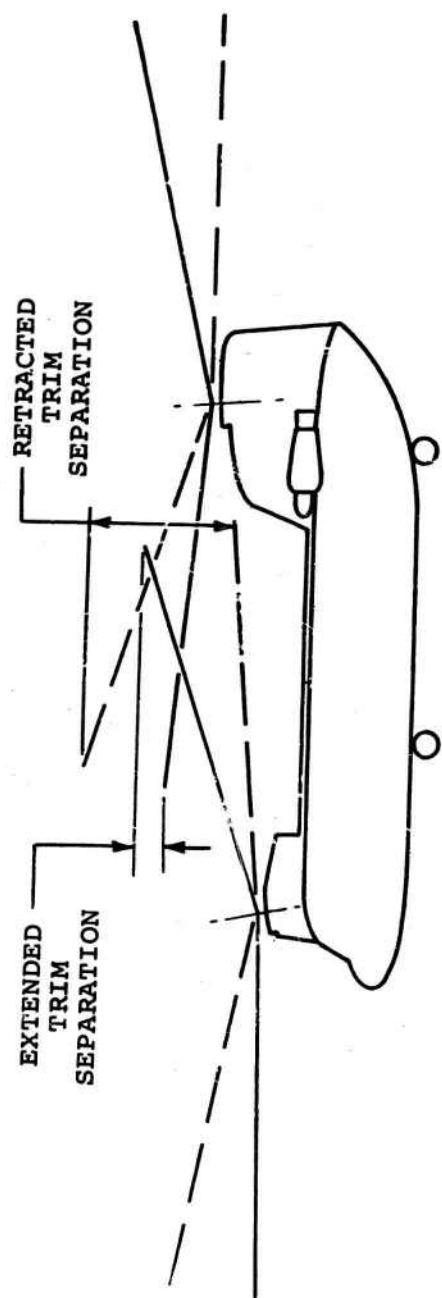
Figure 16. Effect of Cyclic Trim on Rotor Separation.
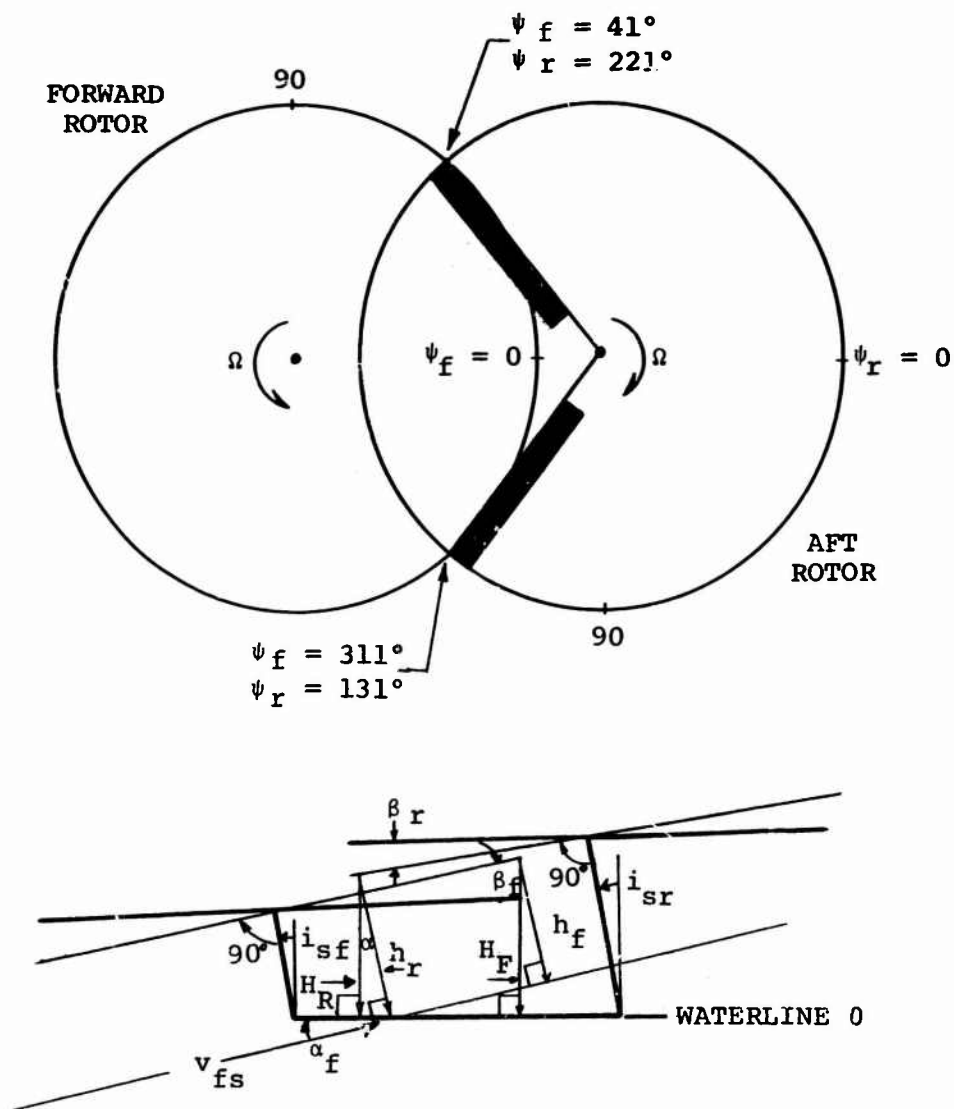
Figure 17. Geometry of CH-47A for Calculation of Blade Separation.

40
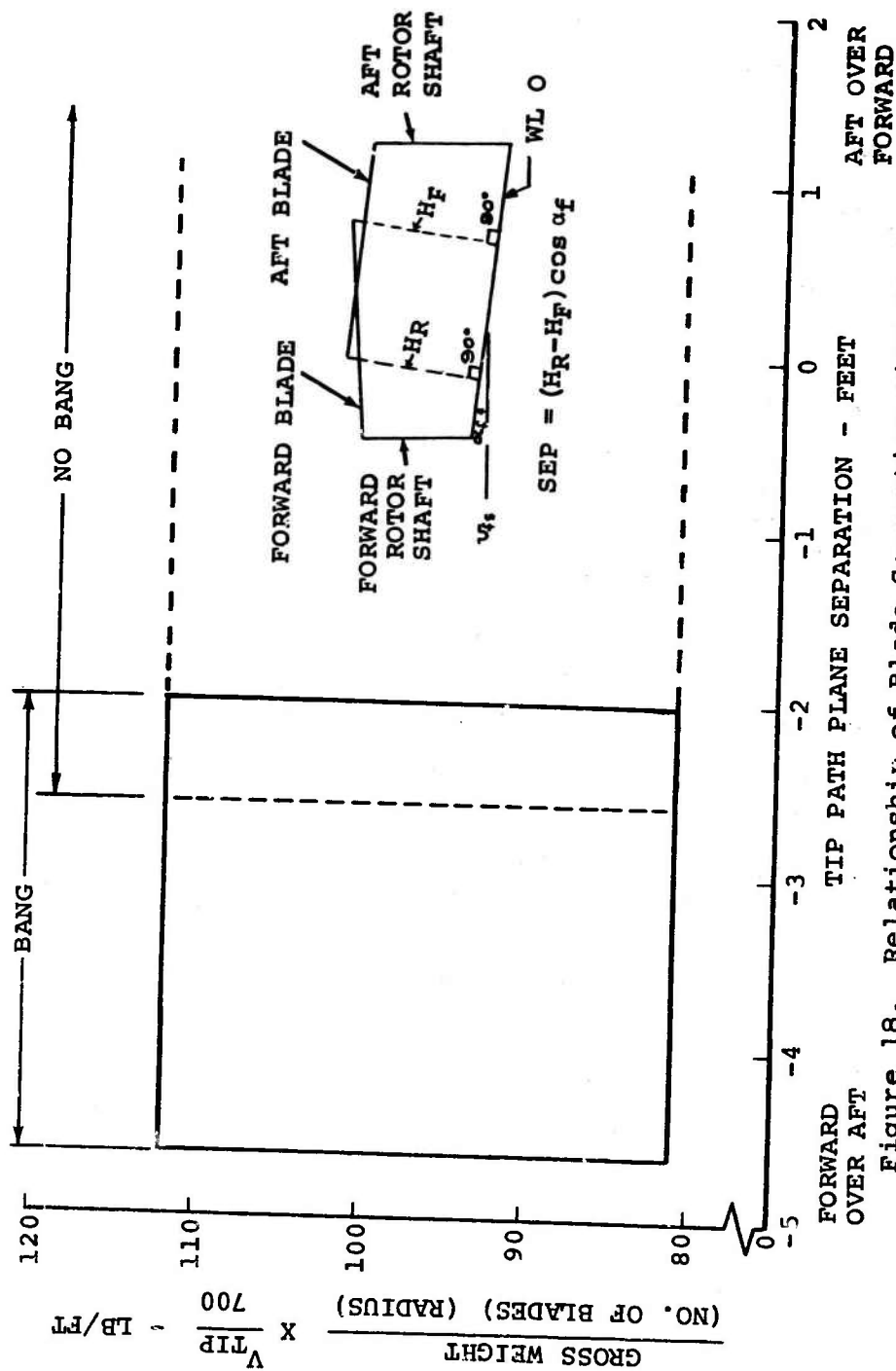
Figure 18. Relationship of Blade Separation With Blade Loading and Tip Speed.

The parameter of distance between blades, in itself, is not a cause of rotor noise, but rather an indicator. There is strong evidence that the interaction between a rotor blade and a trailed tip vortex may be the origin of the rapid pressure rises associated with blade bang. On this assumption, analyses were developed which describe the distance between blade and vortex and correlate it with rotor noise.

This method, which was developed by the Vertol Division of Boeing, is described in Appendix I. Figure 20 shows the application of this method to a slapping and nonslapping condition on the CH-47A. The banging condition, which shows calculated blade-vortex intersections, is Run 4 of Flight 395 of this program; the nonbanging case, which does not show intersection, was selected from other company data. Thus, the only significant difference between the runs was cyclic trim.

A comparison of the waveforms sensed by the microphones for a banging condition is shown in Figure 21. Also shown is an oscillograph stripout of the output of a 95-percent radius blade pressure pickup for a similar flight condition. The high-frequency cutoff of the pressure pickup precludes any direct visual comparison, since the high-frequency content (about 1,600 Hz) of the microphone records is what causes the sharply spiked waveforms.

Comparison of the left-hand and right-hand airborne microphones dramatically illustrates the extremely directional characteristics of the blade bang and shows the basis of selection of the left-hand microphone as the more significant.

The difference between left-hand airborne-to-ground and between nearer and farther ground microphones simply shows the degradation in high-frequency sound experienced during propagation through the atmosphere. In each case the playback attenuation was adjusted to give a good amplitude in order to examine waveform.

Directivity of Hovering CH-47A

Although longitudinal cyclic is not normally used to trim the aircraft below airspeeds of 80 knots, it was useful for test purposes to investigate the extent to which tip path plane position would be effective in modifying rotor bang at this airspeed. It was known that a hovering aircraft trimmed to BITF/BITR = 3.0/5.0 degrees operated at a condition which produced rotor bang, and that at a longitudonal cyclic trim of BITF/BITR = 0.5/0.0 degrees, the rotor did not bang. The directional characteristics of the CH-47A are illustrated in Figure 22 for these two longitudinal cyclic trim positions. Consider first the directivity of the nonbanging rotor.

42
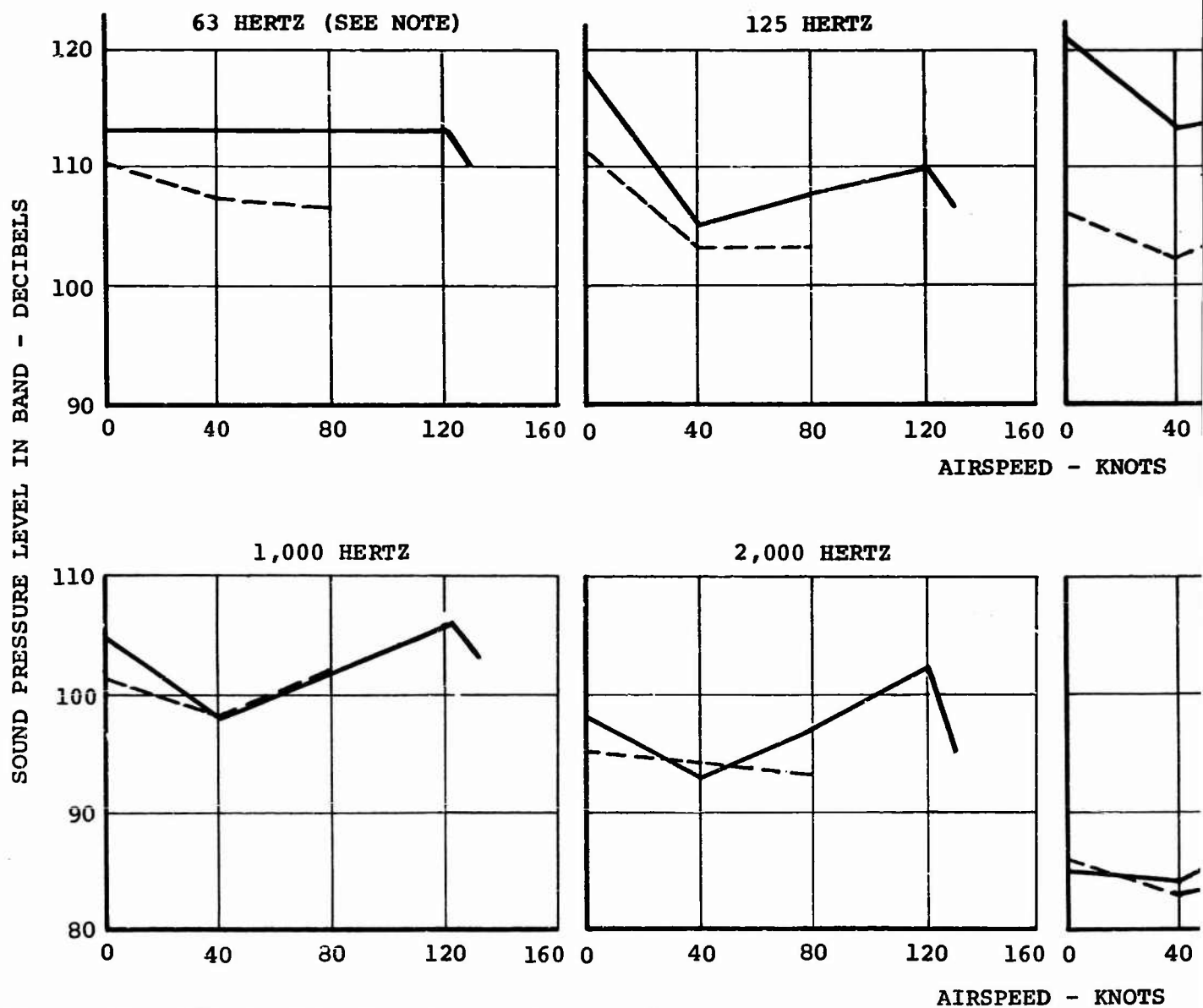
Figure 19. Effect of Cyclic Trim on Rotor Noise.

250 HERTZ

500 HERTZ

120   160   0   40   80   120   160 0   40   80   120   160

AIRSPEED - KNOTS

4,000 HERTZ

120   160   0   40   80   120   16
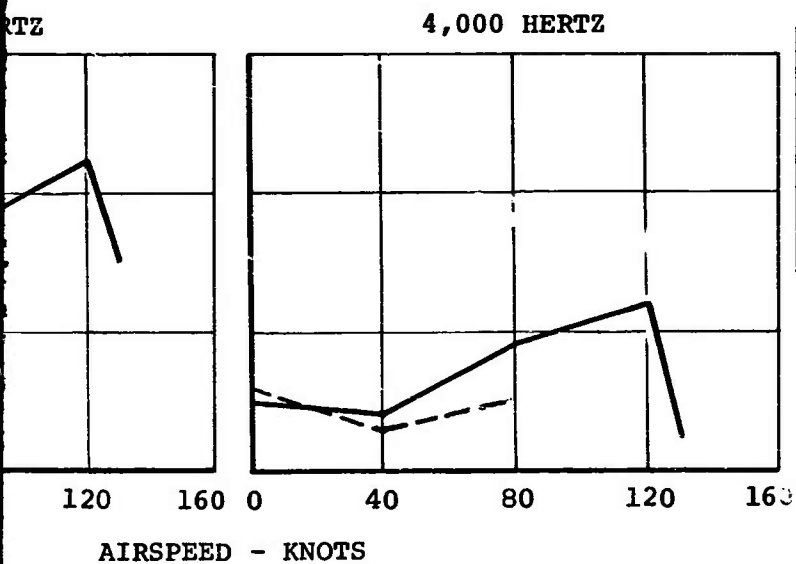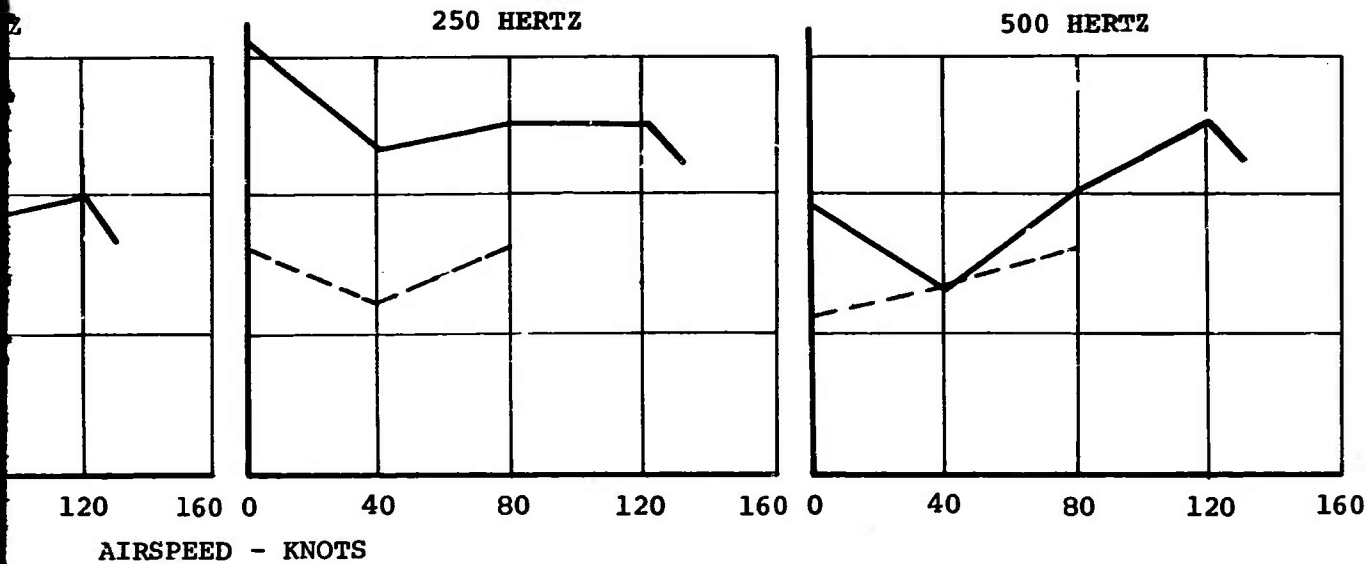
AIRSPEED - KNOTS

LEGEND		
LINE TYPE	TRIM	BITF/BITR
————	EXTENDED	3.0/5.C
- - - -	RETRACTED	0.5/0.0

NOTE: OCTAVE BAND CENTER
FREQUENCY; GIVEN
FOR EACH CURVE.

B
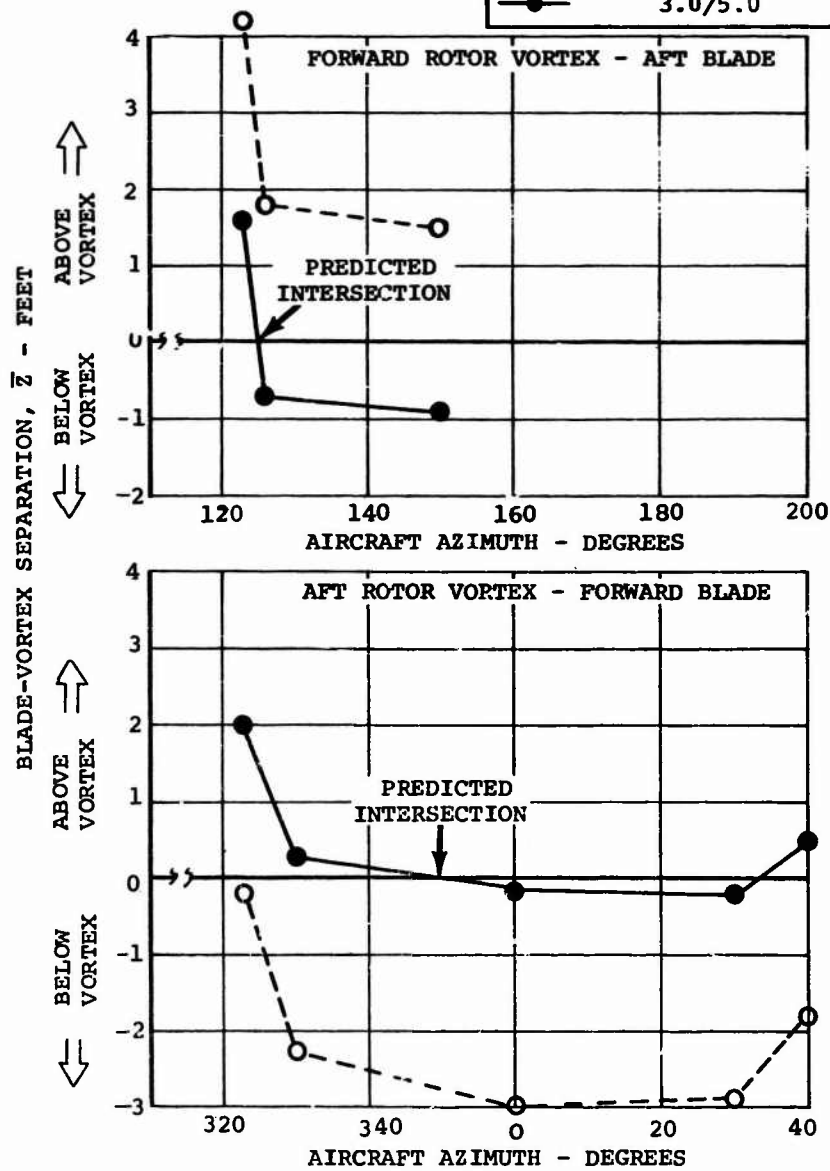
Figure 20. Predicted Blade-Vortex Separations.

45
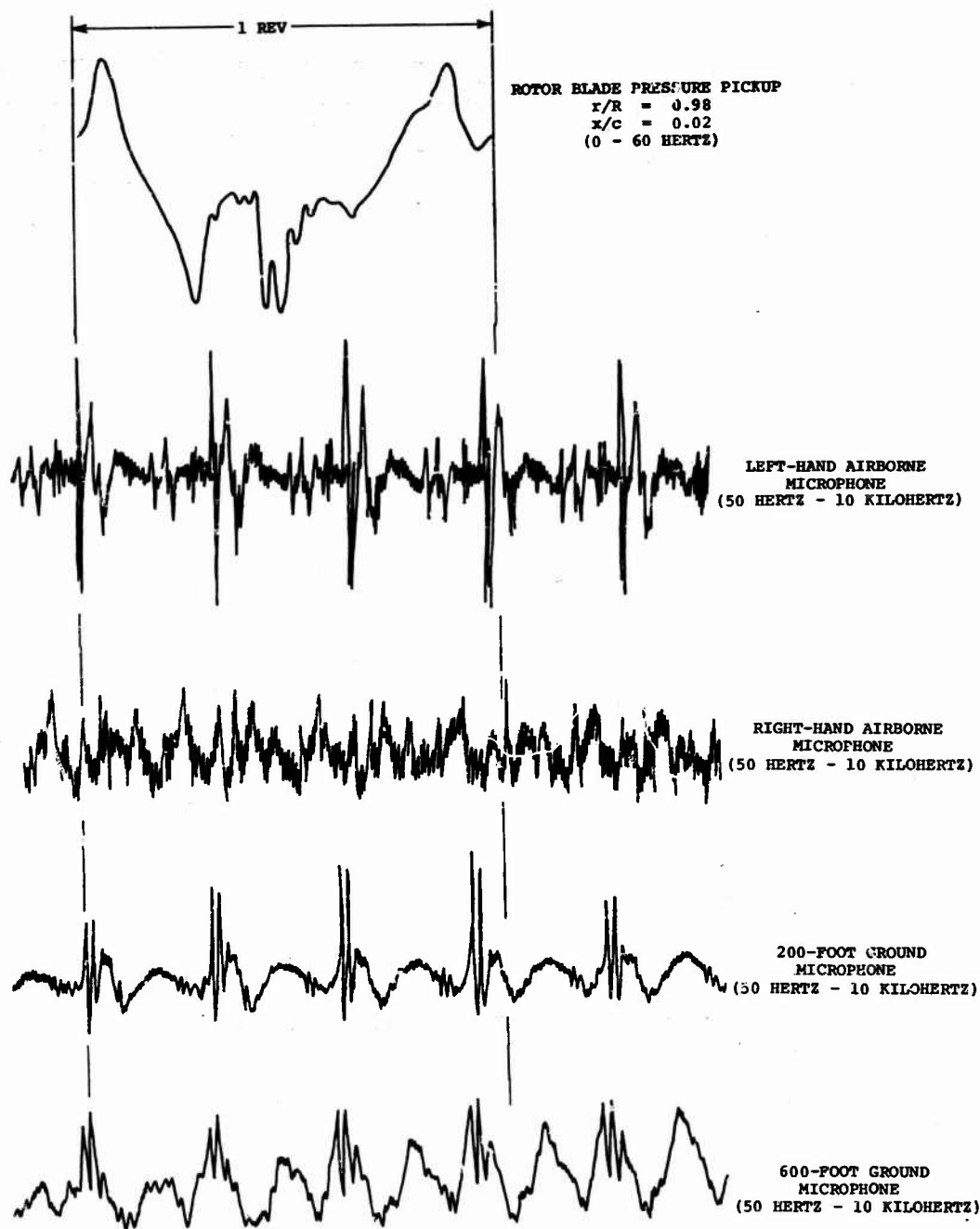
Figure 21. Comparison of Rotor Noise Waveforms.

46
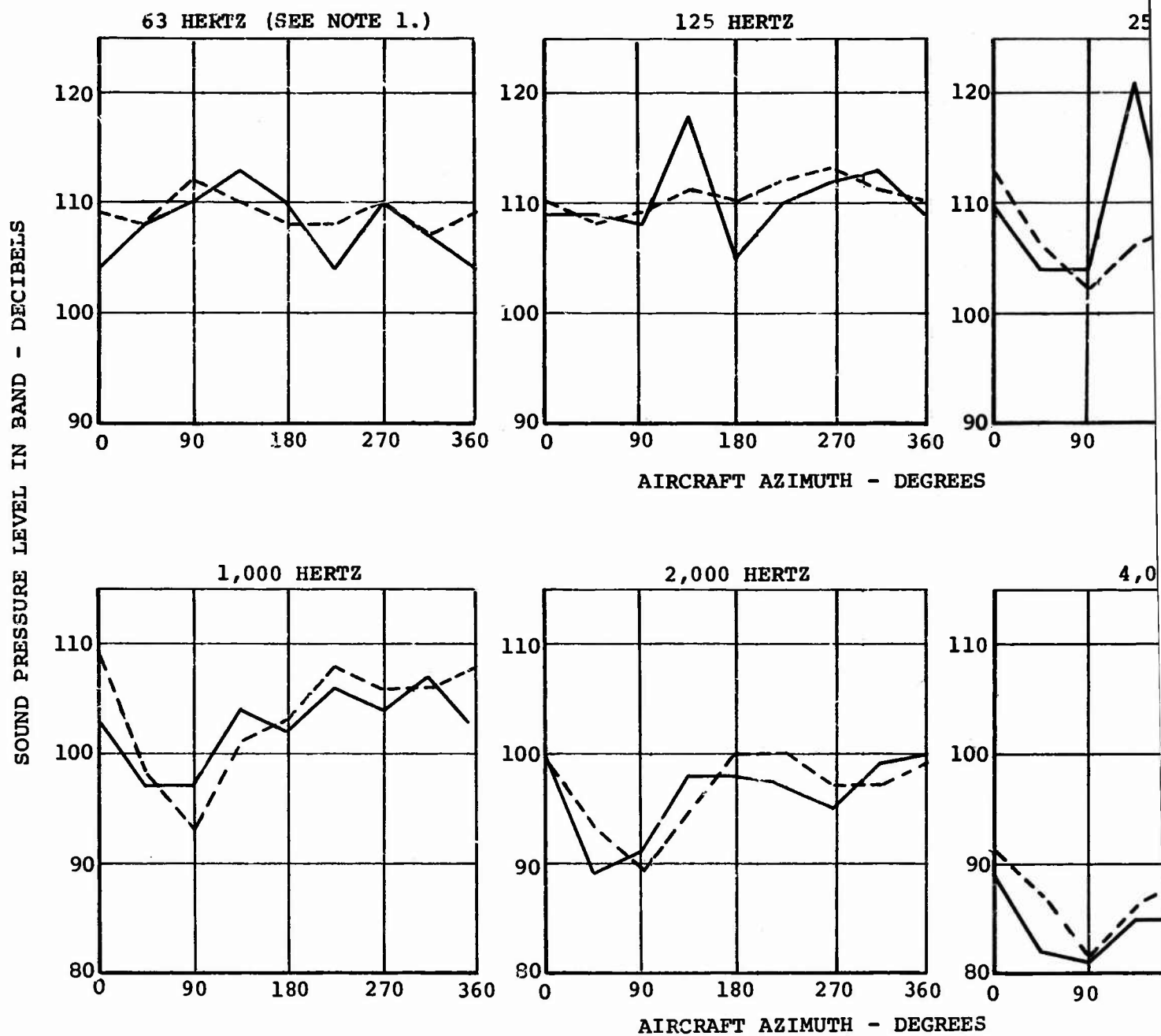
Figure 22. Directional Characteristics of Hovering CH-47A.

47

250 HERTZ

500 HERTZ

DEGREES

4,000 HERTZ

DEGREES
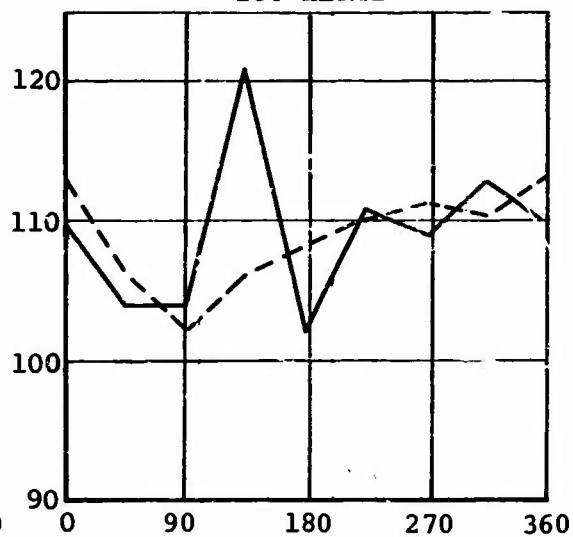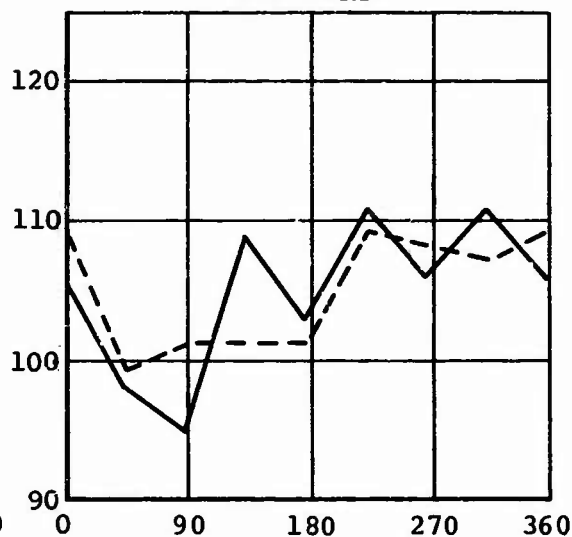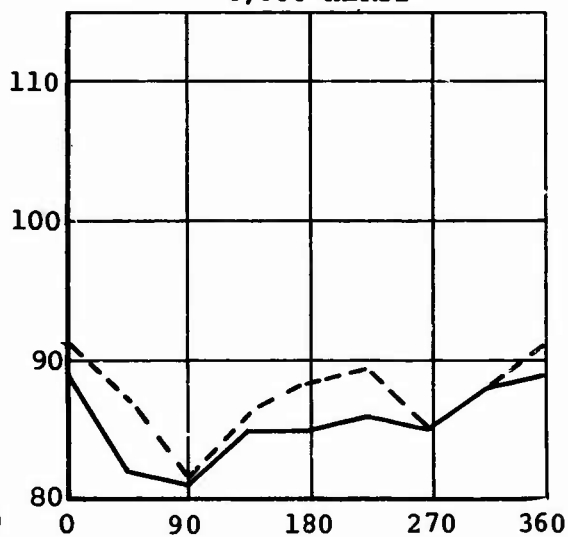
LEGEND		
LINE TYPE	BITF/BITR	CONDITION
———	3.0/5.0	BANGING
------	0.5/0.0	NONBANGING

NOTES:
1. OCTAVE BAND CENTER FREQUENCY; GIVEN FOR EACH CURVE.
2. GROSS WEIGHT = 27,500 POUNDS
3. ROTOR RPM = 230
4. FLIGHT NUMBER 399

B

1.   Retracted Trim

Although measurements were taken at both 200-foot and 600-foot radii, the trends in each case are sufficiently similar to be corroborating. For both extended and retracted trim, the discussion is based on measurements at the 200-foot radius since distance tends to exaggerate anomalies in the data. Distribution and propagation of low frequencies (63, 125 Hz) are generally constant in all directions. Beginning at 250 Hz, a trend toward lower sound pressure levels from 45 degrees to 180 degrees azimuth is observed and continues through the high-frequency end of the spectra. No verified theory currently exists to explain this distribution.

2.   Extended Trim

The CH-47A in hover with extended longitudinal cyclic trim displays high noise levels (rotor bang) over its entire gross weight range. The most notable characteristic of the data with standard tips is the high noise level at the 135-degree azimuth position at 250 Hz. It is 16 to 18 db higher than the adjacent azimuth locations. This characteristic is also noted at a lower frequency (125 Hz) and a higher frequency (500 Hz).

The extremely sharp definition of azimuth corresponding to the blade bang lends further credence to the theory that blade bang arises from the interactions between rotor blades and shed tip vortices at a discrete location rather than from a source which is continuously varying around the azimuth.

Correlation With Other Parameters

No significant correlation was obtained between measured sound pressure level and the following parameters:

> Gross Weight
> Airspeed
> Advancing Tip Speed
> Sideslip Angle

This is probably due to a combination of low sensitivity of noise to these parameters over the range of variation obtainable on the aircraft, and to the overpowering effect of blade-vortex intersections, which, when they occur, mask effects which might otherwise be observable.

It was also found that no significant correlation could be established between sound pressure level and the following:

49

Pitch Link Load (Forward and Aft)
Cockpit Vibration (Vertical and Lateral)
Cabin Vibration (Vertical and Lateral)

In this case, the indication is that the causes of these phenomena and the rotor noise are mutually independent.

EVALUATION OF THE POROUS TIP - PHASE II

Rotor Noise - Hover

In hover, the porous tip proved to be extremely effective in reducing the intensity of rotor slap when it occurred. From the 200-foot microphone data, this is clearly shown in Figure 23 at the critical azimuth of 135 degrees. With a retracted trim (Figure 24), the effect is less pronounced since vortex interaction effects play a less important role.

It is notable that no azimuth position for any hovering test point displayed more than a moderate rotor slap with the porous tip. However, the porous tip did display somewhat higher sound levels above 2,000 Hz than the standard tip. This may be due to the cylindrical ports in the tip which are open-ended pipes of wavelength $\lambda = 2L$.

For the CH-47A rotor blade which has a chord of 1.92 feet and an NACA 0012 section, the maximum port length is

$$L_{max} = c \cdot t/c = 1.92(0.12) = 0.23 \text{ ft}$$

where t/c is blade thickness ratio.

The corresponding wavelength of a resonant port is

$$\lambda = 2L = 2(0.23) = 0.46 \text{ ft}$$

with a frequency of

$$f = \frac{C}{\lambda} = \frac{1,125}{0.46} = 2,450 \text{ Hz}.$$

Frequencies associated with other port lengths in the tip range up to 9,750 Hz for the shortest wavelength, and the illustrations for the porous tip hovering cases reflect this increase in sound level at 2 kHz and 4 kHz. In general, the porous tips tend to have lower sound pressure amplitudes in the low frequencies than the standard tips (see Figure 25). It was noted that when the local flow over the tip was normal to the axis of the port, as in flat pitch during ground idle conditions, excitation of standing waves in the tubular ports was particularly noticeable. When the blade angle of attack was increased to that required for hovering, these standing waves were virtually eliminated. A comparison of noise levels during flat pitch and hover is shown in Figure 25.

50
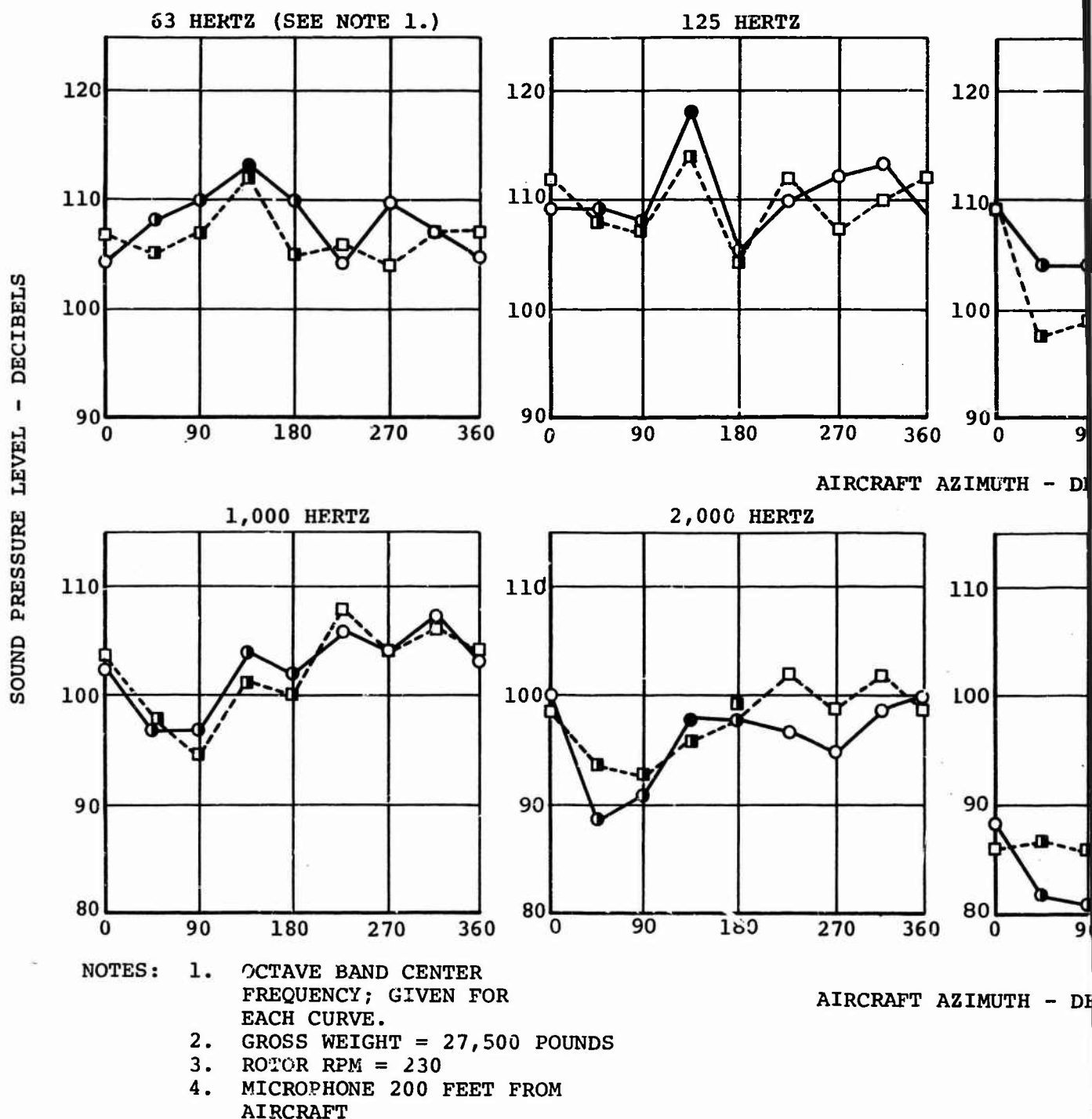
Figure 23. Comparison of Standard and Porous Tips in
Hover - Extended Trim.

NOTES: 1. OCTAVE BAND CENTER
FREQUENCY; GIVEN FOR
EACH CURVE.
2. GROSS WEIGHT = 27,500 POUNDS
3. ROTOR RPM = 230
4. MICROPHONE 200 FEET FROM
AIRCRAFT

51

250 HERTZ

500 HERTZ

4,000 HERTZ

IRCRAFT AZIMUTH - DEGREES

IRCRAFT AZIMUTH - DEGREES

FORWARD

0°

270° ——————————— 90°

1 ƕ0°

VIEW LOOKING DOWN

LEGEND			
SYMBOL	SUBJECTIVE RATING	LINE TYPE	TIP CONFIGURATION
O ☐	NONBANGING	————	STANDARD
● ■	HEAVY BANGING	-----	POROUS
◐ ◪	INTERMEDIATE BANGING		

NOTES: 1. OCTAVE BAND CENTER
FREQUENCY; GIVEN FOR
EACH CURVE.
2. GROSS WEIGHT = 27,500 POUNDS
3. ROTOR RPM = 230
4. MICROPHONE 200 FEET FROM
AIRCRAFT
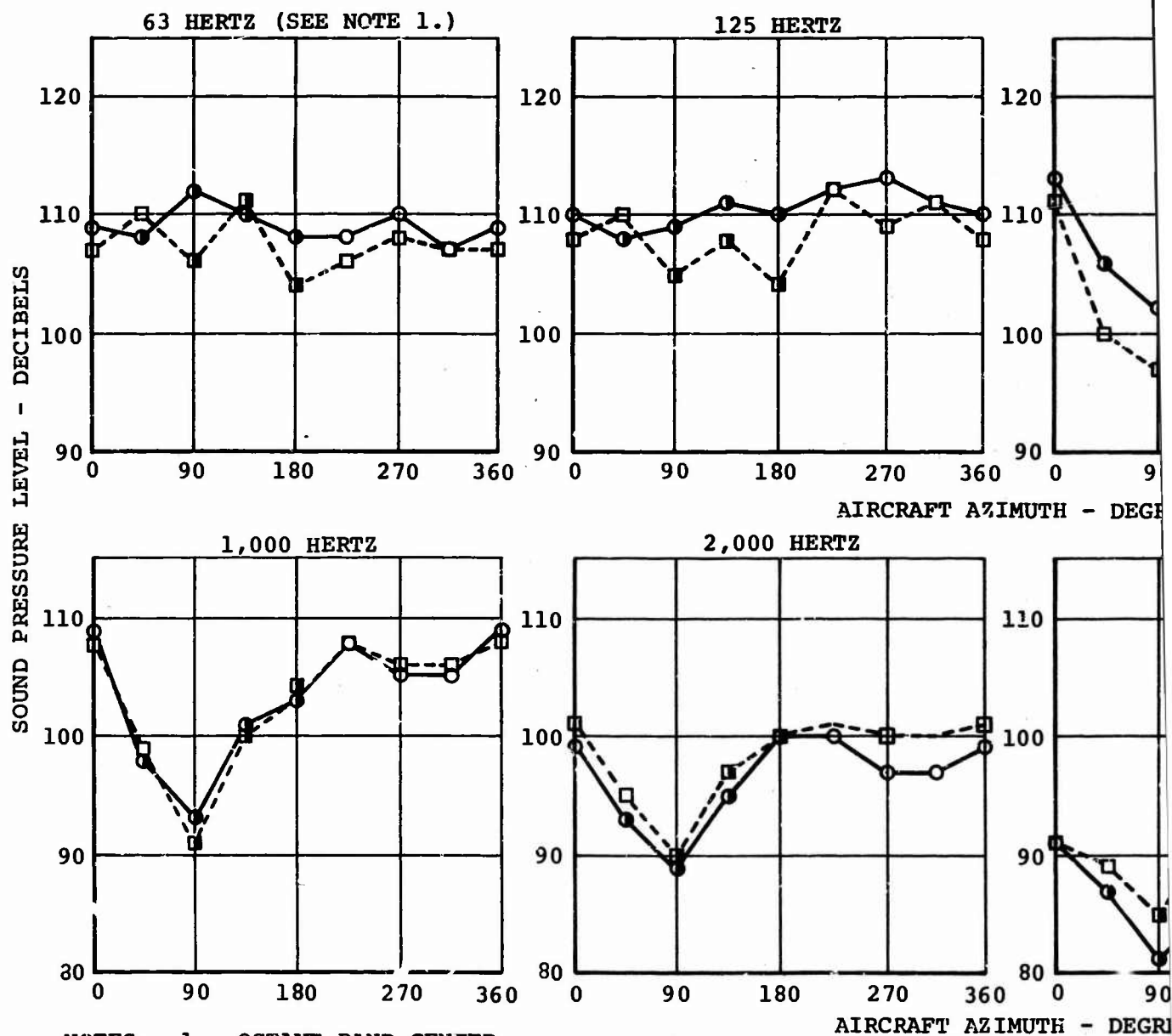
Figure 24. Comparison of Standard and Porous Tips in
Hover - Retracted Trim.

53

250 HERTZ

500 HERTZ

4,000 HERTZ

RCRAFT AZIMUTH – DEGREES

FORWARD
0°

270° ———— 90°

180°

VIEW LOOKING DOWN

LEGEND			
SYMBOL	SUBJECTIVE RATING	LINE TYPE	TIP CONFIGURATION
○ □ ● ◼ ◑ ◪	NONBANGING HEAVY BANGING INTERMEDIATE BANGING	———— - - - -	STANDARD POROUS

B

1

Figure 25. Comparison of Porous Tip Noise During Flat Pitch and Hover.

55

Rotor Noise - Forward Flight

The far field forward flight data are shown in Figure 26. An appreciable reduction in sound pressure level with the porous tips was achieved at 80 knots but is not evident at other airspeeds. Detailed examination of the data confirmed the validity of the values shown but failed to indicate any verifiable explanation.

Flight with standard blades demonstrated that rotor-bang levels are established by blade-to-vortex separation: when intersections occurred, blade pressures (Figure 15) and noise levels (Figure 19) were higher. It is reasonable to assume that blade/vortex intersections also occurred during hover with the porous tips; however, for the reasons given on page 4, no blade pressures were measured to confirm this. Thus, the reduction in noise level measured with the porous tip (Figure 25) must result from a modification in the vortex trailed by the blade with the porous tip.

Measurements of the vortex diameter in the wake of a full-scale helicopter rotor would have conclusively demonstrated this modification, but this was not within the scope of this program and would be the subject of a separate investigation. The increased size of the vortex core with its associated reduction in induced velocity, while sufficient to produce significant noise reductions for the hovering aircraft, was generally insufficient for forward speeds even as low as 40 knots.

Subjective Effects of the Porous Tip

Oscillographic records of hover noise level for the standard and porous tip were stripped out through a C-network filter. The comparisons are illustrated in Figure 27.

The large amplitude of the pulse at blade-passage frequency, which is characteristic of the standard tip, is considerably reduced with the porous tip; and the rise time is significantly increased, indicating a reduction in the sharpness of the noise. This characteristic is not evident from the sound pressure data above; for this reason, all the data in the subject program have been subjectively rated for comparison purposes only. This information is shown in Appendix V.

It is noteworthy that observers described the flyby noise with the porous tip as having a more "hollow" sound than the standard tip flyby, a characteristic evidently arising from modifications in the trailed vorticity.

56

NOTE:
MICROPHONE 200 FEET FROM
AIRCRAFT AT 90° AZIMUTH
(FLAT-PITCH DATA AVAILABLE
ONLY AT 90° AZIMUTH)

	LEGEND		
LINE TYPE	CONDITION	ROTOR RPM	WEIGHT (LB)
	STANDARD TIP, HOVER	230	27,850
	POROUS TIP, HOVER	230	28,200
	POROUS TIP, FLAT PITCH	180	27,500

FREQUENCY - HERTZ

SOUND PRESSURE LEVEL - DECIBELS

Figure 25. Comparison of Porous Tip Noise During Flat Pitch
and Hover.

55
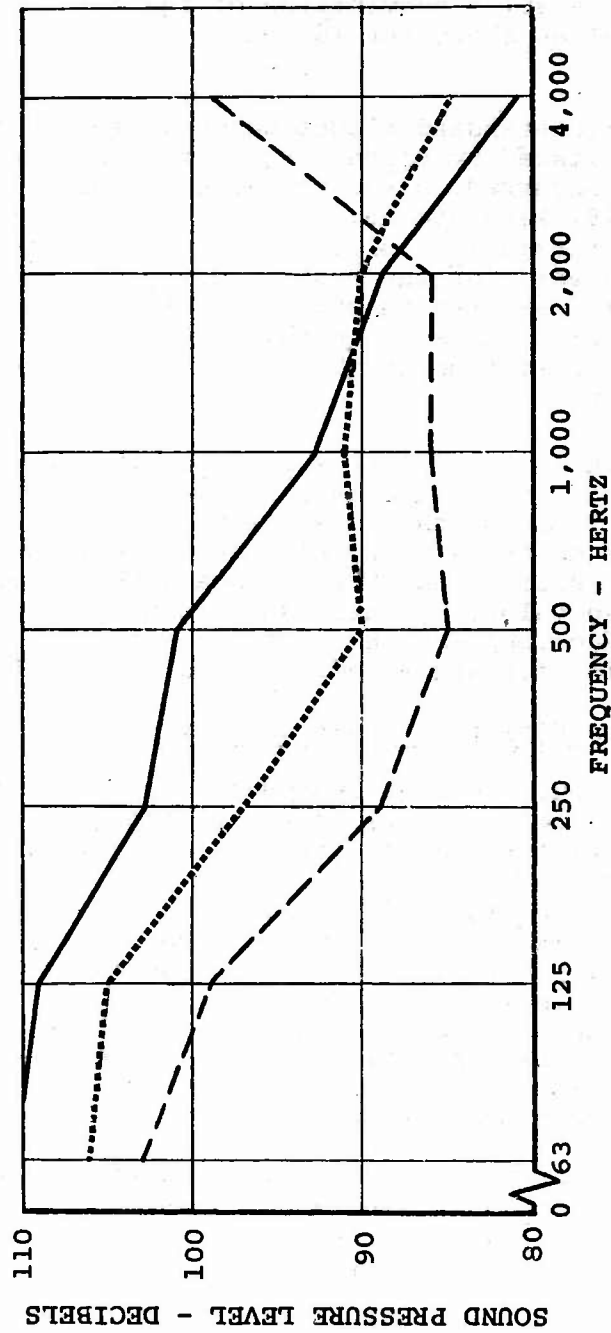
	TRIM SCHEDULE			
A/S (KNOTS)	0	40	80	120
BITF/BITR	0.5/0	0.5/0	0.5/0	3.0/5
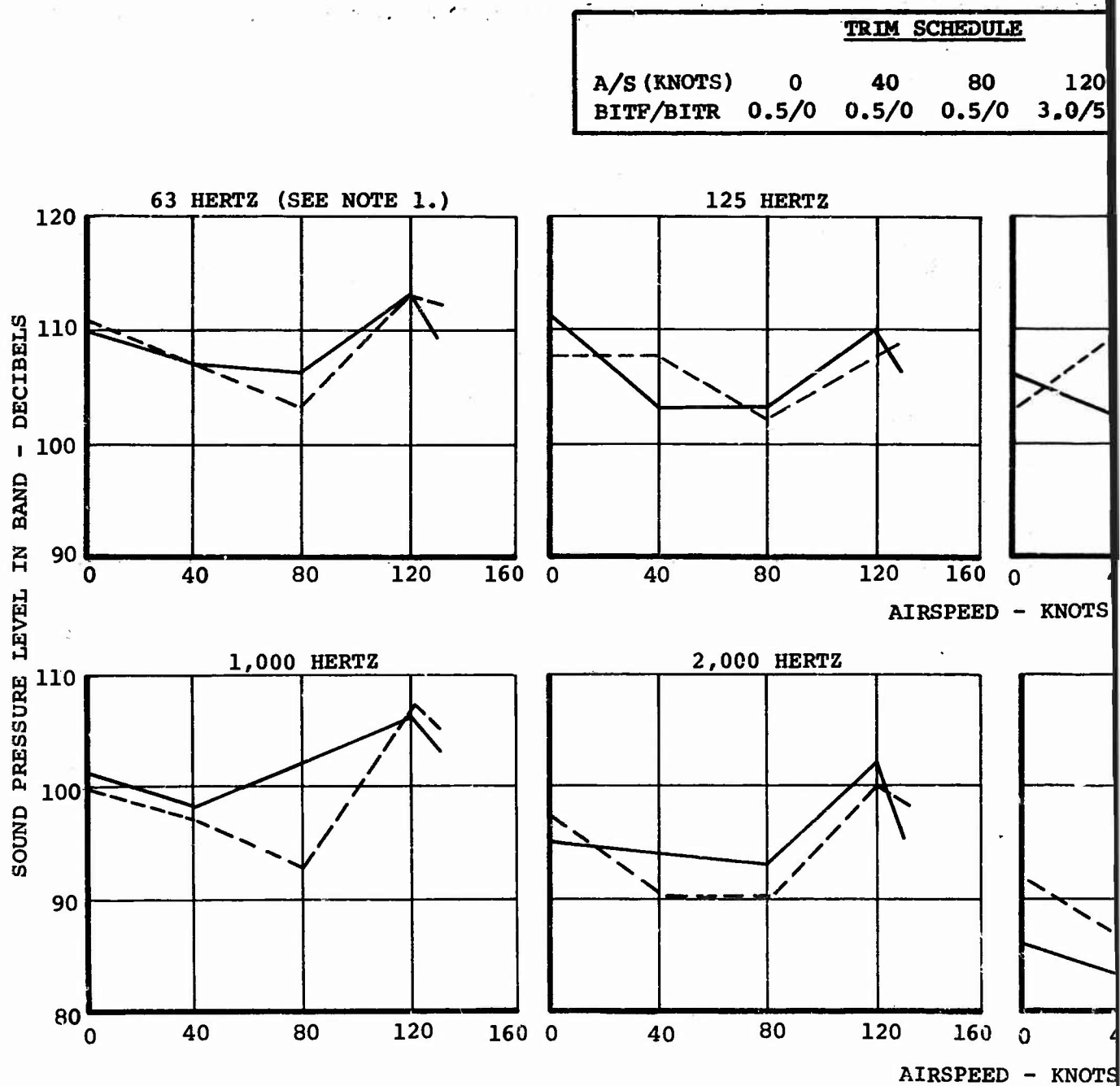
Figure 26. Comparison of Standard and Porous Tip Fly-By
Noise - Scheduled Trim.

57

A

0	80	120	130
/0	0.5/0	3.0/5.0	3.0/5.0

250 HERTZ

500 HERTZ

0   160   0   40   80   120   160   0   40   80   120   160

AIRSPEED - KNOTS

4,000 HERTZ

0   160   0   40   80   120   160

AIRSPEED - KNOTS
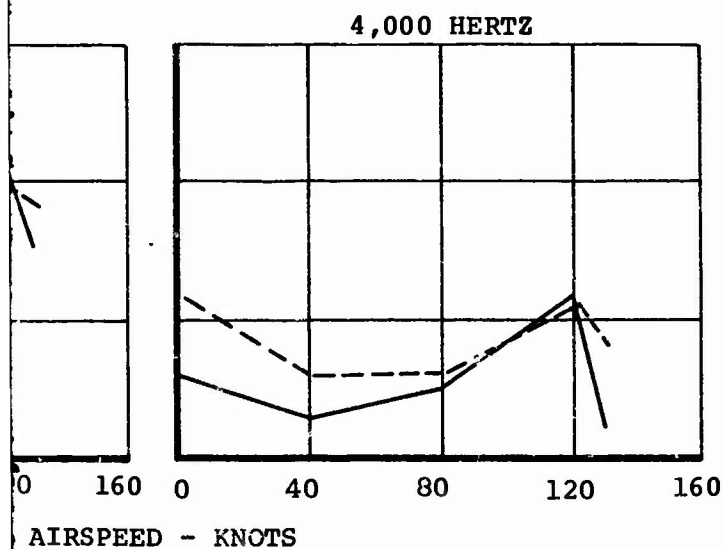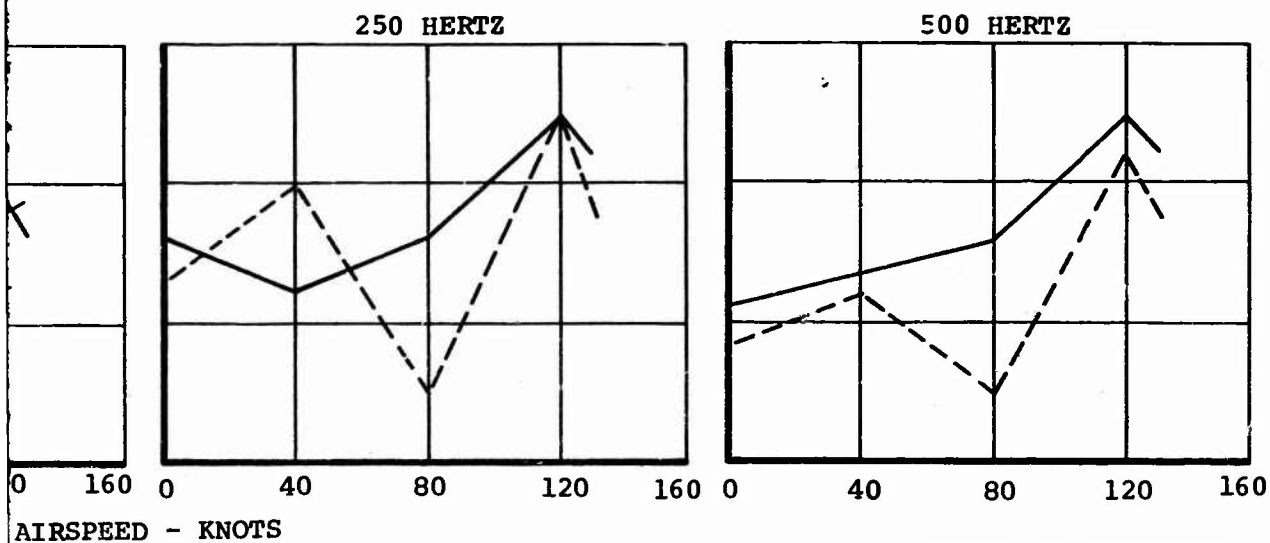
LEGEND	
LINE TYPE	TIP CONFIGURATION
————	STANDARD
– – – –	POROUS

NOTES:
1. OCTAVE BAND CENTER FREQUENCY; GIVEN FOR EACH CURVE.
2. GROSS WEIGHT = 27,500 POUNDS
3. ROTOR RPM = 230
4. DATA IS MAXIMUM VALUE FOR EACH AIRSPEED, AS FOLLOWS:

    HOVER – 135 DEG AZIMUTH

    FORWARD FLIGHT – MAXIMUM VALUE MEASURED ON SIDELINE MICROPHONE DURING FLYBY

B

STANDARD TIP

POROUS TIP

NOTES: 1. GROSS WEIGHT = 27,500 POUNDS
        2. ROTOR RPM = 230
        3. BITF/BITR = 3.0/5.0
        4. MICROPHONE 200 FEET FROM
           AIRCRAFT AT 135° AZIMUTH

Figure 27. Comparison of Standard and Porous Tip
            Time History - Hover.

Power Required

It was recognized that the drag due to the porosity of the blade tip would require significant increases in helicopter power required over the airspeed envelope. Based on preliminary wind tunnel measurements, the increment required for the porous tips was estimated (Reference 4) to be 120 horsepower in hover for a CH-47A helicopter, but measured rotor shaft torque values converted to horsepower indicate that increases of about 600 horsepower were actually required. This is shown in Figure 28 for all airspeeds. At 130-knot airspeed, the power-required curves for the porous and standard tip converge. The increase in power required for the porous tip does not limit the CH-47A from a power-available standpoint, however, and the aircraft was able to achieve 130 knots at the test gross weight. Noise levels at the high forward speeds are similar for both the standard and porous tips. It appears that, above 135 knots, the porous tip might require less power than the standard tip.

NOTES: 1. GROSS WEIGHT = 27,500 POUNDS
       2. ROTOR RPM = 230

LEGEND

LINE TYPE	TIP CONFIGURATION
——————	STANDARD
- - - - -	POROUS
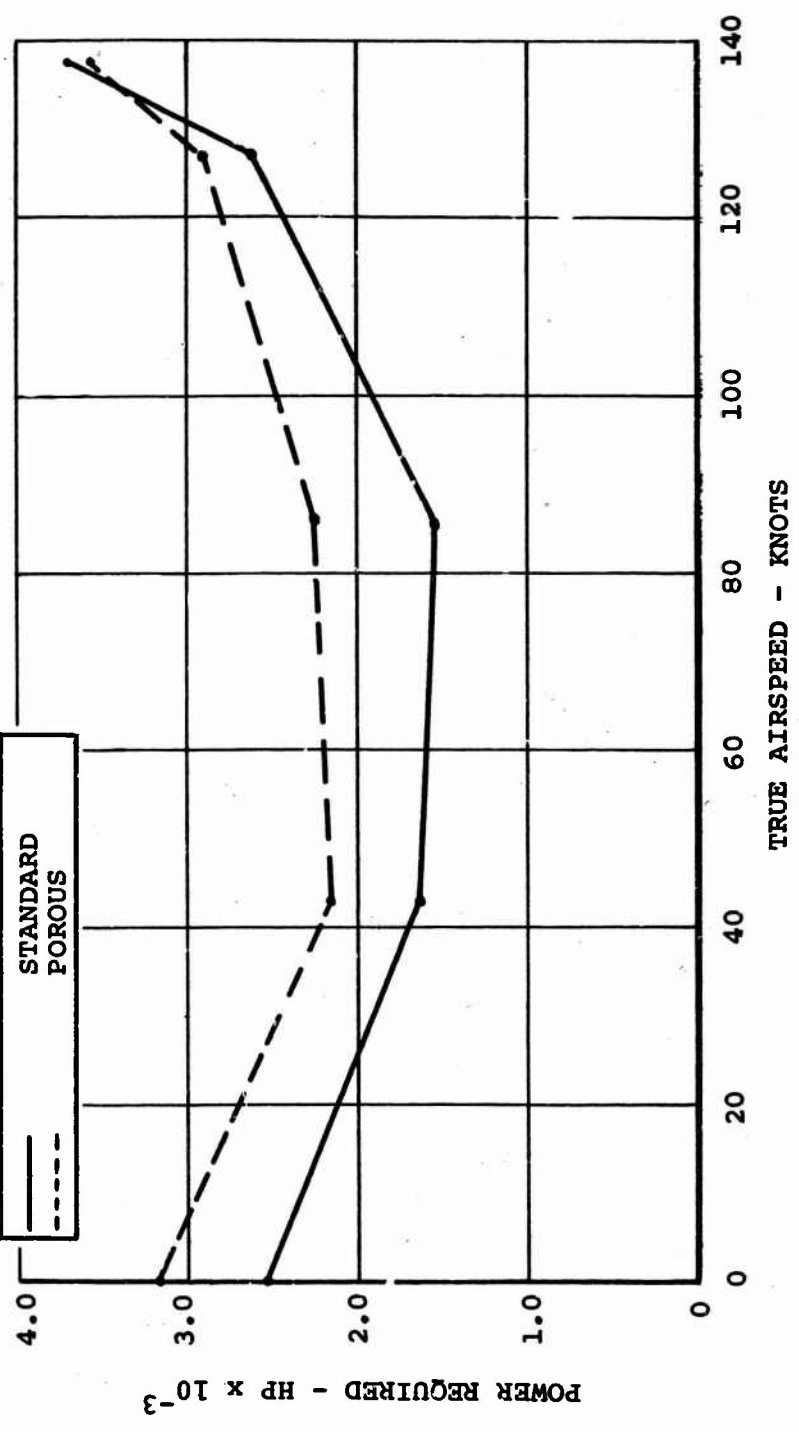
Figure 28. Comparison of Blade Tip on Power Required at Various Airspeeds.

CONCLUSIONS AND RECOMMENDATIONS

The experimental investigation which comprised Phase I of this program and which resulted in a detailed correlation study of rotor noise with other variables and parameters revealed that, in essence, one critical factor exists in the generation of rotor noise on the CH-47A helicopter. This factor is the intersection of a rotor blade with the rolled-up tip vortex shed from another on the opposite rotor. When an intersection occurs, particularly over the outer sections, the rotor noise may be as much as 10 to 15 db higher (at specific frequencies) than when these intersections do not take place. The effects of all other variables which were considered in the subject program are nearly an order of magnitude lower in importance. In a program of this extent, where large numbers of data points are gathered over relatively long periods of time, particularly in terms of many weeks (flight 393 occurred on 4/5/66, flight 400 on 5/2/66), variations in a specific parameter can be difficult to control. This in no way implies that any of the data is insignificant, but rather bolsters the fact that the important variable, blade-vortex separation, was notable throughout the program, whereas many of the secondary parameters appeared to have some inconsistent effects. It is nevertheless apparent that control of rotor noise on a tandem rotor helicopter is strongly dependent on blade-vortex intersections.

The modification of the trailed vorticity with the porous tip was measured only in terms of the noise produced when intercepted by a rotor blade. In hover, this amounted to a reduction of 15 db at 250 Hz. It is noteworthy also that the blade noise during hover with the porous tip never displayed more than a moderate amount of banging at any location. In forward flight the porous tip did not show a consistent effect on rotor noise although at 80 knots a 10-db reduction was achieved.

When blade banging occurs, any effects which materialize from the mechanism of generation are apparently localized in the rotating system of the rotors and are not transmitted to the control system or airframe, since none of the measured parameters, with the exception of rotor blade pressures, showed a substantial correlation with noise.

Based on the premise that blade bang results from a blade-vortex intersection, further study should be made to determine more precisely how these intersections may be avoided in all flight regimes. This study might well be one of vortex visualization on full-scale aircraft or a wind tunnel model combined with a comparison with up-to-date theory to permit an accurate prediction technique for the trailed vorticity. With this technique available to the designer, the major external noise source of the tandem rotor helicopter undoubtedly could be eliminated.

62

LITERATURE CITED

1. Loewy, R.G., and Sutton, L.R., A THEORY FOR PREDICTING THE ROTATIONAL NOISE OF LIFTING ROTORS IN FORWARD FLIGHT INCLUDING A COMPARISON WITH EXPERIMENT, USAAVLABS Technical Report 65-82, U.S. Army Aviation Materiel Laboratories, Fort Eustis, Virginia, January 1966, AD 629377.

2. Schlegel, R., King, R., and Mull, H., HELICOPTER ROTOR NOISE GENERATION AND PROPAGATION, USAAVLABS Technical Report 66-4, U.S. Army Aviation Materiel Laboratories, Fort Eustis, Virginia, October 1966, AD 645884.

3. Pruyn, R.R., IN-FLIGHT MEASUREMENT OF ROTOR BLADE AIRLOADS, BENDING MOMENTS, AND MOTIONS, TOGETHER WITH ROTOR SHAFT LOADS AND FUSELAGE VIBRATION, ON A TANDEM ROTOR HELICOPTER, The Boeing Company, Vertol Division; USAAVLABS Technical Reports 67-9A, -9B, -9C, -9D, and -9E, U.S. Army Aviation Materiel Laboratories, Fort Eustis, Virginia, April 1968, AD 670952, AD 671661, AD 671662, AD 671664, AD 671665.

4. Spencer, R.H., Sternfeld, H., Jr., and McCormick, B.W., TIP VORTEX CORE THICKENING FOR APPLICATION TO HELICOPTER ROTOR NOISE REDUCTION, USAAVLABS Technical Report 66-1, U.S. Army Aviation Materiel Laboratories, Fort Eustis, Virginia, September 1966, AD 644317.

5. American Standards Association, PREFERRED FREQUENCIES FOR ACOUSTICAL MEASUREMENTS, Doc. S1.6, 1960.

6. Davis, J.M., TANDEM HELICOPTER TRIM AND STABILITY ANALYSIS, The Boeing Company, Vertol Division, Aerodynamics Document III-264, Program A-97, March 29, 1965.

SELECTED BIBLIOGRAPHY

Beranek, L.L. (ed), NOISE REDUCTION, McGraw-Hill, New York, 1960.

Croxton, Frederick, E., and Cowder, Dudley J., APPLIED GENERAL STATISTICS, Prentice-Hall, New York, 1947, Pages 685-6.

MIL-C-45662A, CALIBRATION SYSTEM REQUIREMENTS, 17 May 1960.

Schaffer, E.G., HELICOPTER ROTOR NOISE ANALYSIS 1966 INDEPEN-DENT RESEARCH AND DEVELOPMENT, D8-0598, The Boeing Company, Vertol Division, 22 December 1966.

Spreiter, John R., and Sacks, Alvin H., THE ROLLING UP OF THE TRAILING VORTEX SHEET AND ITS EFFECT ON THE DOWNWASH BEHIND WINGS, Journal of the Aeronautical Sciences, January 1951.

Technical Document, 'N' POINT HARMONIC ANALYSIS, The Boeing Company, Vertol Division, Philadelphia, Pennsylvania, IBM Program D44.

Von Gierke, Henning E., EFFECTS OF SONIC BOOM ON PEOPLE: REVIEW AND OUTLOOK, Journal of the Acoustical Society of America, Vol. 39, No. 5, Part 2, May 1966, Page S 50, Figure 7.

Wetmore, Joseph W., AIRCRAFT TRAILING VORTICES - A HAZARD TO OPERATIONS, Astronautics and Aeronautics, July 28, 1950, Pages 44-49.

Wiley, C.R., Jr., ADVANCED ENGINEERING MATHEMATICS, McGraw-Hill, New York, 1951.

APPENDIX I

CALCULATION OF BLADE-VORTEX INTERSECTIONS

X-Y PLANE

The locus of possible blade-vortex filament intersections and intersecting blade element radial positions in the two-dimensional X-Y plane are determined graphically for both hover and forward flight conditions. The appropriate rotor advance ratios (μ) with respect to the rotor disc plane were used in the forward flight cases. Because of the insignificant error involved, the blade flapping was ignored in the X-Y plane representation.

1. <u>Hover</u> - In hover, the possible blade-vortex intersection occurs in the rotor overlap area. Emphasis was applied to the segments of the overlap area where the blade element experiencing the intersection has an outboard radial location of from 48 to 100 percent blade radius, and where the blade angle between the blade element chord axis and line tangent to the vortex-trail becomes large.

2. <u>Forward Flight</u> - In forward flight, where the rotor advance ratio becomes important, each airspeed had to be considered separately. Only the intersections for the initial 240 degrees of trailed filament are considered. The emphasis is on the intersection points where the blade and vortex paths approach tangency.

Z AXIS

Once the possible intersections in the X-Y plane are established, the next step is to determine the relationship of the blade-vortex in the vertical plane, for at this point an intersection can occur only if the vertical position of the vortex filament coincides with that of a blade element. Only hover and straight, level forward flight cases were considered in this study. The aircraft motion along the Y and Z axes was zero in all cases. The geometry of the blade shedding the vortices and the possible intersecting blade element for any particular rotor azimuth location is obtained by computing the total blade flapping.

$$\beta = a_o - a_1 \cos \psi - b_1 \sin \psi + i_s \cos \psi \tag{3}$$

where

a_o = rotor blade mean coning angle with respect to the rotor disc plane.

a_1 = first harmonic longitudinal flapping angle with respect to the rotor disc plane.

b_1 = first harmonic lateral flapping angle with respect to the rotor disc plane.

i_s = angle of incidence of the rotor shaft in the helicopter X-Z plane.

ψ = azimuth position of the blade.

The coordinates for a point on the vortex filament are then found by resolving the vector into its components (normalized to radius r)

$$C_x = \cos \beta_\psi \cos \psi + P(\mu_x) \frac{\Delta\psi}{360} (2\pi) \qquad (4)$$

$$C_y = -\cos \beta_\psi \sin \psi + P(\mu_y) \frac{\Delta\psi}{360} (2\pi) \qquad (5)$$

$$C_z = -\sin \beta_\psi + P(\mu_z + \lambda_z) \frac{\Delta\psi}{360} (2\pi) \qquad (6)$$

where

β_ψ = the azimuth position on the blade occupied when shedding the vortices; obtained from the geometrical representations.

$\Delta\psi$ = the equal blade azimuth angle steps to be considered along the vortex trail (in this study was 30°).

μ = rotor advance ratio with respect to the rotor disc plane.

λ = rotor inflow ratio with respect to the rotor disc plane.

P = the order of points to be computed in equal increments of ψ in obtaining the geometry of the filaments.

The origin of the coordinates is the hub of the rotor. With no lateral motion of the aircraft, in cases studied, μ_y and the last term of C_y become zero.

66

In stabilized hover cases, where μ_x approaches zero, only the first terms of the components c_x and c_y are considered. For forward flight where both the rotor advance ratio and blade geometry become important, the full terms of C_x and C_z are computed. Upon resolution of the appropriate components, the vortex filaments were traced as a function of blade azimuth angle increments (vertical position being defined as Z_v with respect to the forward rotor hub). The possibility of a blade from the opposing rotor intersecting this filament was determined by computing its vertical position (also with respect to the forward rotor hub and defining it as Z_β). The subsequent differential in height is $\bar{Z}$ where $\bar{Z} = Z_\beta - Z_v$ with $\bar{Z}$ positive when the blade element is above the filament and negative when below. $\bar{Z} = 0$ indicates a calculated intersection in the X-Z plane.

The method described provides the ability to calculate blade-vortex separations. Although the simplifying assumptions listed below are inherent in the calculation, the results appear to correlate with the measured noise levels. The major assumptions are:

1. The blade reacts like a rigid body.

2. The trailed wake does not distort.

Assumption number 2 is valid within 60 degrees of rotation after the vortex is shed, where blade-vortex intersections generally occur.

FLIGHT TEST PROGRAM, PHASES I AND II

This appendix presents the specific data points and operating conditions obtained during both Phase I and Phase II of this program. The 'Run' conditions are to be used in identifying all data presented in Appendixes III, IV, and V.

	Run Gross Weight	Run CG (in.	True Air- speed	Rotor	Longitudinal Cyclic Trim (deg) (Nominal)		Fuselage Attitude (deg)		
Run	(lb)	fwd)	(kn)	RPM	Fwd	Aft	Pitch	Roll	Side- slip
Flight No. 393									
1	36,873	3.6	27	230	-0.5	0.0	5.3	-3.7	+0.4
2	36,823	3.6	27	231	-0.5	0.0	5.3	+0.5	-7.5
3	36,823	3.6	27	229	-0.5	0.0	5.3	-1.1	-15
4	36,773	3.6	27	231	-0.5	0.0	5.3	+0.3	+7.5
5	36,773	3.6	27	231	-0.5	0.0	5.3	+0.8	+15
6	36,573	3.5	28	231	-0.5	0.0	4.9	-0.8	-0.2
7	36,473	3.5	28	229	-0.5	0.0	5.2	-0.2	+7.5
8	36,423	3.4	28	231	-0.5	0.0	5.0	+0.4	+15
9	36,373	3.4	28	229	-0.5	0.0	5.0	+1.8	+30
10	36,323	3.4	28	229	-0.5	0.0	5.0	-1.6	-15
11	36,273	3.4	25	231	-0.5	0.0	5.2	-2.4	-30
12	35,973	3.3	63	231	-0.5	0.0	2.7	-0.7	0.0
13	35,923	3.3	70	241	-0.5	0.0	2.4	-0.9	+0.1
14	35,873	3.3	59	240	-0.5	0.0	3.0	+0.3	-0.1
15	35,273	3.1	57	231	-0.5	0.0	3.0	+0.2	+0.1
16	N/A	N/A	N/A	N/A	N/A	N/A	N/A	N/A	N/A
17	35,123	3.0	0	229	-0.5	0.0	2.2	-2.8	-0.3
18	35,073	3.0	0	230	-0.5	0.0	3.5	-1.5	0.0
19	35,023	3.0	0	230	-0.5	0.0	3.4	-0.2	0.1
20	34,998	3.0	0	229	-0.5	0.0	3.3	+0.1	-0.4
21	34,973	3.0	0	231	-0.5	0.0	3.4	+0.6	-0.1
Flight No. 394									
0	33,200	5.3	0	231	-0.5	-0.8	–	-1.3	+5.5
1	33,300	5.3	58	231	-0.8	-0.8	+2.8	-1.2	-2.4
2	33,200	5.3	101	231	-1.3	-1.0	-0.8	+0.4	+0.2
3	33,200	5.3	85	231	-1.0	-1.0	+1.3	+0.3	-2.3
4	33,150	5.3	99	230	-2.5	-2.8	+1.3	-0.6	-3.9
5	33,100	5.2	100	229	-3.0	-4.9	+3.3	-1.5	-3.5
6	33,050	5.2	101	229	-3.5	-5.8	+3.4	-1.7	-4.0

	Run	Run	True		Longitudinal Cyclic Trim		Fuselage Attitude (deg)		
	Gross	CG	Air-						
	Weight	(in.	Speed	Rotor	(deg) (Nominal)				Side-
Run	(lb)	fwd)	(kn)	RPM	Fwd	Aft	Pitch	Roll	slip

TABLE III - Continued

Flight No. 394 (Continued)

	Run	Run	True		Longitudinal Cyclic Trim		Fuselage Attitude (deg)		
7	33,000	5.2	76	222	-1.2	-1.0	+1.2	-1.7	-9.0
8	32,950	5.2	59	214	-1.1	-0.9	+2.0	-0.1	-5.2
9	32,850	5.2	59	213	-1.2	-0.9	+4.2	-0.8	-6.2
10	-	-	-	-	-	-	+2.3	-	-
11	32,700	5.1	28	202	-0.9	-0.8	+4.4	-1.7	-8.9
12	32,550	5.1	28	202	-0.5	-0.8	+4.1	-2.1	-4.8
13	32,500	5.1	28	202	-2.0	-2.3	+6.3	-2.1	-13.0
14	32,450	5.1	82	235	-1.0	-1.1	+1.4	-0.2	-3.9
15	32,300	5.0	99	231	-1.1	-1.8	+3.3	-	-
16	32,150	5.0	59	231	-2.6	-4.7	-	-1.0	-15.2

Flight No. 395

	Run	Run	True		Longitudinal Cyclic Trim		Fuselage Attitude (deg)		
2	25,600	-0.2	0	230	-0.7	-0.7	+7.1	0.0	-3.9
3	25,500	-0.3	54	229	-1.1	-0.9	+2.5	0.0	-3.2
4	25,450	-0.3	98	229	-3.3	-5.2	+4.1	+0.7	-0.7
5	25,450	-0.3	138	229	-3.9	-5.4	-0.8	-1.1	-2.4
6	25,400	-0.3	55	204	-1.3	-0.8	+3.2	-0.8	-4.0
7	25,200	-0.5	53	216	-1.2	-0.8	+2.6	+0.5	-0.1
8	25,200	-0.5	69	216	-1.3	-0.9	+2.5	-0.2	-2.6
9	25,200	-0.5	96	215	-3.0	-3.7	+2.2	-3.0	-1.6
10	25,200	-0.5	102	216	-3.7	-5.6	+2.1	-0.6	-2.6
11	25,150	-0.5	76	229	-0.8	-1.1	+1.4	-26.4	-
12	25,150	-0.5	74	229	-1.0	-1.0	-1.2	+27.2	-5.2
13	25,150	-0.5	79	229	-1.2	-0.8	+2.9	+3.4	-10.9
14	25,100	-0.5	72	229	-0.9	-1.1	+1.3	-2.5	-9.8
15	24,950	-0.6	77	229	-1.1	-1.0	-1.1	+22.8	-9.4
16	24,950	-0.6	78	229	-0.9	-1.0	+0.8	+3.9	-7.4
17	24,950	-0.6	76	229	-0.8	-0.8	-18.3	-13.2	-2.4
18	24,900	-0.6	72	229	-1.0	-1.1	+3.0	+0.2	-5.4
19	24,900	-0.6	73	227	-1.1	-0.9	+3.8	-0.4	-

Flight No. 398

	Run	Run	True		Longitudinal Cyclic Trim		Fuselage Attitude (deg)		
1	23,900	3.2	129	225	-3.3	-5.2	-2.8	3.5	4.0
2	23,850	3.2	138	225	-3.3	-5.2	-6.1	1.0	2.4
3	N/A	N/A	N/A	N/A	N/A	N/A	N/A	N/A	N/A
4	23,700	3.1	126	235	-3.1	-5.2	-1.4	-0.4	1.9
5	23,650	3.1	133	235	-3.3	-5.3	-3.8	0.6	1.3
6	23,600	3.0	147	235	-3.4	-5.3	-5.6	1.0	3.9
7	23,550	3.0	122	230	-3.1	-5.1	-1.8	1.0	1.7
8	N/A	N/A	N/A	N/A	N/A	N/A	N/A	N/A	N/A
9	23,400	2.9	148	230	-3.4	-5.4	-5.7	0.3	2.5

69

	Run Gross Weight	Run CG (in.	True Air- speed	Rotor	Longitudinal Cyclic Trim (deg) (Nominal)		Fuselage Attitude (deg)		Side-
Run	(lb)	fwd)	(kn)	RPM	Fwd	Aft	Pitch	Roll	slip

TABLE IV. FLIGHT TEST PROGRAM - PHASE II

Flight No. 399

Run	Gross Weight (lb)	CG (in. fwd)	Airspeed (kn)	Rotor RPM	Fwd	Aft	Pitch	Roll	Side-slip
1	29,000	5.2	109	230	3.55	4.63	-0.70	0.30	4.40
2	28,200	4.9	128	230	3.60	5.62	-1.69	-1.83	-2.22
3	28,000	4.9	128	230	3.65	5.53	-0.68	-1.24	0.37
4	27,850	4.8	0	230	0.60	0.74	6.27	-0.08	27.36
5	27,850	4.8	0	230	0.93	0.59	6.75	-2.03	-52.45
6	27,850	4.8	0	230	0.97	0.57	7.40	-1.84	14.59
7	27,750	4.8	0	230	0.76	0.55	7.36	-2.67	70.73
8	27,700	4.8	0	230	2.93	4.97	10.61	-0.86	26.04
9	27,700	4.8	0	230	2.95	4.93	10.73	-1.81	-24.44
10	27,650	4.7	0	230	3.07	4.90	10.59	-2.51	-30.53
11	27,600	4.7	0	230	2.98	4.94	11.65	-2.59	-48.91
12	27,600	4.7	43	230	3.17	5.11	10.32	-1.13	-15.67
13	27,500	4.7	85	230	3.25	5.36	5.76	-4.24	-4.53
14	27,500	4.7	127	230	3.53	5.54	3.74	-1.37	-1.92
15	27,400	4.7	138	230	3.82	5.45	-1.53	-1.22	0.77
16	27,300	4.6	43	230	0.84	0.71	7.66	-1.061	-3.40
17	27,200	4.6	85	230	1.37	1.35	3.19	-0.69	-2.92
18	27,000	4.5	43	230	3.06	4.98	7.29	0.36	1.32
19	26,924	4.5	85	230	3.41	5.17	6.00	3.14	1.67
20	26,900	4.5	128	230	3.80	5.42	1.63	2.14	1.71
21	26,800	4.5	138	230	3.52	5.75	-1.93	0.004	-1.93
22	26,700	4.4	43	230	0.81	0.71	6.99	0.75	0.63
23	26,700	4.4	85	230	1.80	1.85	-0.87	-0.09	4.28
24	26,650	4.4	64	230	1.23	1.11	17.32	-2.30	-20.06
25	26,600	4.4	117	230	2.41	3.62	14.40	0.69	-1.64
26	26,550	4.4	140	230	3.91	5.48	-2.40	0.30	2.82
27	26,550	4.4	110	220	2.91	3.99	-2.62	1.00	1.81

Flight No. 400

Run	Gross Weight (lb)	CG (in. fwd)	Airspeed (kn)	Rotor RPM	Fwd	Aft	Pitch	Roll	Side-slip
2	28,250	4.6	0	230	0.75	0.68	6.77	-1.75	26.48
3	28,250	4.6	0	230	0.68	0.65	7.93	-3.16	-8.16
4	28,200	4.6	0	230	0.83	0.63	8.01	-3.38	-6.17
5	28,200	4.6	0	230	0.80	0.62	7.05	-2.64	15.96
6	28,150	4.6	0	230	2.96	5.03	10.93	-2.49	10.22
7	28,100	4.6	0	230	2.96	4.98	11.31	-2.22	-14.75
8	28,050	4.6	0	230	2.97	4.98	11.63	-3.36	-51.4
9	28,000	4.5	0	230	3.01	5.04	12.04	-2.95	-23.65
10	28,000	4.5	126	230	3.38	5.32	1.11	-1.18	1.14
11	28,000	4.5	126	230	3.40	5.43	0.38	-4.03	0.10
12	27,850	4.5	43	230	3.14	5.16	7.54	-1.51	-20.82
13	27,850	4.5	84	230	3.16	5.18	7.26	-3.62	-2.14
14	27,800	4.5	126	230	3.67	5.37	3.38	-0.06	1.19

70

TABLE IV - Continued

Run	Run Gross Weight (lb)	Run CG (in. fwd)	True Air-speed (kn)	Rotor RPM	Longitudinal Cyclic Trim (deg) (Nominal) Fwd	Aft	Fuselage Attitude (deg) Pitch	Roll	Side-slip
Flight No. 400 (Continued)									
15	27,700	4.4	136	230	3.63	5.48	0.13	-0.97	1.34
16	27,600	4.4	42	230	1.25	0.94	4.81	-1.90	-19.76
17	27,550	4.4	84	230	1.03	0.94	0.93	-2.13	-3.88
18	27,500	4.4	42	230	2.89	5.15	9.82	0.06	-2.99
19	27,500	4.4	84	230	3.19	5.20	4.25	-1.24	-0.66
20	27,450	4.4	125	230	3.63	5.38	0.61	1.03	2.01
21	27,450	4.4	136	230	3.65	5.39	-1.107	-0.71	1.54
22	27,400	4.3	42	230	0.91	0.64	3.55	-0.64	2.99
23	27,100	4.2	84	230	1.54	0.79	0.14	0.02	4.22
24	27,100	4.2	63	230	0.78	0.82	16.29	-1.33	-5.52
25	26,800	4.1	84	230	0.91	0.98	-1.92	-3.37	-2.83
26	26,750	4.1	110	230	3.22	5.16	18.48	-2.96	-0.64

71

APPENDIX III

AIRBORNE NOISE DATA

TABLE V. AIRBORNE NOISE DATA - LEFT-HAND MICROPHONE						
Octave Band Center Frequencies - Hz						
Run	63	125	250	500	1,000	2,000	4,000
(Sound pressure level in db given below)						

Flight No. 393

Run	63	125	250	500	1,000	2,000	4,000
1	132	129	131	126	122.5	119	115
2	133	130	132	126.5	124	118	116
3	132.5	129.5	133	128	124	119	127.5
4	131.5	131.5	132	126	124	117	113.5
5	134	129	134.5	125	125	119.5	112
6	131	126	132	125	120.5	108	115.5
7	133	129	132	128	124	117.5	116
8	133.5	130.5	133.5	126.5	126.5	121	119.5
9	133.5	132.5	132	127.5	126	122	121
10	131.5	126.5	133.5	125	121	117	114
11	133.5	128	133	128	123	119	115
12	133	127	130.5	124	120.5	114	107.5
13	130	134	124	124	114.5	113.5	107.5
14	132.5	130.5	132	127.5	120.5	113	112.5
15	113	130.5	132.5	127.5	122.5	122	118
16	N/A	N/A	N/A	N/A	N/A	N/A	N/A
17	133	128.5	131	125.5	123.5	118.5	116.5
18	131	129	129.5	126.5	126	122	118.5
19	130	126.5	129.0	125	125	123	119.5
20	128.5	126.5	128	126.5	127.5	127.5	120.5
21	130	126	130	124.5	125.5	120.5	116.5

Flight No. 394

Run	63	125	250	500	1,000	2,000	4,000
0	(Calibration run - no acoustical data.)						
1	132	127	128.5	122	120	117	114
2	130	127	133	126.5		111.5	109
3	132	127.5	127.5	124	116	113.5	109.5
4	130.5	127.0	132.5	128.5	120.5	116.5	111
5	134.5	129	129	124.5	119	111.5	108.5
6	133.5	131.5	134.5	131	125.5	120	116.5
7	134.5	132.5	136.5	130.5	124	120	114
8	128	124	127	124	115.5	111	107.5
9	131.5	128	135	130	123.5	120	115.5
10	127.5	124	129.5	125.5	116.5	112.5	107.5
11	130.5	125	130	122.5	116	118.5	114.5
12	128.5	122.5	129	121	113	113.5	105.5
13	130	124	129.5	120.5	114	112.5	108

TABLE V - Continued

	Octave Band Center Frequencies - Hz						
Run	63	125	250	500	1,000	2,000	4,000
		(Sound pressure level in db given below)					

Flight No. 394 (Continued)

14	130	124	128	127	119	115	109
15	132.5	130.5	133.5	131	122.5	118	113.5
16	129	123	126.5	123	113	107.5	106

Flight No. 395

2	131	128.5	133	126.5	121.5	118.5	114.5
3	130	126	128	121	122.5	119	117.5
4	127.5	126	130.5	126.5	121	119	111
5	134	132	136.5	129.5	118	114	111.5
6	134.5	131	130.5	124.5	118.5	115	112
7	127.5	123.5	127.5	119.5	113	108.5	102
8	138	126.5	134.5	126	119	116.5	112
9	127.5	125	130	125	120	113.5	113
10	132	129	131.5	122	117.5	114.5	114
11	134	130.5	137.5	131.5	122	118	112.5
12	128	120	119	126.5	119.5	113	110.5
13	128	126	131	123.5	116.5	109.5	112
14	135.5	133.5	131	128.5	122.5	120.5	118
15	126.5	121.0	126.5	126	116	116	112
16	127	126	129.5	128.5	117.5	117	114
17	127	124	127.5	129	118.5	115.5	112
18	131.5	128	129.5	123	122.5	116.5	113.5
19	127	126	132.5	127.5	123	115.5	121

Flight No. 398

1	134.5	135	137.5	137	136.5	135	134.5
2	133.5	134	135	135	134.5	135.5	136
3	131.5	130.5	133.5	135.5	139.5	138.5	139.5
4	135.5	136	143	146	143	139	138
5	134.5	135.5	138.5	138	135	136	136.5
6	136	134.5	135.5	137.5	138.5	138.5	140.5
7	136	135.5	142.5	145.5	139.5	136	134.5
8	135	135	135.5	136	133.5	135	133.5
9	134	133	134	136.5	137.5	137.5	138.5

Flight No. 399

1	144	133	137	131	124.5	120	115.5
2	132	129.5	126.5	122	115.5	113.5	113
3	133	131	127.5	121	117	113.5	112.5

TABLE V - Continued

	Octave Band Center Frequencies - Hz						
Run	63	125	250	500	1,000	2,000	4,000
			(Sound pressure level in db given below)				

Flight No. 399 (Continued)

4	129	126.5	127	123.5	122	117.5	116
5	131	127.5	132	125	120	116	113
6	131	128	132.5	125	121.5	115	112.5
7	129.5	126.5	131	124	119	114	112.5
8	128	125.5	128	122.5	116	112	110
9	132	129	130.5	122.5	118	115.5	111.5
10	130	126.5	130	124	119.5	116.5	114
11	130	125.5	129	124	119	113	113
12	129	127.5	126	122	116	112	108.5
13	129	128	132	128	121.5	115.5	112
14	132	131	127	125	119	118.5	115.5
15	132	129	125.5	125.5	123	119	116
16	127.5	125	130	125	120.5	115.5	111.5
17	127	125	127.5	128	118.5	115	113
18	127	126	131	127.5	119.5	113	110
19	131	126.5	134	128	121	114	111
20	134	133	128	124	122	118	113.5
21	132	130	126	124	119	118	114
22	127.5	127.5	132	128.5	122.5	116	117
23	133	128	125.5	122	116.5	114	112
24	129	125	129.5	122	116.5	112	107
25	132	130.5	127	120	117	114	111
26	133.5	132	127.5	123	117.5	113.5	112
27	133	128.5	127.5	118.5	111.5	119.5	108

Flight No. 400

2	130.5	127	127.5	123	119	114.5	112.5
3	130.5	129.5	117	121	118.5	114	112.5
4	130	126	128	121.5	120.5	115.5	112.5
5	129	127	127.5	123.5	118	114	112
6	131	124	126	120	117	114	112.5
7	129.5	125.5	126	121.5	119.5	116.5	114
8	129	125.5	126.5	122	120	116	113
9	128	125	117	121	119	115	113.5
10	133.5	130.5	130	125	118	114	114
11	132	129	125	124	118.5	116	124.5
12	129	125	124	119	117	115	113
13	127	124.5	127	121	118	116	113
14	135	129.5	132.5	127.5	120	112	115.5
15	132	129	125	125	124	117	118
16	130	126.5	126	122	118.5	113.5	112

74

			TABLE V - Continued				

Octave Band Center Frequencies - Hz							
Run	63	125	250	500	1,000	2,000	4,000
			(Sound pressure level in db given below)				

Flight No. 400 (Continued)

Run	63	125	250	500	1,000	2,000	4,000
17	125	125	123	121	115.5	112.5	112
18	123	125	124	119	115.5	112.5	112
19	123.5	125	127	122	118	113	111.5
20	135	130	130	126	118	116	114
21	134	131	128.5	126	120	117.5	115.5
22	125	123	129	122	120.5	115.5	113.5
23	128.5	128	129.5	125	118	116	112.5
24	123.5	121	121	118.5	115	113	112.5
25	127	125	124.5	119.5	113	111	111.5
26	133	130	132.5	126.5	121	116	111.5

TABLE VI. AIRBORNE NOISE DATA - NOSE-BOOM MICROPHONE						
Octave Band Center Frequencies - Hz						
Run	63	125	250	500	1,000	2,000	4,000
	(Sound pressure level in db given below)						

Flight No. 393

Run	63	125	250	500	1,000	2,000	4,000
1	119	119.5	123.5	120	120	114	113.5
2	119	122	124	121.5	117	112.5	109.5
3	120	123.5	127	123	120	118.5	
4	120	122.5	125.5	121.5	117	115	110
5	120	121.5	123	121	117.5	113.5	108
6	117.5	113.5	120.5	117	113.5	109.5	105.5
7	116	115.5	119.5	115.5	117	109	106.5
8	117.5	116	120	115	114	108	106
9	118.5	115.5	119	116	113	110.5	105.5
10	117.5	113	118	117.5	117.5	115	110.5
11	119.5	121.5	125	123.5	120.5	119	115.5
12	115.5	114	118	119	112.5	114	109
13	117	115	1122	120.5	115	114.5	108
14	116.5	115	121	120	117.5	115.5	110.5
15	118.5	119.5	123	119.5	120	117.5	113.5
16	-	-	-	-	-	-	-
17	118.5	119.5	123	121	118.5	115.5	113
18	120	116.5	122	118	116.5	119.5	112
19	118	117.5	121	117	115	12.5	107
20	117.5	116	119	116.5	113	109.5	104
21	117	114.5	118	114.5	113.5	114	108

Flight No. 394

Run	63	125	250	500	1,000	2,000	4,000
1	117	120	122.5	121.5	122.5	117.5	111
2	118.5	119.5	126.5	121.5	120	118	114
3	118.5	119	122.5	122	119	119.5	114.5
4	119	121	123	122	119	118	114.5
5	120.5	124.5	129	127.5	125.5	122	120.5
6	119.5	123.5	132.5	129	125	124.5	122
7	118	118	123	119.5	117.5	113.5	110.5
8	-	-	-	-	-	-	-
9	117	116.5	123	122	118	115.5	109.5
10	118.5	116	123	121.5	118	115	109.5
11	114.5	116	119	118	119	112	109
12	113.5	111	116	114	113.5	111.5	105.5
13	116	116	118	117	117.5	114	108.5
14	116.5	114.5	123	119	117	116	114
15	121.5	123	131.5	129.5	125	124	121
16	121	122	122	119	117.5	114	109.5

TABLE VI - Continued

		Octave Band Center Frequencies - Hz					
Run	63	125	250	500	1,000	2,000	4,000
		(Sound pressure level in db given below)					

Flight No. 395

2	119	119.5	123.5	120	121	118	117
3	117.5	115	122	122	121.5	119	114
4	120.5	125	134	128.5	127	124	121.5
5	123	123	129	127.5	125.5	123.5	121.5
6	117.5	114.5	120	117	114	111.5	107
7	117	117	121	120	114.5	113	109.5
8	118.5	116	120	119	117	113	109
9	119.5	119.5	124	124	121	118.5	115.5
10	121.5	122	128	126	125	124	121
11	117.5	115	122	116	115	113	108.5
12	119.5	118	123.5	119	118	115	113
13	118.5	118	128	125	119	114	110
14	118.5	114	120	119	116	112.5	111.5
15	119.5	118.5	122	122.5	119	117	114
16	118.5	118.5	122	121	118	114	112
17	117	117	119.5	118	118	116	111
18	120.5	119	124.5	123	122.5	120.5	115
19	124.5	126.5	127	127	125.5	125	122

Flight No. 398

1	119.5	118.5	124.5	126.5	123	120.5	117.5
2	119.5	120	128	127	123.5	124	122.5
3	124.5	120.5	126	122	127	137	116
4	123	125.5	129.5	131	126.5	126.5	126
5	123	121.5	128	126.5	125.5	125	123
6	128.5	127.5	131	127.5	127.5	121	119.5
7	123.5	127.5	129	124.5	124.5	128	125.5
8	122	121.5	127.5	127.5	125.5	125	123.5
9	122.5	120	129.5	126	122.5	122.5	120

Flight No. 399

1	121.5	127.5	134	125	128	126	133
2	122	122.5	124	123	121	121	118
3	122	122	128	126.5	127	125	122.5
4	120.5	121	122.5	122	118	117	112.5
5	120	120	124	119.5	119.5	116.5	113
6	122	123	126	123	122.5	119	114
7	121.5	122.5	125	124	119	118.5	110
8	121	121	123	120.5	125	112.5	109
9	123.5	123.5	124.5	121.5	117.5	116	112

	Octave Band Center Frequencies - Hz						
Run	63	125	250	500	1,000	2,000	4,000
		(Sound pressure level in db given below)					

TABLE VI - Continued

Flight No. 399 (Continued)

10	120	120.5	123	120	114.5	114	110
11	119	122	123	120.5	116.5	116	116.5
12	119	121	123.5	121.5	114.5	116	112
13	122	124	127	126.5	125	125	121.5
14	124	124.5	127.5	127.5	128	126.5	124
15	122	121	126.5	124	123	123.5	117.5
16	120	118.5	121	122	118	118	113
17	123	123	125	124	121.5	120	122
18	119.5	119.5	125	123	122.5	119.5	116.5
19	120	127	129	127	123.5	123	120.5
20	124	128	131	128	130	128	125.5
21	123	124	127	126	122.5	124	119.5
22	120.5	121.5	123	119.5	119	119	116
23	120	117.5	119.5	117	115	115	111
24	123	125	126	125.5	120	118	111.5
25	121	118.5	124.5	123	117	116.5	112.5
26	122.5	124	129	128	126	126	121.5
27	122	123.5	127	125	124	123	

Flight No. 400

2	120.5	122	121.5	121.5	118	115	110
3	121	122	123	121.5	117.5	115	112
4	121.5	121	123	120	117.5	116.5	111.5
5	118.5	120	122	119	115	112	109
6	122	115	123	121.5	119	115.5	114.5
7	118	123	123	119	114.5	112	110.5
8	118	121.5	123.5	118	116	114	111.5
9	117	121	121	116.5	113.5	112	110
10	120.5	124.5	130	126.5	124.5	123.5	118
11	121.5	123	128	126	124	123	117
12	120	124	124	116.5	117	115	110
13	120.5	121	125.5	124.5	120	119	114
14	124.5	126.5	131	128.5	126	124	118
15	123	126	131	129	124	124	118.5
16	122	124	124	124	120	118	113
17	120	123	124	124	122	120	116
18	117	118	121	118	110	116.5	112.5
19	120.5	120	124.5	124	121	120.5	115.5
20	123	127	132.5	128.5	127.5	125.5	120
21	125.5	127	132	128.5	126.5	125.5	119.5
22	120	116	122	121.5	122	121	115.5

TABLE VI - Continued

Run							
	Octave Band Center Frequencies - Hz						
Run	63	125	250	500	1,000	2,000	4,000
	(Sound pressure level in db given below)						

Run	63	125	250	500	1,000	2,000	4,000
Flight No. 400 (Continued)							
23	119	121	125.5	124	121.5	121	115
24	122	120	121.5	120	117.5	114	112.5
25	118.5	115.5	120.5	117.5	116.5	114	111.5
26	127.5	123	128	133	129.5	127	120

TABLE VII. AIRBORNE NOISE DATA - RIGHT-HAND MICROPHONE

	Octave Band Center Frequencies - Hz						
Run	63	125	250	500	1,000	2,000	4,000
	(Sound pressure level in db given below)						
Flight No. 393							
1	126	125	125	121	118	114.5	113
2	125	122	123	119	114	109	110
3	122.5	122.5	120.5	118	114	111	109.5
4	124.5	125.5	126.5	125	118	113	112
5	124.5	123	127	125	118	113	108.5
6	125	121.5	118.5	114.5	112	110	109.5
7	124	123.5	119.5	116	113.5	111.5	112
8	122.5	121	118	115	112.5	110.5	110.5
9	125.5	123.5	122.5	118.5	115	110.5	110.5
10	123.5	121.5	119.5	116	113.5	110.5	110
11	124	121	118	117	111	110	110.5
12	122	121	121	115	114	111	110.5
13	124.5	119.5	120.5	116	113	111.5	111.5
14	124.5	122.5	124	122	118.5	113.5	112
15	129	130	128	127.5	128	125.5	123
16	N/A	N/A	N/A	N/A	N/A	N/A	N/A
17	130	129.5	128.5	127	127	124	126.5
18	129.5	128.0	127	126	121	119.5	117.5
19	126.5	126.5	124	122	122	118	117
20	127	124	126	123	124	121	118.5
21	125.5	127	125	125.5	126	117.5	120
Flight No. 394: No right-hand microphone data available.							
Flight No. 395							
2	124.5	126	125.5	121.5	120.5	119	117.5
3	121.5	120	121	116	112	107.5	106
4	125.5	121	119.5	118.5	113.5	110	107.5
5	128.5	125	121	121.5	118.5	117	117
6	120	117	117	111.5	106	106.5	108
7	123.5	120.5	120.5	113	108	108.5	106.5
8	122	117	118.5	114.5	109.5	107.5	104
9	123.5	119	118	115	114.5	115	111.5
10	123	122.5	121.5	118.5	116.5	112	111
11	128	123	122.5	119.5	116.5	114.5	113.5
12	120.5	118	118	115	108.5	109	109.5
13	121	119	117.5	115	112	111	109.5
14	119.5	117.5	118	114	109	108	109
15	120.5	120	120	115.5	111	110	108.5
16	120.5	120.5	118	115.5	110	108	108
17	125.5	121.5	122.5	119.5	115.5	111	110
18	124	122	123	118	112.5	109	106
19	126	125.5	127	121	118	113	114

TABLE VII - Continued

	Octave Band Center Frequencies - Hz						
Run	63	125	250	500	1,000	2,000	4,000
	(Sound pressure level in db given below)						
Flight No. 398							
1	115.5	116.5	119	125	126	126	129
2	117	117.5	121	128.5	127	128	132
3	117	120.5	122	132.5	132	133	135
4	116.5	122.5	121	127.5	127	125	127
5	116.5	120.5	122	128.5	129.5	128.5	132.5
6	122.5	126	125.5	131.5	131.5	131.5	136
7	117.5	118.5	119.5	127	126.5	124.5	126
8	116.5	120.5	121.5	127	128.5	128	132
9	124	125.5	128	132	133	133.5	134
Flight No. 399							
1	-	-	-	-	-	-	-
2	130.5	129	126	126	122	115	118
3	127	125	121	119	116	118.5	118
4	129	127	128	124.5	122	118.5	118
5	128	127	123	122	118.5	115.5	124.5
6	128	126	123.5	123	132.5	125.5	116.5
7	126	126	123	125.5	125.5	121.5	118.5
8	129	127.5	127	123.5	121.5	121	119.5
9	128	125.5	124.5	125.5	124.5	121.5	118.5
10	126	122	122	124.5	124	122	120.5
11	126	123.5	123	121.5	121	122	114.5
12	126	123.5	121.5	121	115.5	112	110.5
13	123.5	122.5	120	118	113.5	109.5	112
14	125	122	121	120.5	117	116	117
15	130.5	130	129	128.5	124.5	122	120
16	123.5	120.5	122	118	110	109	107
17	122.5	122	121	119	114	112.5	111
18	121	123.5	126	125	119	113.5	110
19	126	125.5	123.5	123.5	119	112	108
20	127.5	127	121	121	120	116	116
21	129.5	125	123.5	126.5	120.5	119	119
22	118.5	123	121	117.5	113	109	109.5
23	127	124	121.5	118	115.5	115	116.5
24	125.5	126	124.5	121.5	116	110	109
25	134.5	113.5	132	129	126	123	116.5
26	129	123	119	120.5	118	118	117
27	125	121	119	119	114.5	111.5	111.5

	TABLE VII - Continued						

	Octave Band Center Frequencies - Hz						
Run	63	125	250	500	1,000	2,000	4,000
			(Sound pressure level in db given below)				

Flight No. 400

Run	63	125	250	500	1,000	2,000	4,000
2	127.5	128	125	124	121.5	118	127.5
3	127	126.5	127	124	123	120	127
4	129	124.5	123	122.5	118	118	116
5	123.5	124.5	123	120.5	119	115.5	115.5
6	127	128.5	126.5	125	122.5	117	117
7	124	123	123	125.5	123	122	119
8	127	123	120.5	122	124	119	119
9	126	123	122	122.5	121	121	117.5
10	126	123	122	120	117.5	117.5	117.5
11	125	124	121	121	123.5	118.5	117.5
12	126	124	121	121	113	111	113
13	124.5	121	123	118.5	113.5	110	108
14	127	123	119.5	120	119	115.5	116
15	127	124	119	121	120.5	119	120
16	123	122	120	116.5	113.5	111.5	113
17	121	120	113.5	116	112.5	112	114
18	124	123.5	124	121.5	118.5	113	114.5
19	125	122	121.5	119	114	112	114
20	127	124	119	121	117	116.5	117
21	127	123.5	120	121	118	119	117.5
22	120.5	120.5	119.5	118	114	111	114
23	122.5	118	119	115	111	110	113
24	123.5	123.5	123	121	116.5	112	115
25	120.5	118	117	114	111.5	111.5	114
26	125	124	123	119.5	116.5	115	116

TABLE VIII. AIRBORNE NOISE DATA - COCKPIT MICROPHONE						
Octave Band Center Frequencies - Hz						
Run	63	125	250	500	1,000	2,000	4,000
	(Sound pressure level in db given below)						

Flight No. 393

Run	63	125	250	500	1,000	2,000	4,000
1	105.5	107.5	101.5	105.5	102.5	107.5	109.5
2	109.5	108	102.5	105	103	107.5	109.5
3	114.5	111	106	105.5	102	106	108.5
4	110	108.5	103.5	105	103	108	111
5	106.5	109	105	105	102.5	106.5	109
6	110.5	108.5	99	104.5	102	106	108.5
7	108	107.5	98	104.5	102.5	106	109
8	108	108	99	104.5	102	106	108
9	114	109	100	103.5	102	106.5	108.5
10	114.5	110	101	104	102	105.5	107.5
11	113	110.5	103	103.5	102.5	106.5	108
12	110.5	108	99	103.5	102	108	112
13	114.5	111	101.5	104.5	103	107.5	111.5
14	108	108	101.5	103	101.5	106	115.5
15	110.5	108.5	102.5	106.5	103.5	107	108
16	-	-	-	-	-	-	-
17	110	108	103	107	103.5	106	110
18	107.5	108.5	101.5	106	102.5	106.5	108
19	107	107	99.5	105.5	102	105	108
20	106.5	107.5	98	105.5	102	106	109
21	108.5	106	97.5	104.5	103	106	108

Flight No. 394

Run	63	125	250	500	1,000	2,000	4,000
1	112.5	108.5	102	104	100	104	106
2	116	107	101.5	103.5	100.5	105.5	106.5
3	113.5	108.5	100.5	103.5	100	104.5	107.5
4	117	109.5	100.5	103.5	100.5	106	106.5
5	115	111	106	104.5	101.5	107	107.5
6	116	111.5	106.5	105	106.5	104.5	106.5
7	112	106	98.5	101	104.5	104.5	107.5
8	-	-	-	-	-	-	-
9	113	108	105.5	100	102.5	108.5	106
10	105	103.5	97.5	103	110	105.5	108
11	104	99.5	97.5	101.5	105	102	107
12	104	99	96	102.5	105	101.5	110
13	105	99.5	96.5	102	105	101.5	108.5
14	116.5	111	103	103.5	101	105	107
15	-	-	-	-	-	-	-
16	-	-	-	-	-	-	-

TABLE VIII - Continued

	Octave Band Center Frequencies - Hz						
Run	63	125	250	500	1,000	2,000	4,000
			(Sound pressure level in db given below)				

Flight No. 395

2	101	103	96	102.5	102	107	108.5
3	103	103.5	97	100.5	101.5	106.5	109
4	-	-	-	-	-	-	-
5	-	-	-	-	-	-	-
6	98.5	99.5	94.5	99	104.5	101	106.5
7	97.5	102.5	98	101.5	108.5	106	109.5
8	100	102	96	101	108	105.5	108
9	104	103.5	96.5	101	107.5	104.5	108.5
10	103.5	104.5	101.5	102.5	108	104.5	107.5
11	111.5	105	96.5	100	100	105.5	107
12	109	105	100	101	100.5	105.5	110
13	101	104.5	100	102	101.5	107	106.5
14	108.5	104.5	97.5	101.5	100	104.5	107.5
15	109.5	105	97	101	100	105	107
16	108	104.5	98.5	101	100	105.5	108
17	108	105	96.5	102	100	104.5	107.5
18	100	104	100.5	101	99.5	104.5	111
19	107.5	108.5	100	101	100	101.5	105

Flight No. 398 Data not available

Flight No. 399

2	110.5	103.5	103	102.5	104.5	106	96.5
3	111.5	111.5	107	103.5	103	106	106
4	106	101.5	103	102	108	110.5	97.5
5	105.5	102.5	101.5	103.5	107.5	107.5	107
6	108	102	102.5	103	107.5	105.5	97.5
7	105	102	102.5	102	107	107	97.5
8	105	101	102	103	106.5	106.5	99
9	106	103	102	102	107	106	97
10	105	101.5	103	103	107	109.5	108.5
11	105.5	100.5	102	103.5	106	105.5	98.5
12	113	103.5	100	102.5	106.5	106	97
13	113.5	109	103	103	107.5	103.5	100.5
14	-	-	-	-	-	-	-
15	-	-	-	-	-	-	-
16	-	-	-	-	-	-	-
17	-	-	-	-	-	-	-
18	108	104	101.5	102.5	107	105	99
19	111	106	102.5	102	105	105	99
20	114	107.5	105	104	105	106	98.5
21	112	107	104.5	103	106.5	106.5	97.5
22	105	102	100	103	108	107.5	97

TABLE VIII – Continued

	Octave Band Center Frequencies – Hz						
Run	63	125	250	500	1,000	2,000	4,000
			(Sound pressure level in db given below)				

Flight No. 399 (Continued)

23	108.5	102.5	101	102	106.5	108	98.5
24	108	103.5	99	103	105.5	107.5	96.5
25	113	107	103	101.5	105	104	98.5
26	110	105.5	105	101.5	104	105.5	97.5
27	106.5	100.5	100	103	106.5	104	96.5

Flight No. 400

2	104	107	100	101.5	101.5	107.5	107
3	108.5	107	101.5	102	101	107	109
4	104.5	106	100	101	102	106	108.5
5	106	106	99	101.5	101	107.5	110
6	102	107.5	99	101	102	106.5	107
7	106	107	100	101.5	102	107	106
8	106	106	97.5	100.5	101.5	106.5	105
9	105.5	106	96.5	100.5	102	107	106
10	115	108	104.5	104	99	104	107
11	113.5	106.5	104.5	103.5	100	103	104.5
12	108	107.5	99.5	100	101	107.5	107
13	111	107.5	102	101	99	104.5	107
14	114	108	104.5	104	100	105	106
15	114	109.5	104.5	104.5	100	104	105.5
16	111	109.5	98	100	100.5	107	107
17	112	107.5	98	101.5	99.5	103.5	109
18	103	104.5	98	99.5	102.5	108.5	107.5
19	108	107	102	102	100	104.5	107.5
20	113	109	104.5	103.5	100.5	103.5	105.5
21	115	109	104.5	103	101	104.5	105
22	107	104	98	100.5	102	108.5	107
23	104	105	100	102.5	100.5	104.5	107.5
24	104	109	97	100	101	107	110.5
25	111	106	95	102	99.5	105.5	106
26	116	110.5	105	101.5	99.5	104.5	106

APPENDIX IV

GROUND NOISE DATA

TABLE IX. GROUND DATA - MICROPHONE AT 600 FEET NORTH SIDE (FLIGHT 399)							

Run	Azimuth re A/C (deg)	Octave Band Center Frequencies - Hz						
		63	125	250	500	1,000	2,000	4,000
		(Sound pressure level in db given below)						
2	090	102	101	102	109	99	93	80
3	090	105	102	98	105	104	98	77
4	180	98	96	93	93	91	84	70
5	135	99	99	84	84	82	78	69
6	090	100	96	82	81	79	74	64
7	045	97	95	82	80	74	77	60
8	180	93	82	78	81	85	76	56
9	135	99	103	95	86	76	65	52
10	090	100	96	87	79	79	62	46
11	045	96	97	84	80	80	73	61
12	090	102	98	95	96	91	81	65
13	090	98	97	99	105	96	90	71
14	090	105	103	100	109	99	93	77
15	090	104	104	99	103	95	96	79
16	090	99	86	88	90	88	79	64
17	090	-	-	-	-	-	-	-
18	270	-	-	-	-	-	-	-
19	270	103	100	94	100	100	89	74
20	270	105	104	98	100	95	83	68
21	270	102	102	93	96	91	76	59
22	270	101	98	90	93	89	90	63
23	270	98	94	92	91	88	83	65
24	090	104	100	92	100	96	88	76
25	090	102	101	98	104	99	87	74

TABLE X. GROUND DATA - MICROPHONE AT 200 FEET NORTH SIDE (FLIGHT 399)

Run	Azimuth re A/C (deg)	Octave Band Center Frequencies - Hz						
		63	125	250	500	1,000	2,000	4,000
		(Sound pressure level in db given below)						
2	090	112	114	116	115	107	100	90
3	090	111	109	116	113	105	-	91
4	180	108	110	108	101	103	98	88
5	135	110	111	106	101	101	95	86
6	090	112	109	102	101	93	89	81
7	045	108	108	106	99	98	93	87
8	180	110	105	102	103	102	98	85
9	135	113	118	121	109	104	98	85
10	090	110	108	104	95	97	91	81
11	045	108	109	104	98	97	89	82
12	090	113	105	113	103	98	93	84
13	090	113	108	115	110	102	97	89
14	090	113	110	115	115	106	102	92
15	090	109	106	112	112	103	95	82
16	090	107	103	102	102	98	94	83
17	090	106	103	106	106	102	93	85
18	270	-	-	-	-	-	-	-
19	270	111	110	116	117	110	107	95
20	270	113	107	114	111	103	98	86
21	270	110	106	105	103	96	89	81
22	270	110	104	103	106	101	91	85
23	270	107	101	97	97	97	92	82
24	090	115	113	108	110	103	97	88
25	090	110	110	108	105	98	96	81

87

TABLE XI. GROUND DATA – MICROPHONE AT 200 FEET SOUTH SIDE (FLIGHT 399)

Run	Azimuth re A/C (deg)	Octave Band Center Frequencies – Hz						
		63	125	250	500	1,000	2,000	4,000
		(Sound pressure level in db given below)						
2	270	111	106	106	105	99	83	80
3	270	112	108	108	106	100	94	81
4	360	109	110	113	114	109	99	91
5	315	107	111	110	107	105	97	88
6	270	110	113	111	108	105	97	85
7	225	108	112	110	109	108	100	89
8	360	104	109	110	106	103	100	89
9	315	107	113	113	111	107	99	88
10	270	110	112	109	106	104	95	85
11	225	104	110	111	111	106	97	86
12	270	109	108	109	111	104	96	82
13	270	113	109	116	114	108	97	85
14	270	112	110	111	106	102	95	80
15	270	114	111	105	104	101	96	85
16	270	112	111	111	116	110	99	88
17	270	110	109	109	109	108	99	86
18	090	108	107	110	112	106	96	85
19	090	111	110	118	119	112	102	90
20	090	114	113	116	115	106	97	84
21	090	117	109	116	116	102	88	70
22	090	109	110	106	108	105	96	84
23	090	107	106	114	111	93	94	83
24	270	112	115	110	109	109	101	88
25	270	112	107	106	103	100	94	80

TABLE XII. GROUND DATA – MICROPHONE AT 600 FEET SOUTH SIDE (FLIGHT 399)

Run	Azimuth re A/C (deg)	Octave Band Center Frequencies – Hz						
		63	125	250	500	1,000	2,000	4,000
		(Sound pressure level in db given below)						
2	270	104	102	102	94	94	83	66
3	270	103	107	105	97	94	82	64
4	360	97	99	95	88	81	74	68
5	315	95	97	91	87	79	70	60
6	270	98	95	91	87	80	71	57
7	225	97	98	94	90	83	77	60
8	360	93	94	89	81	78	71	55
9	315	98	99	94	86	82	73	55
10	270	95	96	92	86	79	72	57
11	225	94	94	87	81	85	70	51
12	270	101	102	101	100	98	89	68
13	270	103	105	106	102	98	–	75
14	270	104	107	106	100	93	85	67
15	270	103	101	99	97	91	81	68
16	270	100	102	102	99	98	86	71
17	270	101	101	99	92	92	84	62
18	090	98	99	101	97	93	84	66
19	090	101	103	105	108	104	92	75
20	090	106	110	108	106	102	93	73
21	090	104	105	104	108	103	93	72
22	090	95	98	96	90	91	83	58
23	090	95	98	96	90	91	83	58
24	270	98	101	98	96	94	85	63
25	270	100	101	98	84	88	79	56

89

TABLE XIII. GROUND DATA - MICROPHONE AT 600 FEET NORTH SIDE
(FLIGHT 400)

Run	Azimuth re A/C (deg)	Octave Band Center Frequencies - Hz						
		63	125	250	500	1,000	2,000	4,000
		(Sound pressure level in db given below)						
2	180	91	91	77	80	84	79	71
3	135	97	97	82	82	88	78	74
4	090	95	89	74	74	74	70	65
5	045	98	97	84	79	83	78	70
6	180	91	90	78	78	81	80	70
7	135	100	103	89	81	75	80	73
8	090	95	89	77	74	75	74	72
9	045	92	98	81	79	84	79	71
10	090	103	97	94	101	98	92	83
11	090	101	100	97	105	98	93	88
12	090	99	95	95	99	93	87	79
13	090	97	93	96	101	94	91	81
14	090	100	98	100	99	93	88	81
15	090	100	102	100	103	100	96	84
16	090	101	93	98	92	91	84	75
17	090	95	93	91	87	86	85	79
18	270	103	104	103	100	94	88	81
19	270	103	106	109	104	110	94	87
20	270	109	112	107	109	102	101	95
21	270	111	112	105	101	95	89	88
22	270	104	104	104	102	98	95	87
23	270	-	-	-	-	-	-	-
24	090	102	99	86	89	90	84	77
25	270	-	-	-	-	-	-	-
26	090	101	98	100	101	100	93	87

90

TABLE XIV. GROUND DATA – MICROPHONE AT 200 FEET NORTH SIDE (FLIGHT 400)

Run	Azimuth e A/C (deg)	Octave Band Center Frequencies – Hz						
		63	125	250	500	1,000	2,000	4,000
		(Sound pressure level in db given below)						
2	180	104	104	99	102	103	100	93
3	135	111	108	103	98	100	97	92
4	090	106	105	97	90	91	90	85
5	045	110	110	100	97	99	95	89
6	180	105	104	96	99	100	98	90
7	135	112	114	106	103	101	96	91
8	090	107	107	99	93	95	93	86
9	045	105	108	98	96	98	94	87
10	090	110	105	110	108	98	93	86
11	090	112	107	111	106	101	99	88
12	190	110	104	110	105	99	96	89
13	090	106	103	111	108	101	91	88
14	090	113	108	116	112	107	100	91
15	090	112	109	108	108	105	98	88
16	090	107	108	110	102	97	90	86
17	090	103	102	95	95	93	90	86
18	270	96	92	94	95	85	81	74
19	270	95	96	94	91	89	82	74
20	270	105	97	104	102	95	94	86
21	270	106	102	97	97	88	85	77
22	270	100	95	99	91	88	85	75
23	270	–	–	–	–	–	–	–
24	090	116	111	103	109	105	98	90
25	270	–	–	–	–	–	–	–
26	090	109	109	114	108	104	101	91

91

	Azimuth re A/C (deg)	Octave Band Center Frequencies - Hz						
Run		63	125	250	500	1,000	2,000	4,000
		(Sound pressure level in db given below)						
2	360	107	108	111	108	108	101	91
3	315	107	111	109	105	106	100	91
4	270	108	109	107	103	106	100	90
5	225	106	112	110	107	108	101	91
6	360	107	112	110	107	104	99	86
7	315	107	110	108	106	106	102	92
8	270	104	107	104	103	104	99	89
9	225	106	112	109	108	108	102	93
10	270	111	108	109	100	96	96	86
11	270	111	109	108	107	99	95	88
12	270	107	110	109	108	104	96	38
13	270	107	107	114	110	103	99	87
14	270	111	111	112	115	111	98	94
15	270	111	111	107	104	101	96	87
16	270	104	110	114	108	102	95	80
17	270	103	100	99	100	98	93	85
18	090	102	114	117	110	94	108	89
19	090	107	111	114	108	104	98	88
20	090	110	117	121	113	106	98	86
21	090	113	115	112	111	105	96	86
22	090	110	108	114	109	105	98	87
23	090	104	113	113	106	103	107	83
24	270	111	111	107	106	105	101	91
25	90	-	-	-	-	-	-	-
26	270	109	112	111	105	99	93	86

TABLE XV. GROUND DATA - MICROPHONE AT 200 FEET SOUTH SIDE (FLIGHT 400)

TABLE XVI. GROUND DATA - MICROPHONE AT 600 FEET SOUTH SIDE (FLIGHT 400)

Run	Azimuth re A/C (deg)	Octave Band Center Frequencies - Hz						
		63	125	250	500	1,000	2,000	4,000
		(Sound pressure level in db given below)						
2	360	98	99	94	92	88	83	73
3	315	97	99	93	86	85	80	68
4	270	95	96	91	80	81	77	66
5	225	96	98	92	83	85	82	72
6	360	96	98	95	86	82	79	68
7	315	98	98	93	89	87	83	74
8	270	92	97	91	87	89	83	73
9	225	94	100	92	90	88	86	73
10	270	103	103	99	94	97	90	78
11	270	105	105	102	95	93	89	78
12	270	97	102	99	98	96	89	78
13	270	101	101	99	100	97	86	76
14	270	106	107	106	108	102	94	90
15	270	106	106	102	102	92	89	78
16	270	101	98	97	97	93	85	73
17	270	97	95	92	95	88	86	74
18	090	101	98	106	103	98	89	77
19	090	105	99	107	104	98	89	78
20	090	106	108	103	107	102	93	79
21	090	109	107	106	104	103	93	78
22	090	102	100	96	100	96	90	76
23	090	99	100	100	104	96	91	74
24	270	99	100	90	91	92	88	77
25	090	-	-	-	-	-	-	-
26	270	107	105	105	104	94	85	69

APPENDIX V

SUBJECTIVE RATING OF AIRBORNE
AND GROUND DATA

Run No.	True Air-speed (kn)	Rotor RPM	Long. Cyclic BITF/BITR (deg)	Subjective Rating		
				Microphone		
				Left Hand	Nose Boom	Right Hand
TABLE XVII. SUBJECTIVE RATING OF ROTOR NOISE AIRBORNE DATA						
Flight No. 393. Nominal Gross Weight - 36,000 pounds						
1	25	230	0.5/0.0	M	M	W
2	25	230	0.5/0.0	L-M	L-M	W
3	25	230	0.5/0.0	M	M	W
4	25	230	0.5/0.0	M	L-M	W
5	25	230	0.5/0.0	L	None	None
6	25	230	0.5/0.0	L	L	None
7	25	230	0.5/0.0	M	None	None
8	25	230	0.5/0.0	M	M-L	None
9	25	230	0.5/0.0	M	L	L
10	25	230	0.5/0.0	M	L	L
11	22	230	0.5/0.0	M	L	None
12	56	230	0.5/0.0	M-H	M	L
13	61	243	0.5/0.0	M-H	M	L
14	52	243	0.5/0.0	M	M-L	L
15	55-70	230	0.5/0.0	-	N/A	-
16	-	230	0.5/0.0	-	N/A	-
17	0	230	0.5/0.0	M	M	W
18	0	230	0.5/0.0	M	M	W
19	0	230	0.5/0.0	W	L-M	W
20	0	230	0.5/0.0	W	None	W
21	0	230	0.5/0.0	W	None	W
Flight No. 394. Nominal Gross Weight - 32,500 pounds						
0	0	230	0.5/0.0	-	N/A	-
1	51	230	0.5/0.0	M	M-L	None
2	90	230	0.0/0.0	M	M-L	None
3	75	230	0.5/0.0	M-H	M	None
4	38	230	2.0/2.0	M		None
5	88	230	2.86/4.73	H	M	None
6	88	230	3.0/5.0	H	M	None
7	66	222	0.5/0.0	M	L	None
8	51	215	0.0/0.0	-	N/A	-
9	51	215	2.0/2.0	H	M	None
10	51	215	0.5/0.0	M	L	None

Run No.	True Air- speed (kn)	Rotor RPM	Long. Cyclic BITF/BITR (deg)	Subjective Rating		
				Microphone		
				Left Hand	Nose Boom	Right Hand

<table>
<tbody>
<tr><td colspan="7">TABLE XVII - Continued</td></tr>
</tbody>
</table>

Flight No. 394.   Nominal Gross Weight - 32,500 pounds (Continued)

Run No.	True Air-speed (kn)	Rotor RPM	Long. Cyclic BITF/BITR (deg)	Left Hand	Nose Boom	Right Hand
11	23	204	0.5/0.0	L-M	L	None
12	23	204	0.0/0.0	L-M	L-None	None
13	23	204	2.0/2.0	M	L-M	None
14	72	235	0.5/0.0	M	M	None
15	93	230	2.9/4.7	M-H	M-H	None
16	55-0	230	0.5/0.0	L-M	L-M	None

Flight No. 395.   Nominal Gross Weight - 25,500 pounds

Run No.	True Air-speed (kn)	Rotor RPM	Long. Cyclic BITF/BITR (deg)	Left Hand	Nose Boom	Right Hand
2	0	230	0.5/0.0	L-M	None	L
3	51	230	0.5/0.0	M-H	M	L
4	88	230	2.86/4.73	H	M	L-None
5	123	230	3.0/5.0	H	M	L
6	51	204	0.5/0.0	L-M	L-None	None
7	51	215	0.5/0.0	L-M	L-None	L-None
8	65	215	0.5/0.0	M	L-None	None
9	92	215	2.23/3.47	M-H	L-M	None
10	97	215	3.0/5.0	M-H	L-M	None
11	69	230	0.5/0.0	M	L-None	None
12	69	230	0.5/0.0	L-M	L-None	None
13	69	230	0.5/0.0	M	L-M	None
14	69	230	0.5/0.0	L-M	None	L-None
15	69	230	0.5/0.0	M	None	None
16	69	230	0.5/0.0	L-M	L	None
17	69	230	0.5/0.0	M-H	L-None	None
18	69	230	0.5/0.0	M-H	L-None	L-None
19	69	230	0.5/0.0	L-M	W	L

Flight No. 398.   Nominal Gross Weight - 23,500 pounds

Run No.	True Air-speed (kn)	Rotor RPM	Long. Cyclic BITF/BITR (deg)	Left Hand	Nose Boom	Right Hand
1	122	225	3.0/5.0	H	M	None
2	132	225	3.0/5.0	H	M-H	None
3	141	225	3.0/5.0	M-H	M-L	None
4	122	235	3.0/5.0	H	L-None	None
5	132	235	3.0/5.0	H	M	None
6	142	235	3.0/5.0	H	M-H	L-None
7	118	230	3.0/5.0	H	M-H	L-None
8	127	230	3.0/5.0	M-H	M	None
9	137	230	3.0/5.0	H	None	None
10	143	230	3.0/5.0	H	M	None

	True Air-		Long. Cyclic	Subjective Rating		
					Microphone	
Run No.	speed (kn)	Rotor RPM	BITF/BITR (deg)	Left Hand	Nose Boom	Right Hand
TABLE XVII - Continued						
Flight No. 398. Nominal Gross Weight - 23,500 pounds (Continued)						
11	138	230	3.0/5.0	M	L	None
12	136	230	3.0/5.0	M	M	None
13	137	230	3.0/5.0	M-H	M-H	L-None
Flight No. 399. Nominal Gross Weight - 27,500 pounds						
1	96	230	3.0/5.0	H	M	L-None
2	120	230	3.0/5.0	-	N/A	-
3	120	230	3.0/5.0	H	M	None
4	0	230	0.5/0.0	M	L	
5	0	230	0.5/0.0	M	L	None
6	0	230	0.5/0.0	M	L	L-None
7	0	230	0.5/0.0	M	L	None
8	0	230	3.0/5.0	M	L	None
9	0	230	3.0/5.0	M	L	None
10	0	230	3.0/5.0	M	L	None
11	0	230	3.0/5.0	L-M	L-None	None
12	40	230	3.0/5.0	M-H	M	L
13	80	230	3.0/5.0	M-H	L-M	None
14	120	230	3.0/5.0	M-H	L-None	None
15	130	230	3.0/5.0	M-H	M	
16	40	230	0.5/0.0	L-M	L-None	None
17	80	230	0.5/0.0	-	N/A	-
18	40	230	3.0/5.0	H	M	L
19	80	230	3.0/5.0	H	M	L-None
20	120	230	3.0/5.0	H	M	L-None
21	130	230	3.0/5.0	H	L-M	L
22	40	230	0.5/0.0	M-H	L-M	L
23	80	230	0.5/0.0	M-H	M-H	L
24	60	230	0.5/0.0	M-H	M	L
25	110	230	0.5/0.0	M	None	L-None
26	123	230	3.0/5.0	M-H	M-H	L-None
27	97	220	3.0/5.0	M-H	None	L-None
23R	80	230	0.5/0.0	-	N/A	-
Flight No. 400. Nominal Gross Weight - 27,500 pounds						
2	0	230	0.5/0.0	None	L	None
3	0	230	0.5/0.0	None	L	L-None
4	0	230	0.5/0.0	L-None	L	L-None
5	0	230	0.5/0.0	None	L	None

				Subjective Rating		
	True Air-		Long. Cyclic		Microphone	
Run No.	speed (kn)	Rotor RPM	BITF/BITR (deg)	Left Hand	Nose Boom	Right Hand
Flight No. 400. Nominal Gross Weight - 27,500 pounds (Continued)						
6	0	230	3.0/5.0	L-None	L	L-None
7	0	230	3.0/5.0	L-None	L	L-None
8	0	230	3.0/5.0	L-None	L	L-None
9	0	230	3.0/5.0	L-None	L	L-None
10	120	230	3.0/5.0	L-M	M	None
11	120	230	3.0/5.0	L-M	M	None
12	40	230	3.0/5.0	L-M	L-M	L-None
13	80	230	3.0/5.0	L-M	M	L-None
14	120	230	3.0/5.0	M	M	None
15	130	230	3.0/5.0	M	M	L-None
16	40	230	0.5/0.0	L-M	L	L-None
17	80	230	0.5/0.0	L	L-None	L-None
18	40	230	3.0/5.0	L-M	L-M	L-None
19	80	230	3.0/5.0	L-M	L-M	L-None
20	120	230	3.0/5.0	M	M	None
21	130	230	3.0/5.0	M	M	L-None
22	40	230	0.5/0.0	L-M	M-L-None	L-None
23	80	230	0.5/0.0	L-M	L-None	L-None
24	60	230	0.5/0.0	L	L-M	L
25	80	230	3.0/5.0	L-M	L-None	L-None
26	110	230	0.5/0.0	L-None	None	None

L - Light Rotor Bang
M - Moderate Rotor Bang
H - Heavy Rotor Bang
W - High Wind Noise

97

				Subjective Rating Microphone 200 Ft North	
Run 399/400	Azimuth (deg)	True Airspeed (kn)	Long. Cyclic BITF/BITR (deg)	Standard Tip X-399	Porous Tip X-400
2/10	90	120	3.0/5.0	M	M
3/11	90	120	3.0/5.0	M	M
4/2	180	0	0.5/0.0	M-H	L-M
5/3	135	0	0.5/0.0	M	M-L
6/4	90	0	0.5/0.0	M	L-None
7/5	45	0	0.5/0.0	M	L
8/6	180	0	3.0/5.0	M-H	L-M
9/7	135	0	3.0/5.0	H	M
10/8	90	0	3.0/5.0	M	M
11/9	45	0	3.0/5.0	M-H	M
12/12	90	40	3.0/5.0	M-H	L-M
13/13	90	80	3.0/5.0	H	M-H
14/14	90	120	3.0/5.0	M-H	H
15/15	90	130	3.0/5.0	M-H	H
16/16	90	40	0.5/0.0	M-H	M
17/17	90	80	0.5/0.0	M	L
18/18	270	40	3.0/5.0	M	L-M
19/19	270	80	3.0/5.0	H	M
20/20	270	120	3.0/5.0	M-H	H
21/21	270	130	3.0/5.0	L-M	M
22/22	270	40	0.5/0.0	M	M
23/23	270	80	0.5/0.0	L-None	L-None
24/24	90	60	0.5/0.0	M-H	M
25/26	90	110	0.5/0.0	M	M

L - Light Rotor Bang
M - Moderate Rotor Bang
H - Heavy Rotor Bang
W - High Wind Noise

TABLE XVIII. SUBJECTIVE RATING - STANDARD TIP AND POROUS TIP - GROUND DATA

DOCUMENT CONTROL DATA - R & D

(Security classification of title, body of abstract and indexing annotation must be entered when the overall report is classified)

1. ORIGINATING ACTIVITY *(Corporate author)*	2a. REPORT SECURITY CLASSIFICATION
The Boeing Company	Unclassified
Vertol Division	2b. GROUP
Philadelphia, Pennsylvania	

3. REPORT TITLE

MEASUREMENT OF ROTOR NOISE LEVELS AND EVALUATION OF POROUS BLADE TIPS ON A CH-47A HELICOPTER

4. DESCRIPTIVE NOTES *(Type of report and inclusive dates)*

Final Report

5. AUTHOR(S) *(First name, middle initial, last name)*

Robert H. Spencer
Harry Sternfeld, Jr.

6. REPORT DATE	7a. TOTAL NO. OF PAGES	7b. NO. OF REFS
September 1969	111	6

8a. CONTRACT OR GRANT NO.	9a. ORIGINATOR'S REPORT NUMBER(S)
DA 44-177-AMC-330(T)	
b. PROJECT NO.	USAAVLABS Technical Report 69-18
Task 1F162203A14801	
c.	9b. OTHER REPORT NO(S) *(Any other numbers that may be assigned this report)*
d.	D8-0439B

10. DISTRIBUTION STATEMENT

This document is subject to special export controls, and each transmittal to foreign governments or foreign nationals may be made only with prior approval of US Army Aviation Materiel Laboratories, Fort Eustis, Virginia 23604.

11. SUPPLEMENTARY NOTES	12. SPONSORING MILITARY ACTIVITY
	US Army Aviation Materiel Laboratories
	Fort Eustis, Virginia

13. ABSTRACT

Two sets of acoustical data were correlated. Relative blade tip-path plane positions influenced noise levels more than other operating parameters such as rotor speed or gross weight.

Porous blade tips were installed on the test aircraft. The tips reduced noise levels in hover but had no consistent effect in forward flight. However, the tips tended to decrease the sharpness of the acoustical signature at all airspeeds.

DD FORM **1473** REPLACES DD FORM 1473, 1 JAN 64, WHICH IS OBSOLETE FOR ARMY USE.

14. KEY WORDS	LINK A		LINK B		LINK C	
	ROLE	WT	ROLE	WT	ROLE	WT
Acoustical Signature Noise Levels Porous Blade Tips						